EFFECT ON HYSTERESIS LOOPS OF SUPERPOSING ALTERNATING MAGNETIZING FORCES

LAURENCE LEROY JACKSON, Jr.
and
WILLIAM CARL NEWELL, Jr.

EFFECT ON HYSTERESIS LOOPS OF

SUPERPOSING ALTERNATING MAGNETIZING FORCES

Artisan Gold Lettering & Smith Bindery

593 - 15th Street Oakland, Calif. GLencourt 1-9827

DIRECTIONS FOR BINDING

BIND IN
(CIRCLE ONE)

BUCKRAM
COLOR NO. 8854

FABRIKOID
COLOR

LEATHER
COLOR

LETTERING ON ~~BACK~~ shelf
TO BE EXACTLY AS
PRINTED HERE.

JACKSON
and
NEWELL

1954

Thesis
J22

OTHER INSTRUCTIONS

Letter on the front cover:

EFFECT ON HYSTERESIS LOOPS OF
SUPERPOSING ALTERNATING MAGNETIZING FORCES

LAURENCE LEROY JACKSON, Jr.
and
WILLIAM CARL NEWELL, Jr.

Jr.

r.

EFFECT ON HYSTERESIS LOOPS OF SUPERPOSING ALTERNATING MAGNETIZING FORCES

By

Laurence Leroy Jackson, Jr.
Lieutenant, United States Navy

and

William Carl Newell, Jr.
Lieutenant, United States Navy

Submitted in partial fulfillment
of the requirements
for the degree of

MASTER OF SCIENCE

in

ELECTRICAL ENGINEERING

United States Naval Postgraduate School
Monterey, California

1954

This work is accepted as fulfilling the thesis requirements for the degree of

MASTER OF SCIENCE
IN
ELECTRICAL ENGINEERING

from the
United States Naval Postgraduate School

PREFACE

The experiment discussed in this report was carried on from September, 1953 to April, 1954, at the U.S. Naval Postgraduate School, Monterey, California. The work was in partial fulfillment of the requirements for the degree of Master of Science. The experimenters are grateful for the advice and suggestions made by Professor Allen E. Vivell, Professor C.H. Rothauge and Professor R.C.H. Wheeler, and for the technical assistance of Mr. A.J. White and Mr. H. Minor.

TABLE OF CONTENTS

LIST OF ILLUSTRATIONS

LIST OF ILLUSTRATIONS

SUMMARY

Objective: To determine the shape of a hysteresis loop when there is simultaneously imposed on the iron alternating magnetizing forces of various frequencies and intensities.

General Methods: Two physically and magnetically similar ring-shaped specimens having identical primary exciting toroidal winding, pickup winding and another exciting toroidal winding (called the A.C. exciting winding) were selected. The cores of these specimens were subjected to alternating magnetizing forces of various frequencies and intensities by applying A.C. current to the A.C. windings which were connected in opposition with respect to the primary exciting windings and the pickup windings. Resultant hysteresis loops were measured by ballistic means using reversal of direct current in the primary exciting windings and galvanometer integration of the impulse voltage in the pickup winding circuit. Mild steel solid core hysteresis loops were obtained at 1100 ampere-turns per meter and superposed alternating magnetizing forces 800 ampere-turns per meter and 1600 ampere-turns per meter, frequencies varying from 12 to 420 c.p.s. Silicon Steel laminated core hysteresis loops were obtained with 700 and 1400 ampere-turns per meter with alternating magnetizing forces 70 to 1050 ampere-turns per meter, freqcuecies varying from 25 to 420 c.p.s.

Findings: The experimenters demonstrated conclusively that the hysteresis loop of both solid and laminated steel specimens is decreased in area when an alternating magnetizing force is superposed on the specimen. Furthermore, the shape of the magnetization curve is also modified, hence the permeability of the iron.

TABLE OF SYMBOLS AND ABBREVIATIONS

A.C.	Alternating current
D.C.	Direct current
DPDT	Double pole double throw
c.p.s.	Cycles per second
Δ	Incremental change
B	Flux density, in webers per square meter
K	Constant of proportionality
I	Current, in amperes
θ	Deflection of galvanometer, in millimeters
μ	Permeability
N	Number of turns
A	Cross sectional area, in square meters
l	Length, in meters
H	Magnetizing force, in ampere turns per meter
CDRX	Critical damping resistance external
mm	Millimeters
R	Resistance
CRO	Cathode ray oscillograph
RMS	Root-mean-square
A.I.S.I.	American Iron and Steel Institute
in.	Inches
no. Number	Number
°F	Degrees Fahrenheit
sq.	Square
μf	Micro farads
L	Inductance
μh	Microhenry
C	Capacitance
VTVM	Vacuum tube voltmeter
g	grams
cm	centimeters
PK	peak
%	percent
v	Volts
lb	Pounds
sq	Square
m	meter
mh	Millihenry
γ	Relative damping constant
S	Flux sensitivity
e	Instantaneous voltage
dt	Incremental change of time
T	Galvanometer period
t	Time
KVA	Kilovolts-ampere
L&N	Leeds and Northrup
KVAR	Kilovolt-ampere reactive
KW	Kilowatt
RPM	Revolutions per minute

G	Gain
ω	angular velocity in radians per second
E	Voltage
i	instantaneous current
τ	Time constant
KG	Transfer function
d	small division on grid of DuMont CRO
k	instantaneous volts per small division on grid of CRO
AT/m	Ampere-turn per meter

Subscripts refer to:

x	Any point on hysteresis loops other than maximum point
c	Calibrating coil of standard inductor
p	Primary coil of standard inductor
s	Sample under test

CHAPTER I

INTRODUCTION AND HISTORY

Although the subject of magnetic hysteresis is at least seventy years old, recent developments in practise have made it very much a contemporary one. To understand the operation of magnetic amplifiers requires the prior understanding of hysteresis. To analyze the performance of these devices one must first understand what factors may influence the magnetic characteristics of the elements of the magnetic amplifier. It was with a realization of the importance of magnetic amplifiers that this investigation was begun.

Perhaps the single factor motivating the choice of a particular study in the field of magnetic hysteresis was the work of Boyajian and Camilli(6). In their development of the "Orthomagnetic Current Transformer" they used a principle accredited by them to Gerosa and Finzi(9). This principle was not fully tested nor explained by Gerosa and Finzi, nor by Boyajian and Camilli, nor by Ewing(8), nor by any of the five persons discussing the paper submitted by Boyajian and Camilli. Nevertheless, as was evident by a perusal of the paper submitted by Boyajian and Camilli, the facts seemed to be that when an alternating magnetizing force was superposed upon a sample of iron something happened to the hysteresis loop of the iron seen at a lower frequency.

In a sense this thesis is an extension of the work of Niwa and Asami(12) as discussed in Spooner(14). See Figures 1,

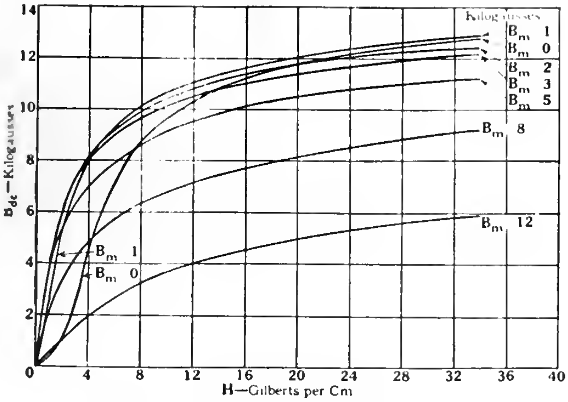

Magnetization curves under superposed alternating field

Figure 1

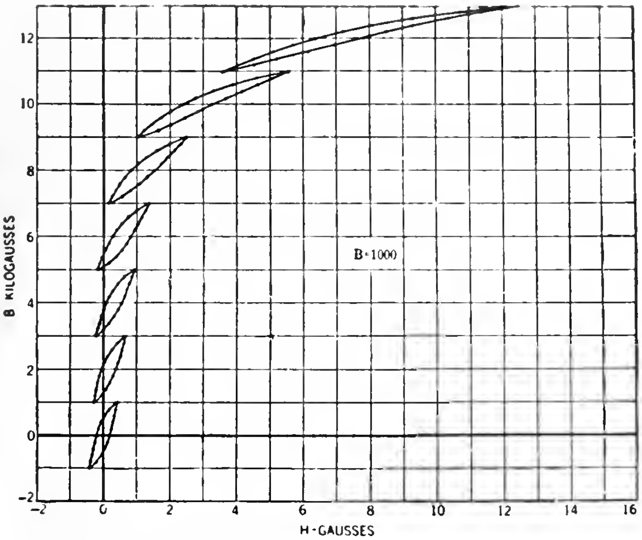

Effect of displacement on hysteresis loops having the same *B*-amplitude (2 kilogausses).

Figure 2

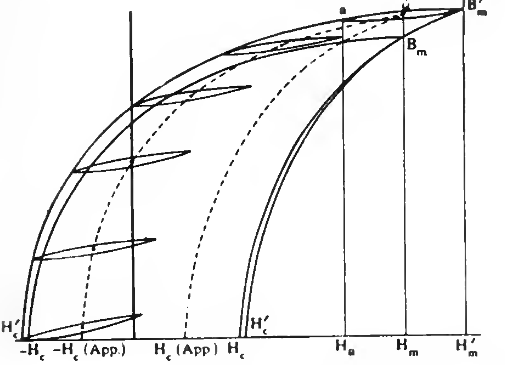

Effect of superposed a.c. on apparent hysteresis loop

Figure 3

2 and 3. Spooner has also cited Ashworth(4), Wright, and Steinhaus and Gumlich as having investigated the "apparent" reduction in hysteresis loss and the "apparent" change in permeability when iron is subjected to a rapidly changing magnetizing force, but, except for Ashworth, these works were not available to these writers.

Perhaps the most comprehensive recent study of ferromagnetism is that prepared by Bozorth(5). In this text, Bozorth (5, pp. 549-554) discusses the effect of superposing an alternating magnetizing force on ferromagnetic materials and reiterates Spooner's(14) contention that the effect is an apparent reduction in the hysteresis loop.

It is the purpose of this thesis to investigate the effect upon the hysteresis loops of several materials of superposing alternating magnetizing forces. These alternating forces will be varied in frequency and in intensity. Data will also be given to show the effect upon the magnetization curve of applying different alternating magnetizing forces. Some of the work done in connection with a study of dynamic effects will be presented, but due to the fact that this phase was not thoroughly investigated, this data is relegated to the appendices.

CHAPTER II

PROCEDURE

To accomplish the purpose of this thesis two ring-shaped specimens were obtained. Each specimen was wound with three windings: a D.C. excitation winding, an A.C. excitation winding, and a detection winding. Particular pains were taken that the two specimens were electrically and magnetically matched insofar as was reasonably possible. There was one primary reason for this: the detection device in the pickup winding circuit should not be influenced by unwanted voltages developed as a result of differences between specimens.

Switches, resistances, meters and galvanometers were so arranged (see Appendix C and Figure 58) that one person could without moving from his seat:

1. Effect a galvanometer calibration by throwing a DPDT switch to CALIBRATE, setting and recording a value of D.C. current, throwing the REVERSING SWITCH, and recording the galvanometer deflection. The ratio of current change to galvanometer deflection was then substituted in the equation:

$$\Delta B_x = K\left(\frac{\Delta I_c}{\Delta \theta_c}\right)\Delta\theta_x$$

where

$$K \mathrel{\hat{=}} \mu_0 \frac{N_c A_c}{N_s A_s}\frac{N_p}{l_p}$$

2. Put the iron in a cyclic state at the B-H point of interest.

3. Change current in a double-step manner from a negative value to any desired positive value or from a positive value in a single step to some other positive value.

4. Arrange for galvanometer deflection to be always in the same direction (black half of scale was used in these experiments) and to record deflection of glavanometer in response to an impulse voltage.

5. Insert critical damping resistance external (CDRX) so that galvanometer would return rapidly to zero.

6. Apply, measure, and record any value of A.C. magnetizing current at a given frequency.

7. Observe wave forms and estimate the magnitude of both the exciting A.C. and the difference A.C. voltage appearing in the galvanometer circuit. This latter was done primarily to protect the galvanometer.

Having obtained some satisfactory specimens (see Appendix A) and having organized the experimental set-up as described above, the taking of data was begun. The procedure outlined in Stout(15) was followed very closely.

First, the galvanometer was adjusted to give deflections in the black sector, made free to swing 250 mm, and set on zero for zero applied signal.

The iron was put in a cyclic state at zero B and H by gradually reducing the D.C. exciting current to zero from some high value, say, 2 amperes, while slowly operating the REVERSING SWITCH.

The D.C. exciting current was then raised to some <u>negative</u> value, the iron cycled several times at this value, the galvanometer put into the circuit, and the current reversed. Half the resultant galvanometer deflection, converted into webers per square meters, and plotted against the magnitude of the current, converted into ampere-turns per meter, established a point on the magnetization curve. When specimens were connected with windings in series the same procedure was used with the exception that now one-quarter of the galvanometer deflection corresponded to the flux density existing in one core.

To determine the static hysteresis loop required two distinct steps, one step for each of two portions of the loop. The method used was capable only of establishing that portion of the hysteresis loop lying in the positive H half-plane; that is, in the right half-plane. The portion of the static loop lying in the left half-plane was plotted by symmetry. The full hysteresis loop was plotted for the sake of clarity and emphasis and with some slight sacrifice of experimental veracity.

The "upper curve" of the positive portion of the loop was determined as follows:

1. The iron was brought to a starting point $+H$, $+B$, as determined both by ammeter reading and by galvanometer deflection occurring when the current was reversed.

2. The iron was then cycled several times by means of the REVERSING SWITCH.

3. With REVERSING SWITCH in $+H$ position and R2 previously adjusted to give some smaller value of positive current the galvanometer was connected in the galvanometer circuit.

4. The resultant step <u>decrease</u> of exciting current caused an impulse to appear in the galvanometer circuit and deflected the galvanometer proportionally. In every case the GALVANOMETER REVERSING SWITCH was so arranged as to give deflections only into the black scale. The <u>change</u> of flux density was negative, and represented a decrease from the flux density existing at $+H1$, $+B1$. The new point, H_x and B_x is thus established as that magnetizing force corresponding to the new value of current and that flux density corresponding to B1 <u>less</u> the change of flux density as read by the galvanometer.

5. R2 was then adjusted for a new value of end current, the BYPASS SWITCH closed, the $+H1$, $+B1$ point checked by reading the galvanometer and ammeter, the iron cycled at $+H1$, $+B1$, and finally, the BYPASS SWITCH opened to obtain a new point as previously described.

To obtain data for the lower portion of the positive half of the hysteresis loop it was necessary to follow a somewhat different procedure:

1. The iron was cycled and left at a point $-H1$, $-B1$, which, in magnitude of current and galvanometer deflection, was exactly the same as $+H1$, $+B1$ but had current passing through the exciting winding in the opposite direction. R1

was left at the same value as for the point +H1, +B1, but after cycling the iron the REVERSING SWITCH was left in the -H position.

2. The BYPASS SWITCH was then opened, introducing R2, but this, of course, had no effect on the current flow while the REVERSING SWITCH was in the -H position. The galvanometer was then connected into the galvanometer circuit.

3. REVERSING SWITCH was then reversed to the +H position. The current almost instantaneously changed from <u>minus</u> I to zero, then from zero to <u>plus</u> I. The value of plus I was dependent upon the pre-set value of R2. A flux density change occurs which is a positive change representing the difference between -B1 and the new value of flux density in the iron corresponding to plus I. Thus, as before, the change in flux density is algebraically subtracted from -B1 and this difference plotted against the new value of H. Since R2 can be varied from zero to 700 ohms, then made infinite by disconnecting a lead, essentially all points on this section of the hysteresis loop can be read or extrapolated.

The procedure for taking points when an A.C. was superposed on the cores was the same as above. The alternating magnetizing force was applied while the iron was at the point corresponding to H1. It was noted that due to change in inductive impedance at the new point the value of the A.C. magnetizing current would change, but for consistency the value

used was always that corresponding to H1.

The magnitude of A.C. magnetizing force superposed was determined primarily as a peak-to-peak value as seen on a CRO. A standard resistance of 0.100 ohm in series with the A.C. exciting winding supplied the voltage signal to the CRO. Since, at the point H1, B1 the magnetizing current was essentially a sine wave (see Figure 4), an A.C. ammeter was also placed in series with this winding to read the RMS value of current.

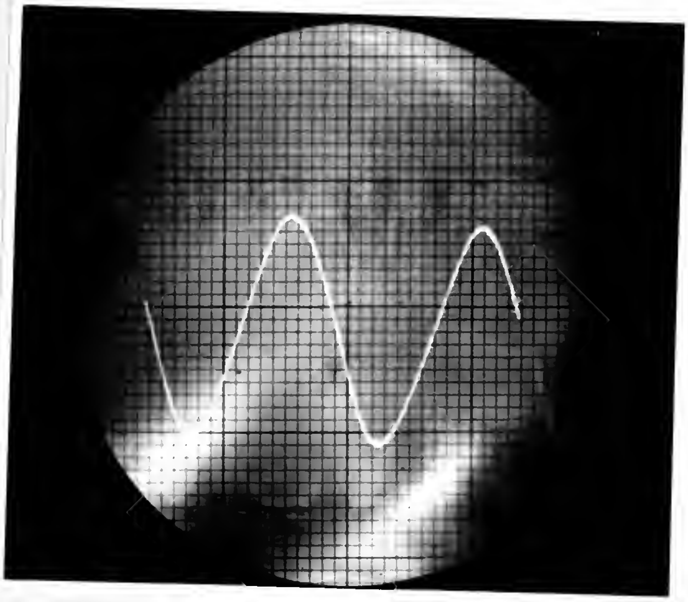

Figure 4

Superposed Current Waveform

180 Cycles

.05 amp/small div.

CHAPTER III

PRESENTATION OF RESULTS

The results of this investigation are presented in this chapter in the form of magnetization curves and hysteresis loops plotted from the laboratory data. The results are divided into two major section - one for each magnetic material studied. The first section deals with the solid core samples, C and D, of annealed low carbon steel; the second section with the laminated core samples, E and F, of silicon steel. The specimens used in the tests are described in detail in Appendix A.

The first section dealing with the solid core samples, consists of Figures 5 through 15. Figure 5 shows the individual normal magnetization curves of samples C and D using 8000 ampere-turns per meter maximum D.C. magnetizing force. Figure 5 serves to identify the magnetic properties of the individual samples used and illustrate the slight mismatch of the cores. The combined normal magnetization curve for samples C and D in series, using 1150 ampere-turns per meter maximum D.C. magnetizing force is shown in Figure 6. This is an average characteristic of the material used.

All of the hysteresis loops for the solid core samples C and D are obtained using a maximum D.C. magnetizing force of 1150 ampere-turns per meter which, as shown in Figure 6, is beyond the saturation point for this material. The individual magnetization curves of specimens C and D are shown in

Figures 7 and 8. The fundamental or reference hysteresis loop, Figure 9, is obtained with the two cores combined in series. Subsequent hysteresis loops in this section should be referred to Figure 9.

Figures 10 through 14 form a series showing the effect of superposing an alternating magnetizing force of a constant maximum value of 810 ampere-turns per meter but of various frequencies. Frequencies of 12, 60, 180 300 and 420 c.p.s. are shown successively. This series of hysteresis loops shows that the area of the hysteresis loop is decreased by the superposed A.C. magnetizing force but that this reduction in area decreases as the frequency of the superposed A.C. is increased. Figures 14 and 15, show the effect of changing the maximum value of the superposed A.C. at one frequency, 420 c.p.s. Figure 14 was plotted with a maximum magnetizing force of 810 ampere-turns per meter, while Figure 15 was plotted with a maximum magnetizing force of 1620 ampere-turns per meter. It is seen by this comparison that increasing the A.C. magnetizing force decreases the area of the hysteresis loop.

Comparing the point of maximum flux density in Figure 9 with those of Figures 10 through 14 it can be observed that the maximum flux density is increased by superposing an A.C. magnetizing force. However, this increase seems to be independent of both frequency and magnitude of the superposed A.C. in the ranges reported.

The second section of these results deals with the effect of a superposed A.C. magnetization force upon specimens E and F, the laminated core specimens. Figure 16* is an averaged or combined magnetization curve taken with the two specimens connected in series. Figure 18 is the combined hysteresis loop of the two specimens with no superposed A.C. excitation. These two figures are the ones which should be used for reference. Individual magnetization and hysteresis curves were not taken because Figures 5 through 9 for specimens C and D indicated that this would be superficial. The two specimens were selected and compared for similar magnetic properties as discussed in Appendix A.

Figure 17 is a study of the effect of a superposed magnetizing force of various amplitudes at a frequency of 180 c.p.s. upon the D.C. normal magnetization curve. It consists of five curves - the D.C. magnetization curve as obtained in Figure 16 and the magnetization curve as modified by a 180 c.p.s. magnetizing force of 70, 175, 350 and 700 maximum ampere-turns per meter superposed. From this figure it is seen that the permeability is first increased and then decreased as the magnitude of the superposed magnetizing force is increased. Also the initial bend in the normal magnetization curve is apparently removed when the alternating magnetizing force is impressed. Within the magnitudes of magnetizing force used the highest point of induction is not decreased.

---

* The B scale of Figures 16-43 should be multiplied by 0.852 to obtain the correct value of flux density in webers per square meter.

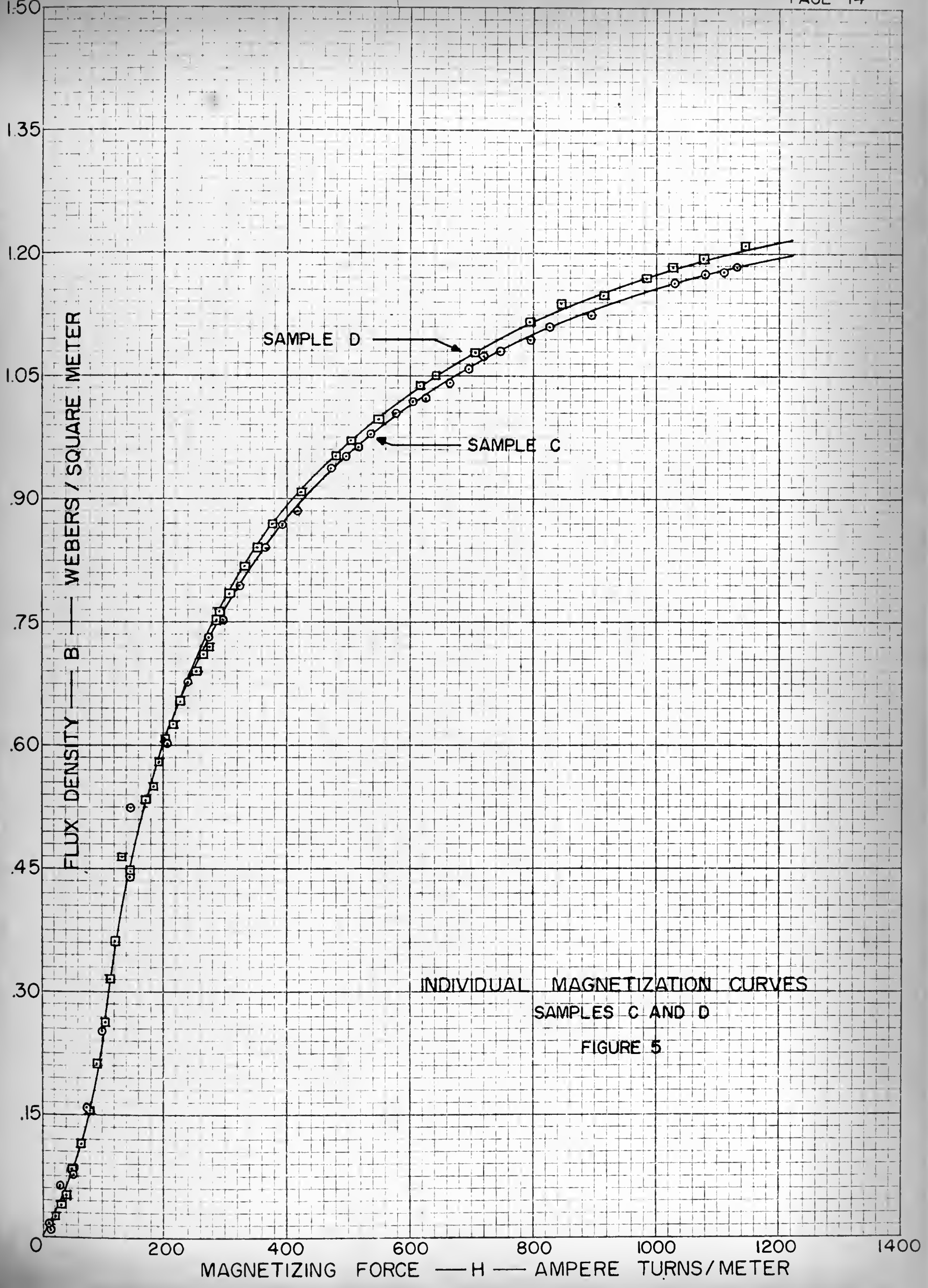

INDIVIDUAL MAGNETIZATION CURVES
SAMPLES C AND D
FIGURE 5

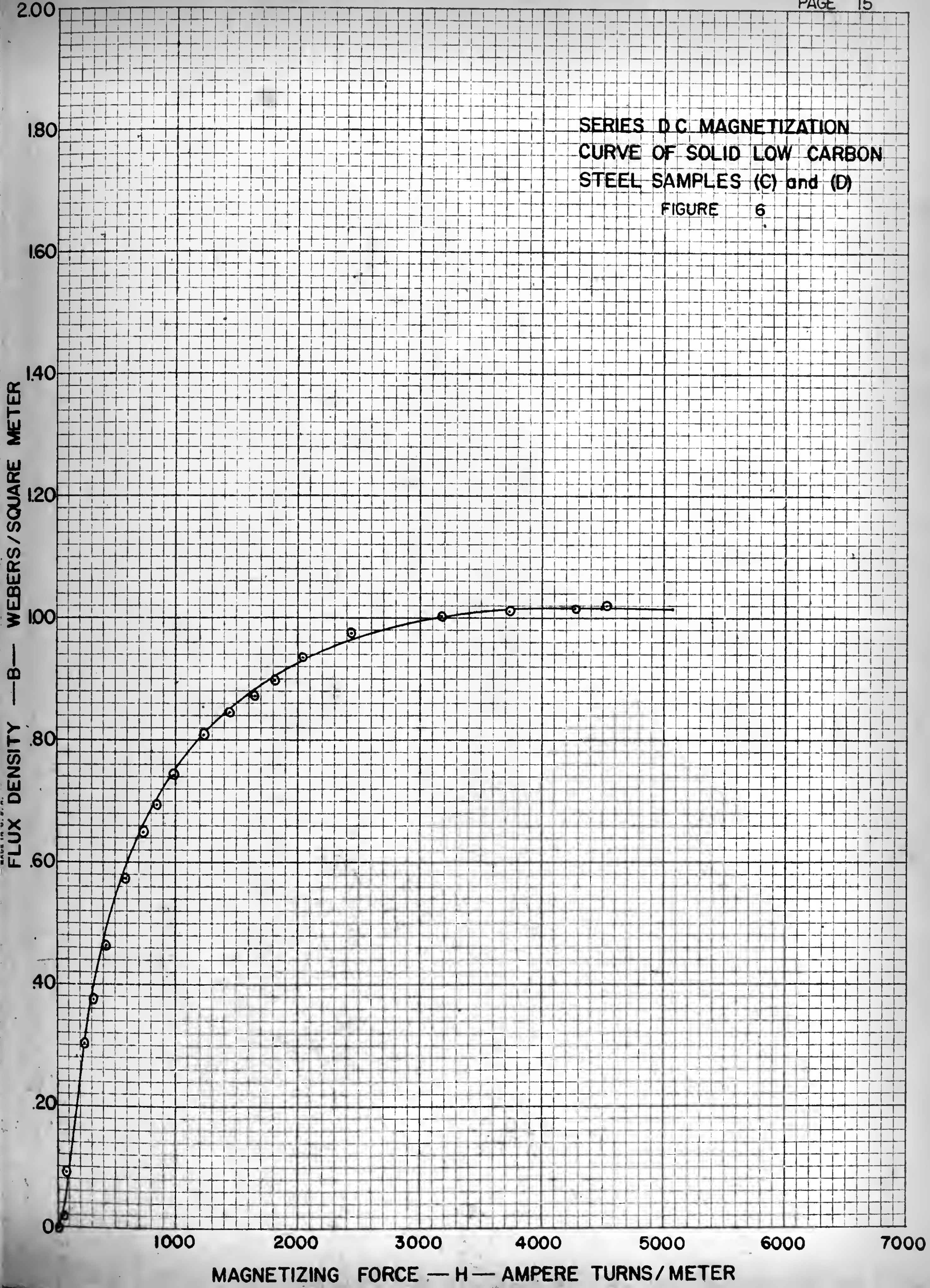

SERIES D.C. MAGNETIZATION CURVE OF SOLID LOW CARBON STEEL SAMPLES (C) and (D)

FIGURE 6

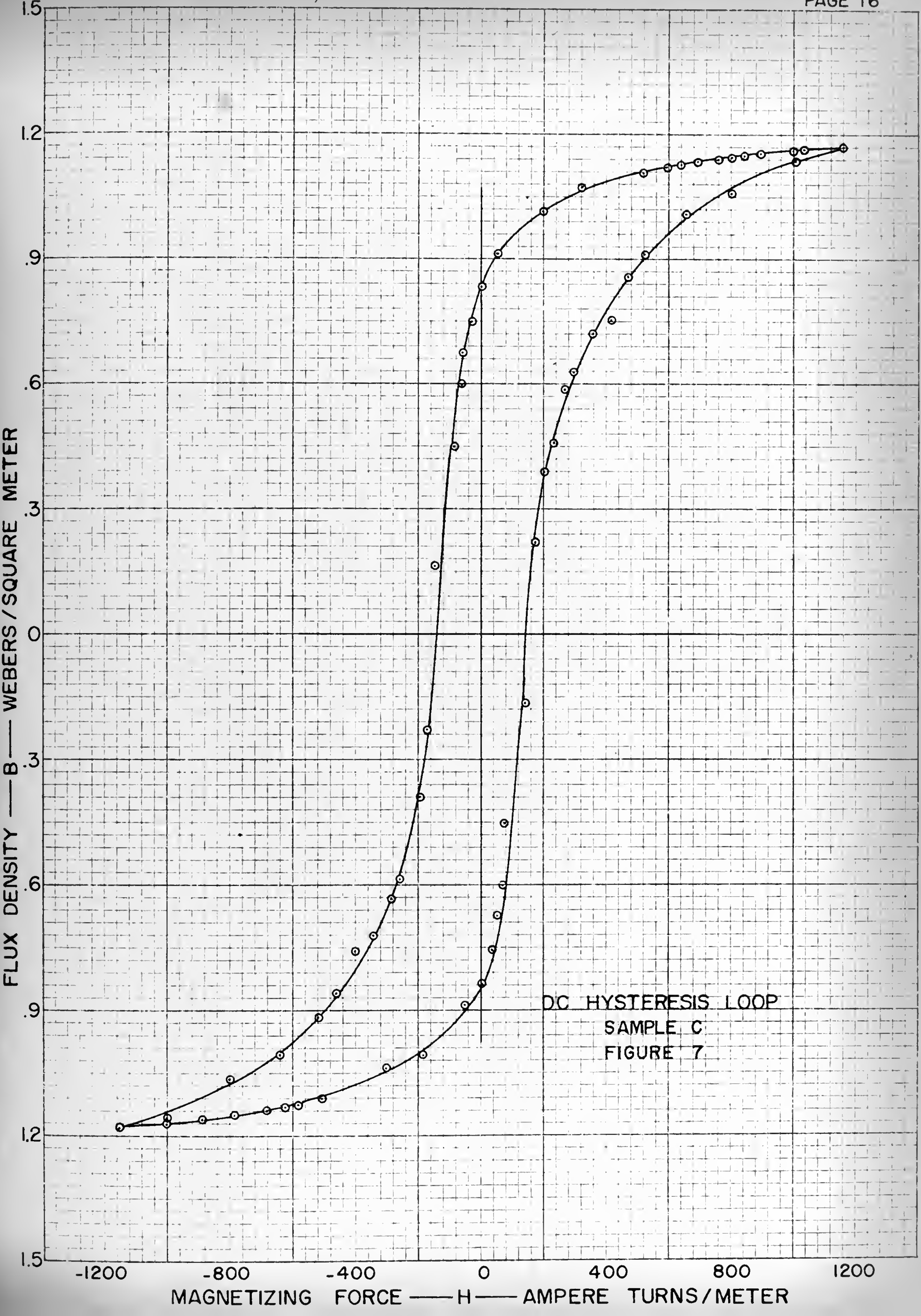

DC HYSTERESIS LOOP
SAMPLE C
FIGURE 7

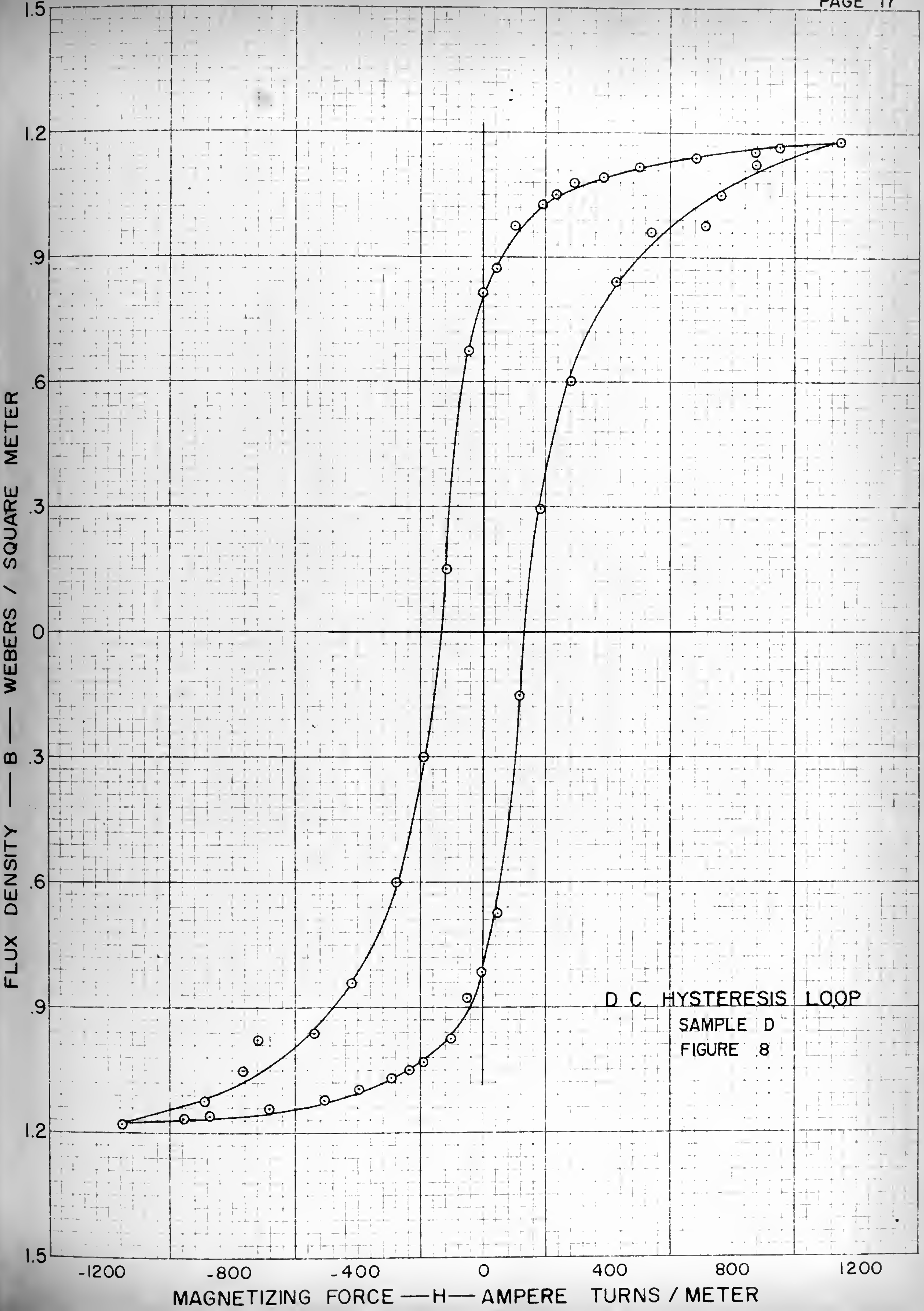

D C HYSTERESIS LOOP
SAMPLE D
FIGURE 8

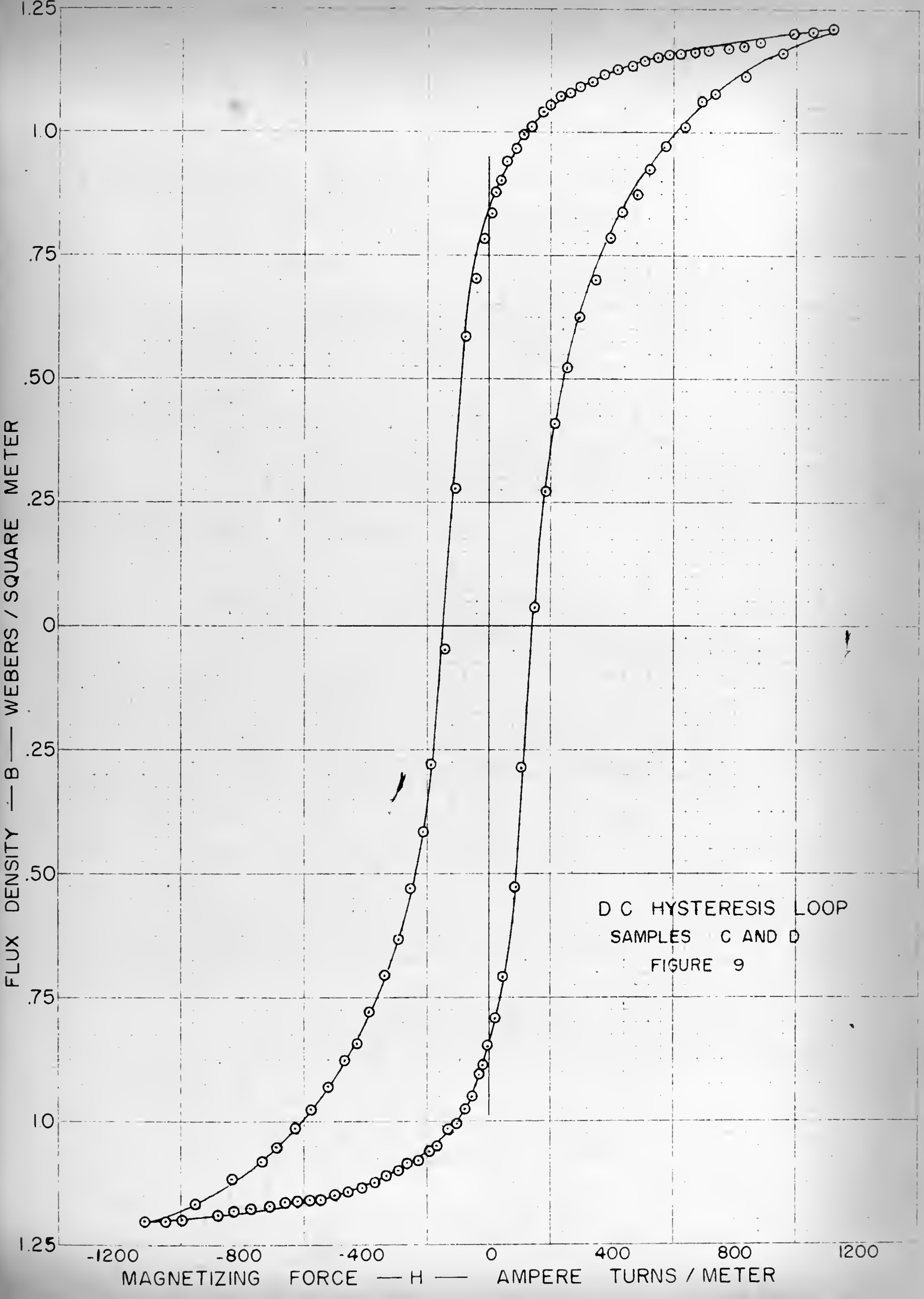

D C HYSTERESIS LOOP
SAMPLES C AND D
FIGURE 9

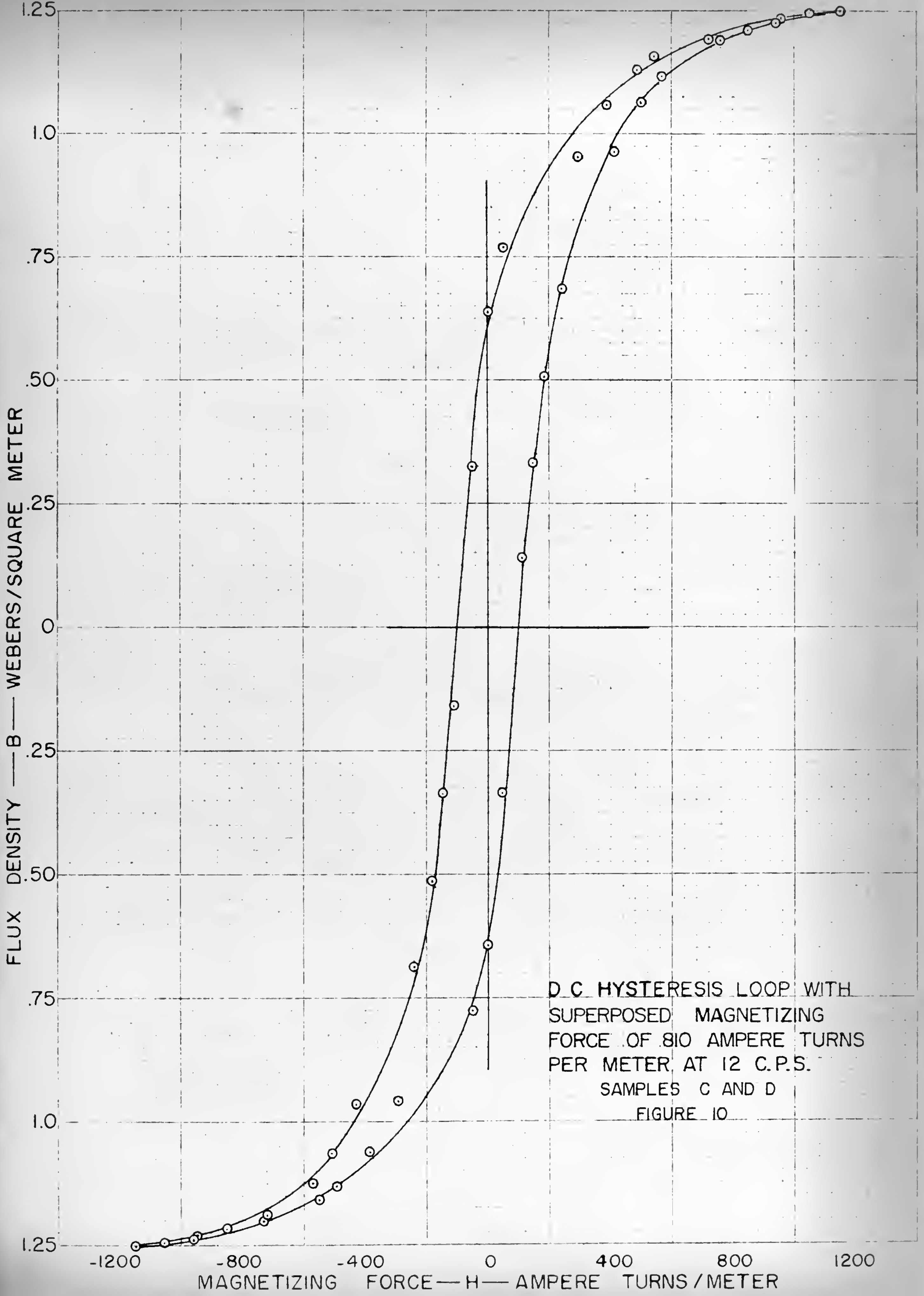

D C HYSTERESIS LOOP WITH SUPERPOSED MAGNETIZING FORCE OF 810 AMPERE TURNS PER METER AT 12 C.P.S.

SAMPLES C AND D

FIGURE 10

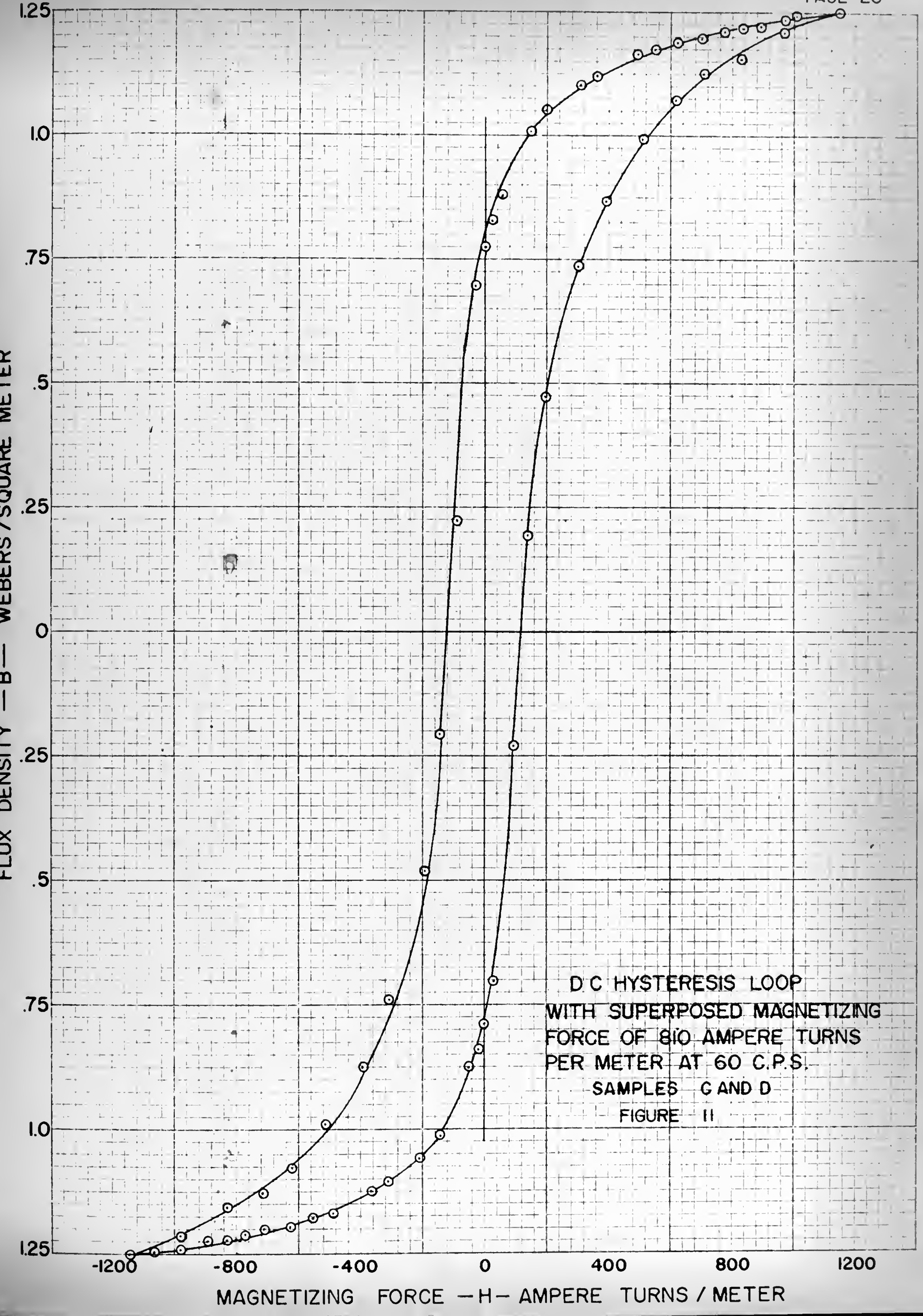

D C HYSTERESIS LOOP
WITH SUPERPOSED MAGNETIZING
FORCE OF 810 AMPERE TURNS
PER METER AT 60 C.P.S.
SAMPLES G AND D
FIGURE 11

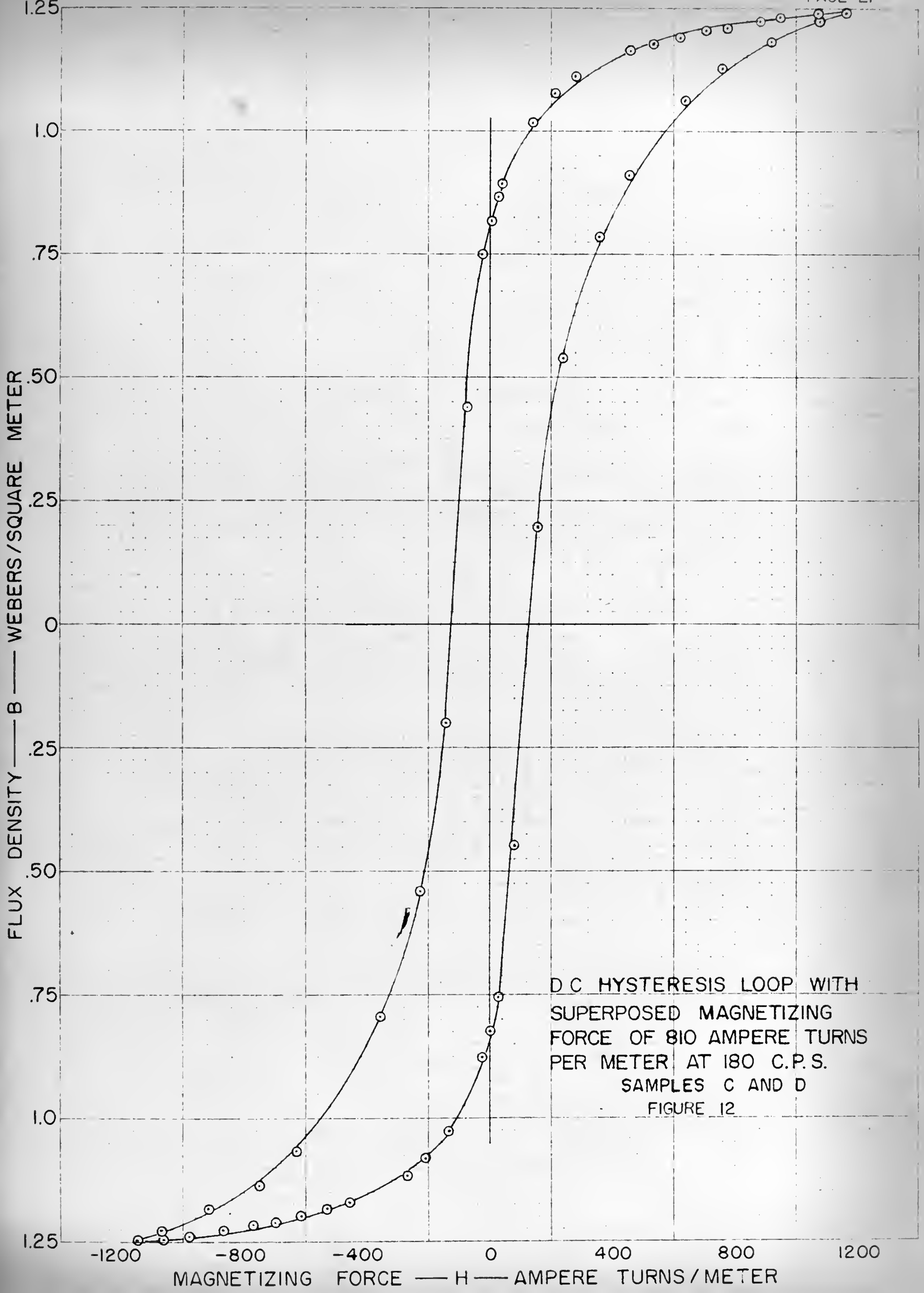

D C HYSTERESIS LOOP WITH
SUPERPOSED MAGNETIZING
FORCE OF 810 AMPERE TURNS
PER METER AT 180 C.P.S.
SAMPLES C AND D
FIGURE 12

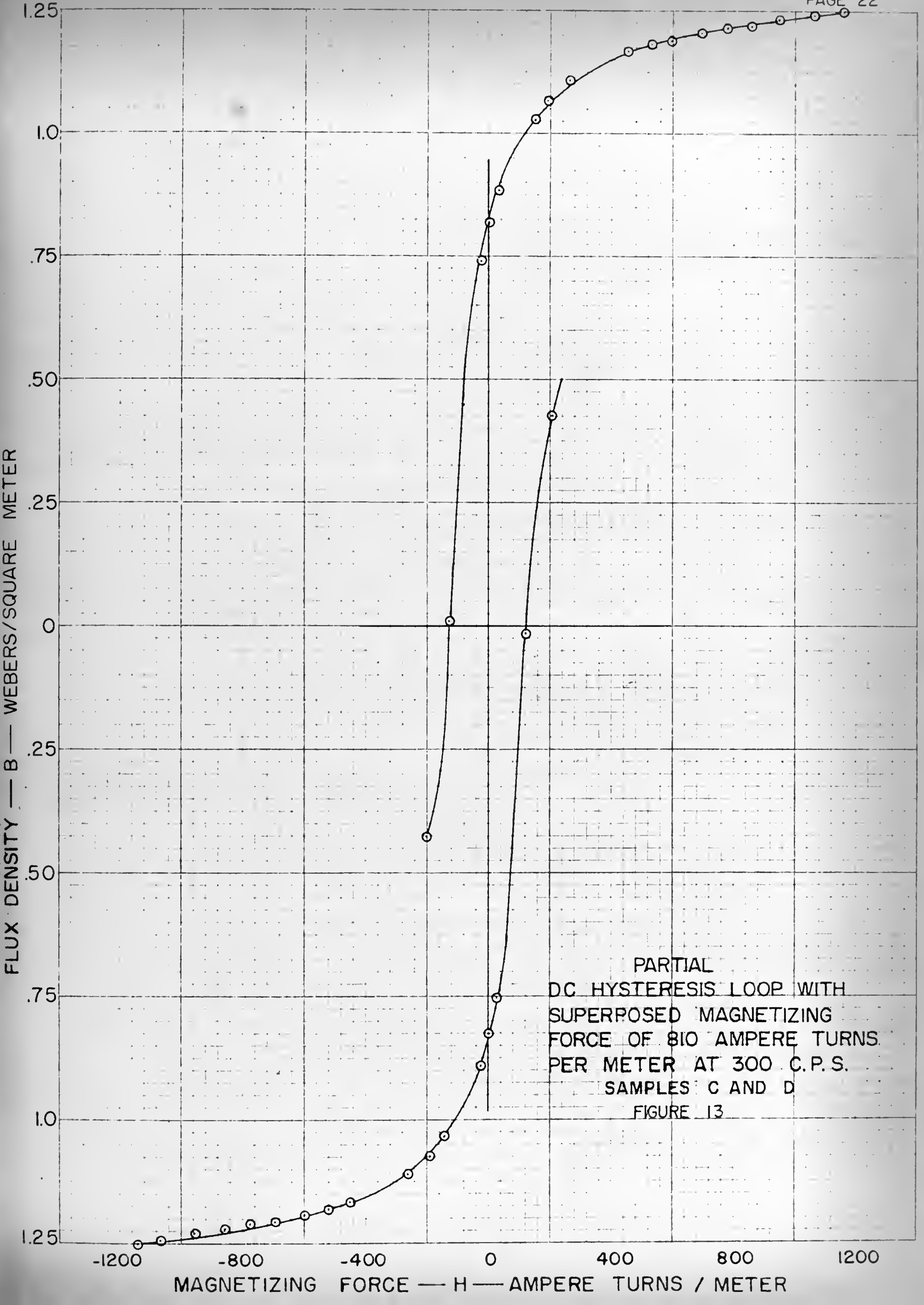

PARTIAL
DC HYSTERESIS LOOP WITH
SUPERPOSED MAGNETIZING
FORCE OF 810 AMPERE TURNS
PER METER AT 300 C.P.S.
SAMPLES C AND D
FIGURE 13

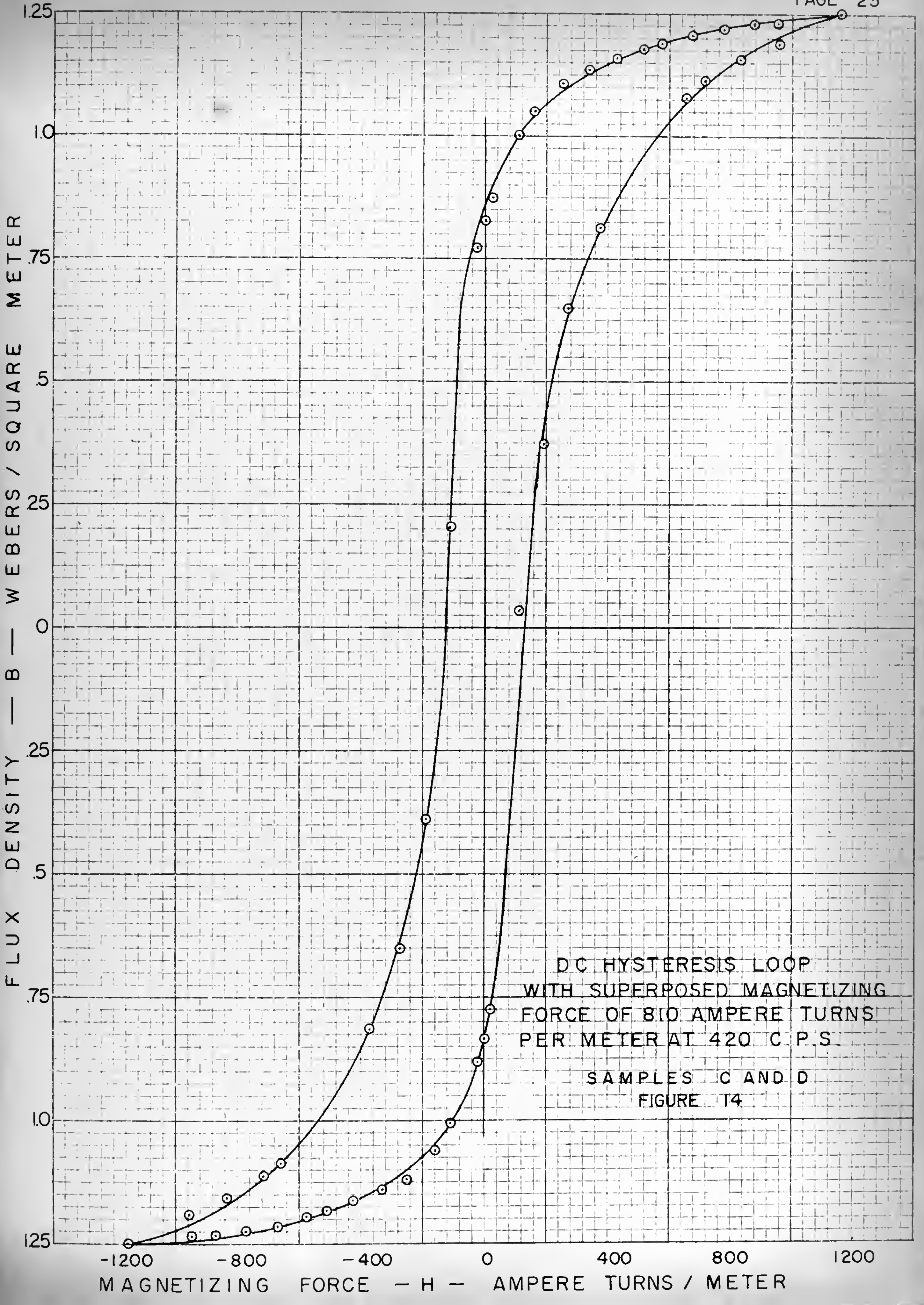

DC HYSTERESIS LOOP
WITH SUPERPOSED MAGNETIZING
FORCE OF 810 AMPERE TURNS
PER METER AT 420 C.P.S.

SAMPLES C AND D
FIGURE 14

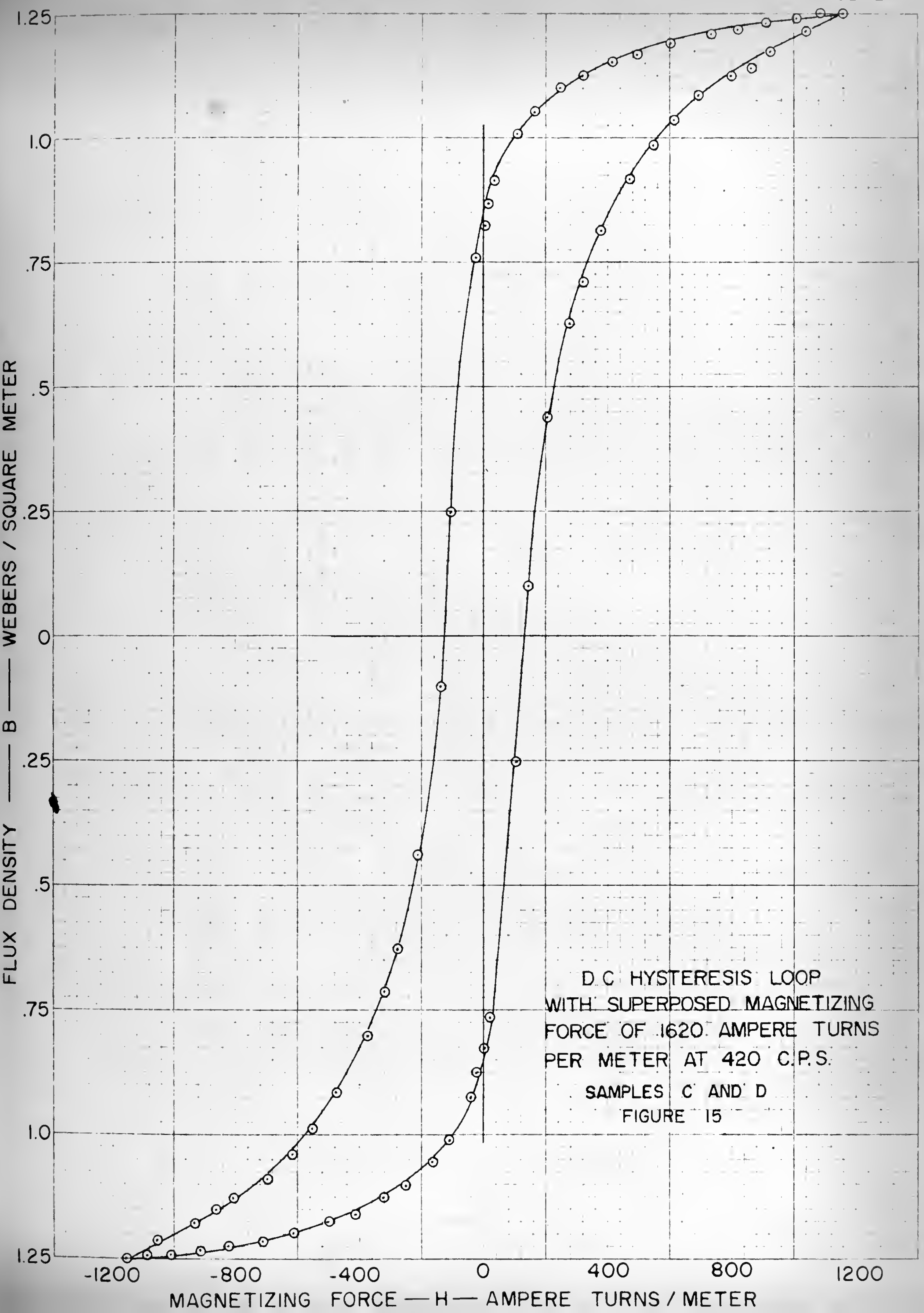

D.C. HYSTERESIS LOOP
WITH SUPERPOSED MAGNETIZING
FORCE OF 1620 AMPERE TURNS
PER METER AT 420 C.P.S.

SAMPLES C AND D

FIGURE 15

The remaining hysteresis loops, except Figures 41 through 43, to allow comparison with Figure 18, use the same D.C. maximum magnetizing force of 700 ampere-turns per meter. They are arranged in order of increasing A.C. frequencies of 28, 120, 180, 300 and 420 c.p.s. and magnitudes of 70, 175, 350, 700 and 1050 ampere-turns per meter.

Within this series of figures a number of comparisons may be made. First considering Figures 18, 19, 20, 21, 22 and 23 which is a study at 28 c.p.s. using various magnitudes of A.C. magnetizing force, it is clearly seen that the area of the hysteresis loop decreases as the magnitude of the superposed field increases.

In this series it is also clear that the point of maximum induction is markedly increased when an A.C. magnetizing force is superposed. However, when figures 19 through 23 are compared with each other it is observed that the point of maximum induction does not change which means that the change in maximum induction is apparently independent of the magnitude of the superposed A.C. magnetizing force.

Also, if Figures 19 through 23 are compared with Figures 24 through 39, it is observed that the change in the point of maximum induction is independent of the frequency of the superposed A.C. magnetizing force.

Considering again the series of Figures 18 through 23, it is observed that the slope of the hysteresis loop is substantially increased when a superposed A.C. magnetizing force

is impressed. It is also seen that the slope slightly decreases as the magnitude of the superposed field is increased. This is also observed in the series of Figures 27 through 32 where the frequency is 420 c.p.s. If it may be allowed that the slope of the hysteresis loop is an indication of the apparent permeability, from the above it may be inferred that the permeability first increases and then decreases as the magnitude of the superposed field is increased.

Next, to observe the effect of a variation of the frequency of the superposed field, Figures 22, 25, 26, 31, 34 and 39 may be compared. These figures form a series of hysteresis loops with a constant maximum magnitude magnetizing force of various frequencies superposed. The frequencies used were 28, 60, 120, 180, 300 and 420 at a maximum magnitude of 700 ampere-turns per meter. There is no consistent detectable change in the hysteresis loops as the frequency changes.

By comparing Figure 18 with Figures 19 through 40 it is seen that the residual magnetism and the coercive force decrease as the magnitude of the superposed field increases. When a series of hysteresis loops where the frequency alone changes, is studied, such as the series of Figures 19, 24, 27, 33 and 35, it is observed that the change in the residual magnetism and coercive force is independent of the frequency of the superposed field.

Figures 41 through 43 form a separate limited study with a higher D.C. magnetizing force of 1400 ampere-turns per meter. Figure 41 is a D.C. hysteresis loop with no A.C. field superposed. Figures 42 and 43 show the effect of varying the frequency of the superposed magnetizing force at a constant maximum magnitude of 700 ampere-turns per meter. The results obtained from this study are in agreement with results previously obtained from Figures 18 through 40.

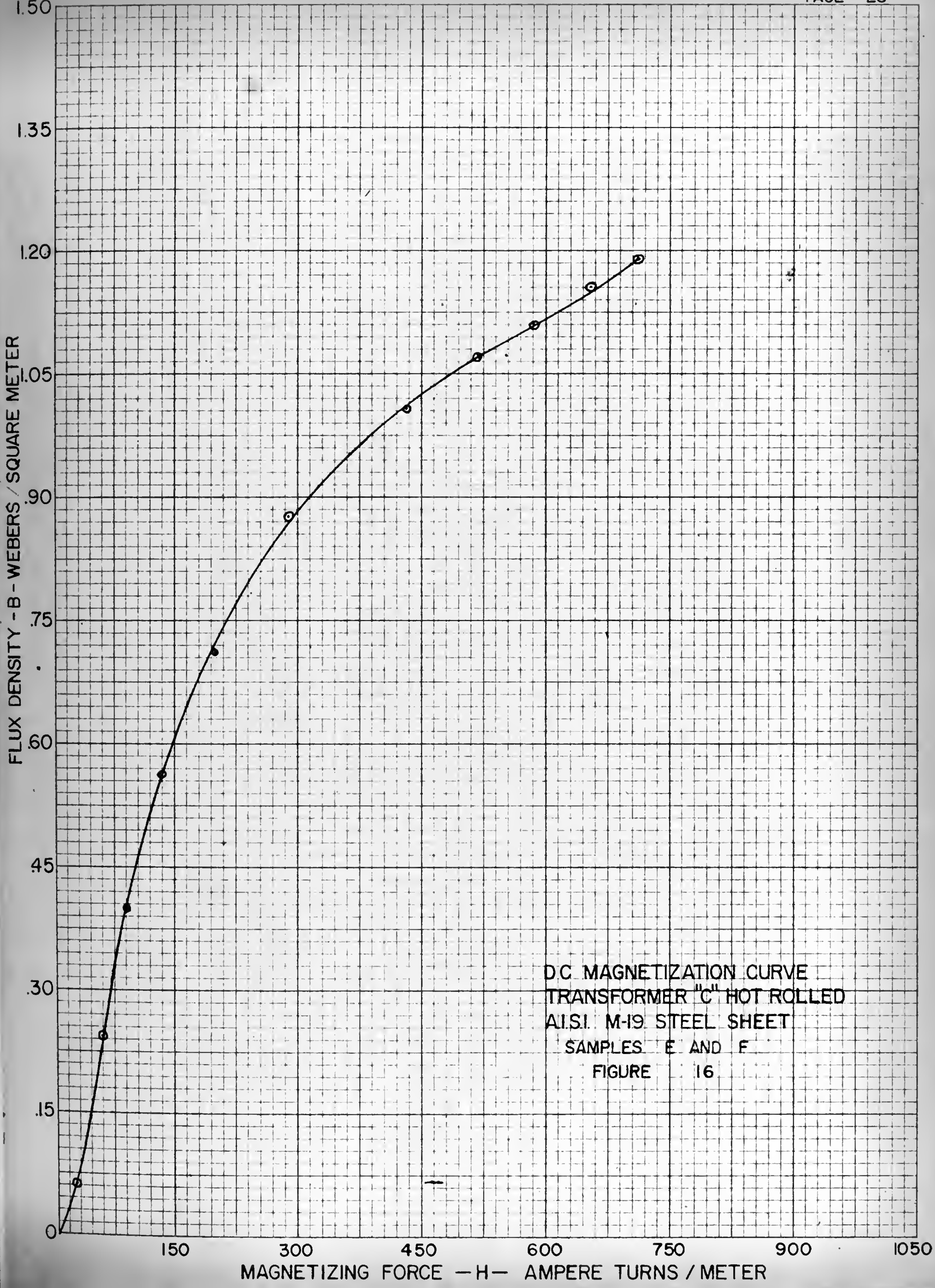

D.C. MAGNETIZATION CURVE
TRANSFORMER "C" HOT ROLLED
A.I.S.I. M-19 STEEL SHEET
SAMPLES E AND F
FIGURE 16

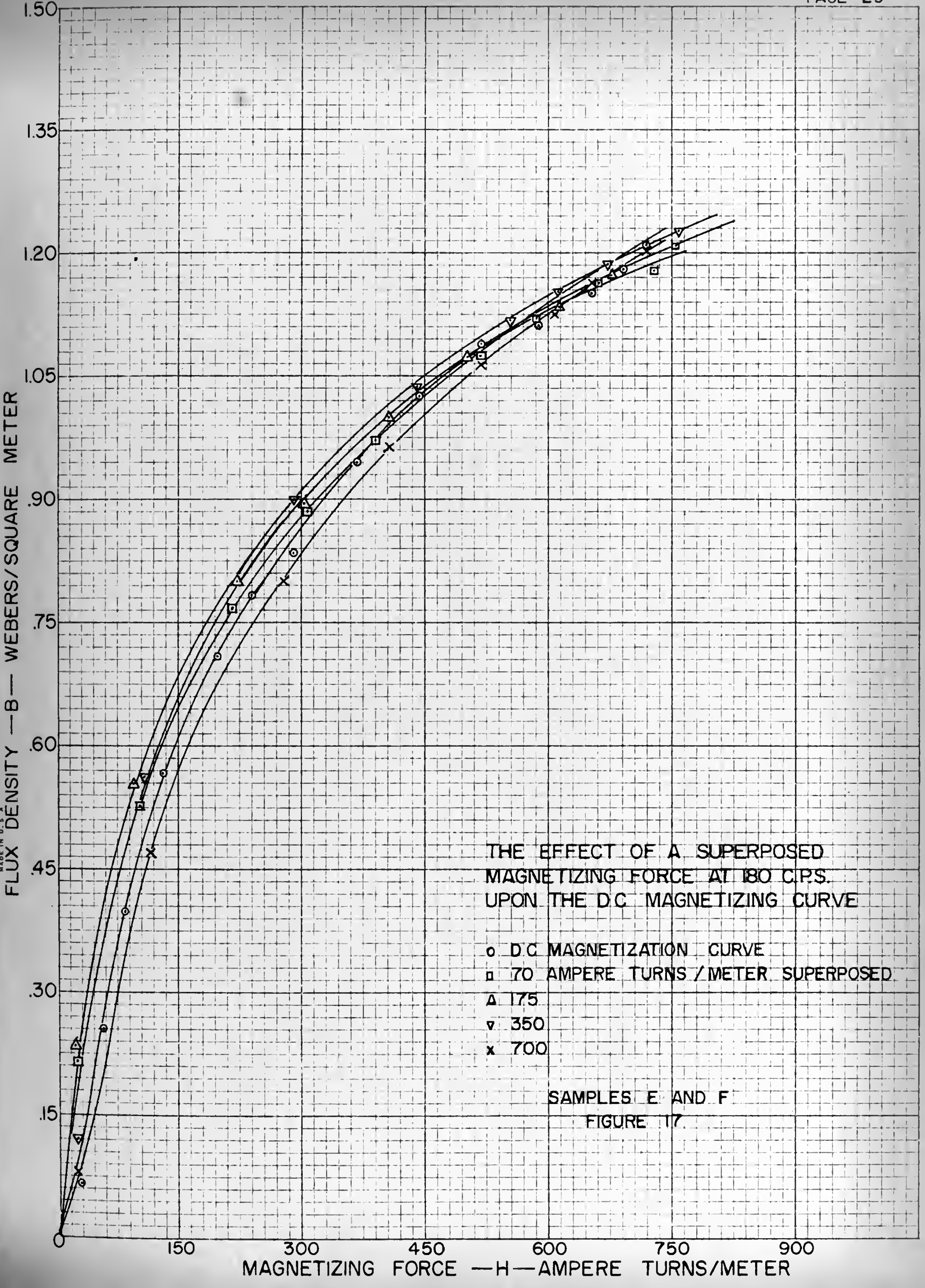

THE EFFECT OF A SUPERPOSED MAGNETIZING FORCE AT 180 C.P.S. UPON THE D.C. MAGNETIZING CURVE

SAMPLES E AND F
FIGURE 17

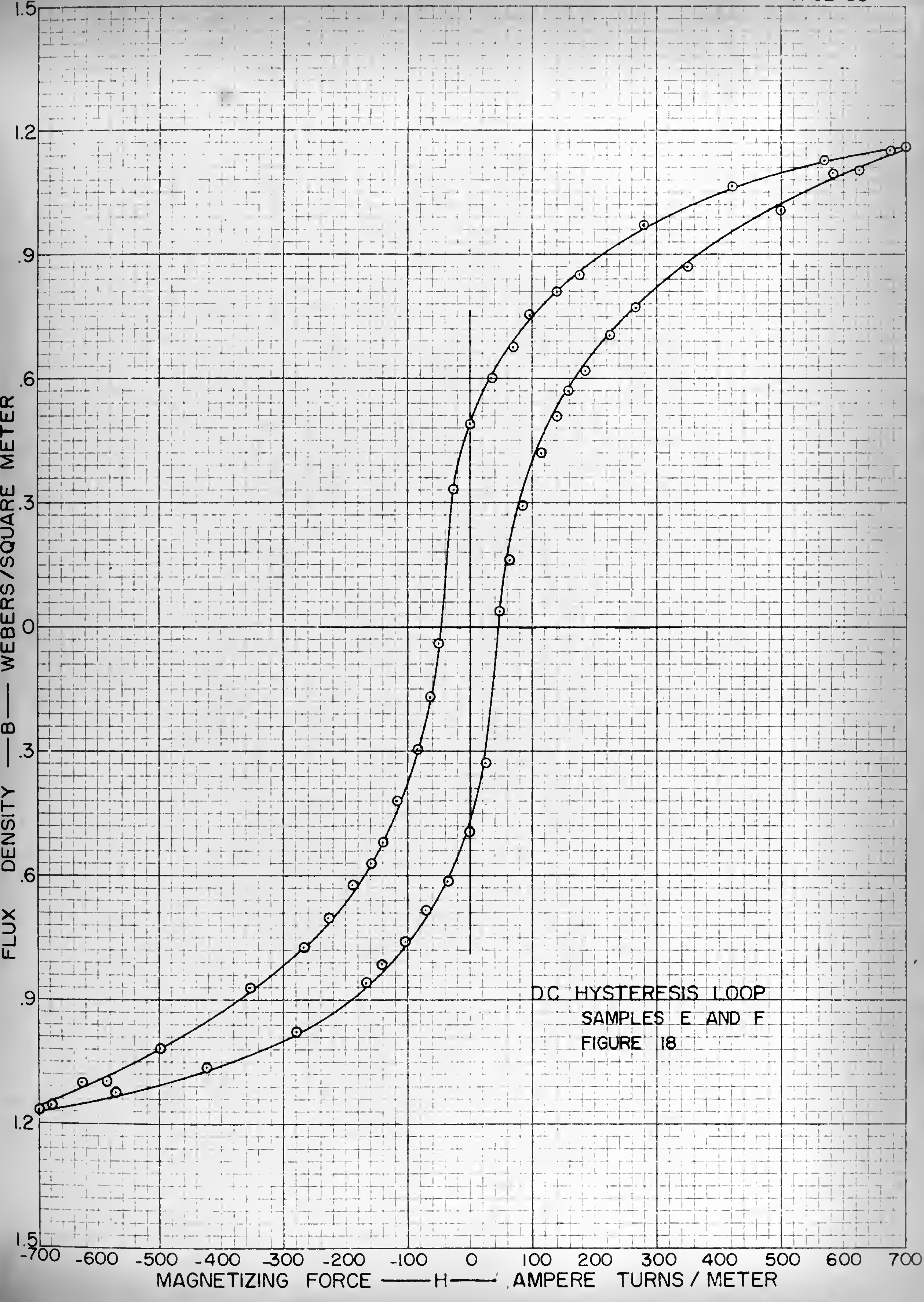

DC HYSTERESIS LOOP
SAMPLES E AND F
FIGURE 18

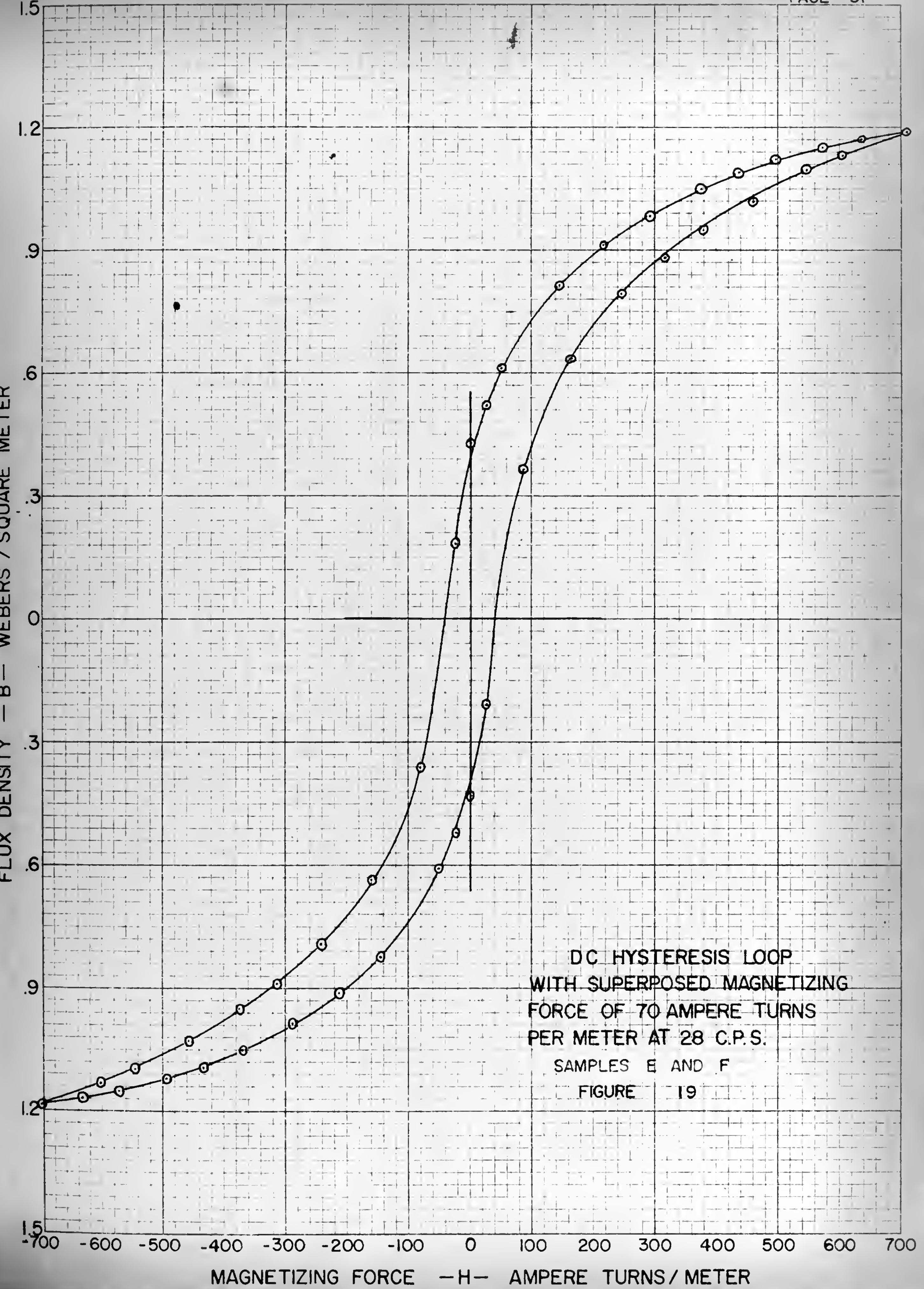

DC HYSTERESIS LOOP
WITH SUPERPOSED MAGNETIZING
FORCE OF 70 AMPERE TURNS
PER METER AT 28 C.P.S.
SAMPLES E AND F
FIGURE 19

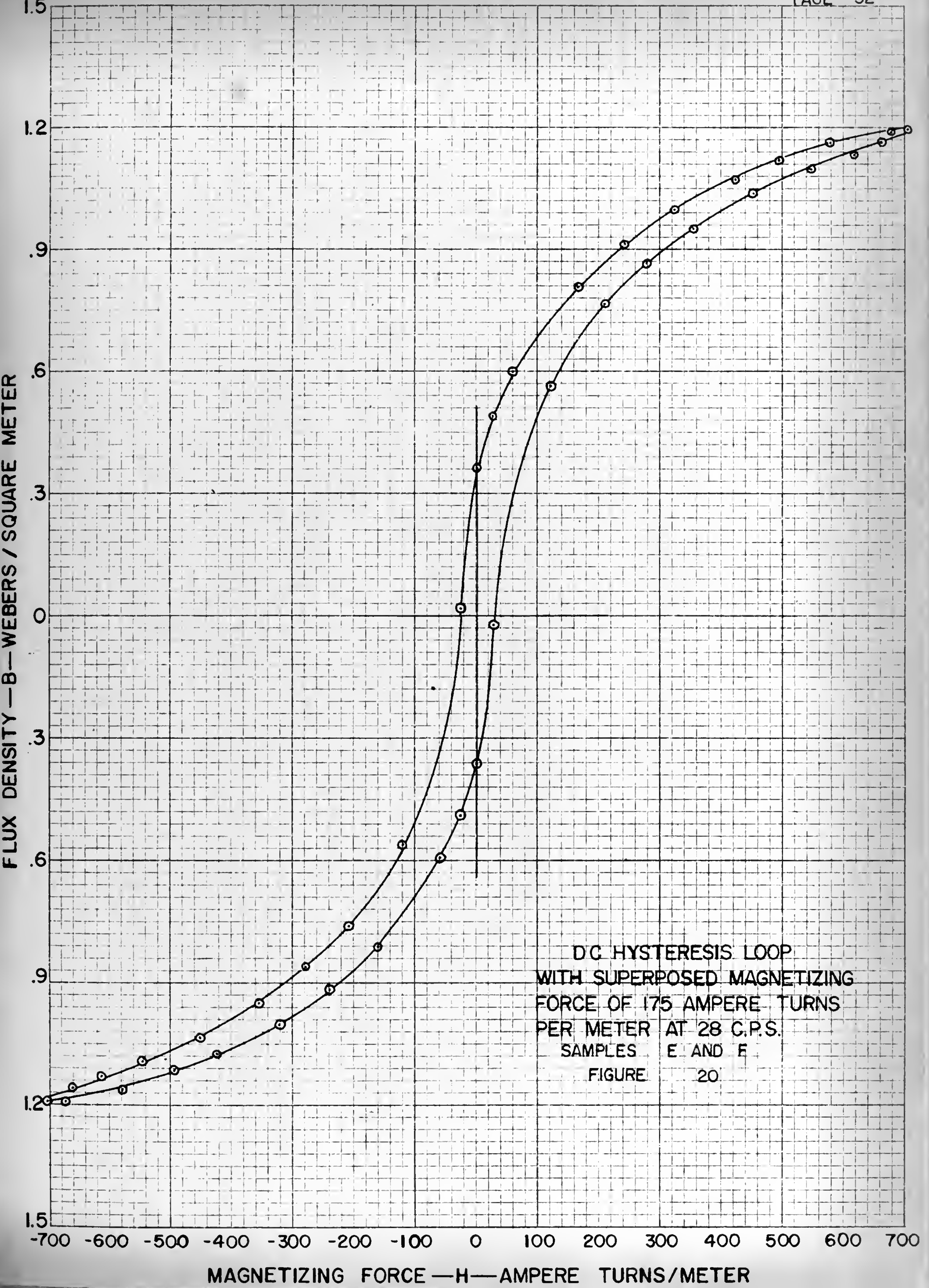

DC HYSTERESIS LOOP
WITH SUPERPOSED MAGNETIZING
FORCE OF 175 AMPERE TURNS
PER METER AT 28 C.P.S.
SAMPLES E AND F
FIGURE 20

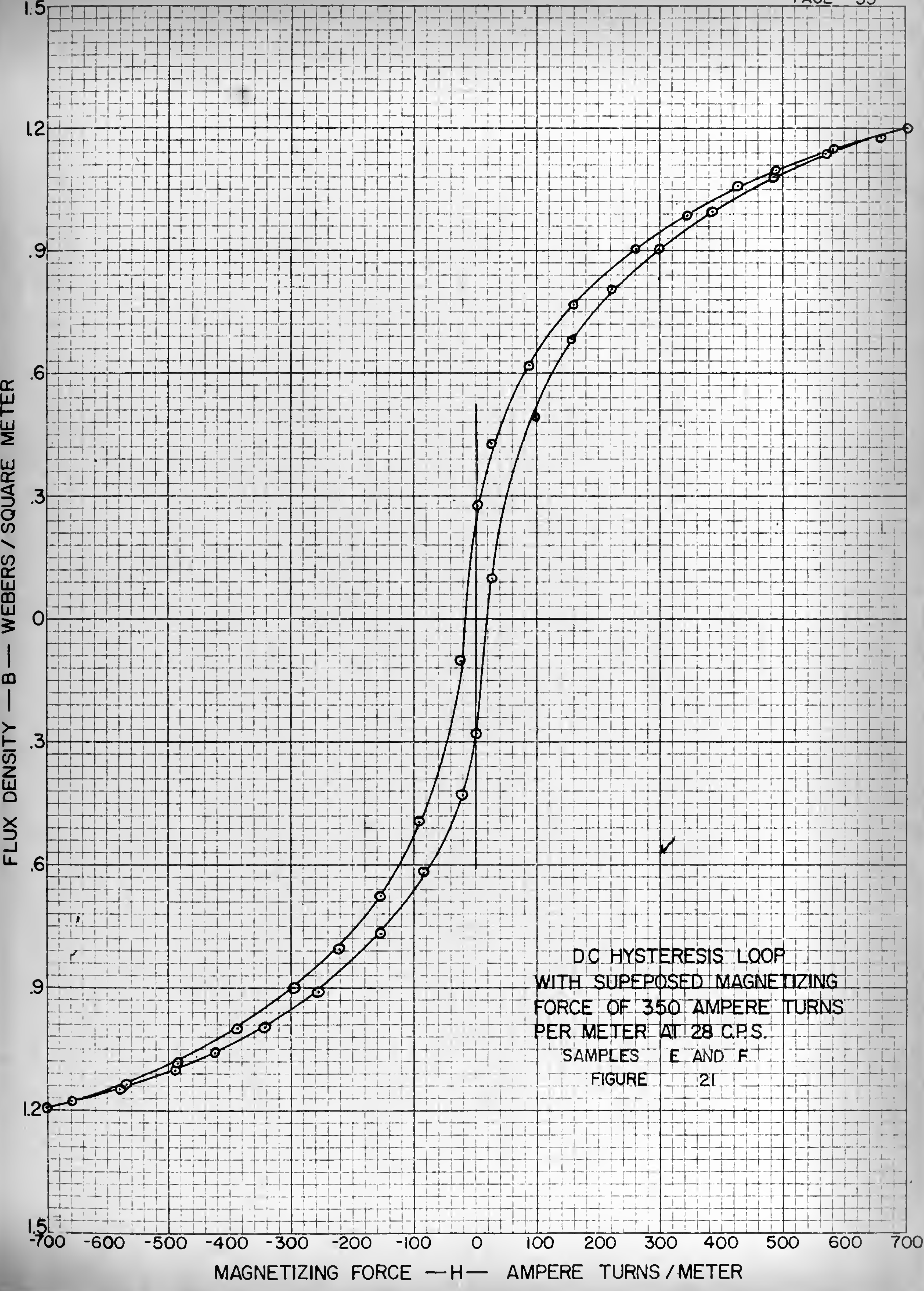

D.C HYSTERESIS LOOP
WITH SUPEPOSED MAGNETIZING
FORCE OF 350 AMPERE TURNS
PER METER AT 28 C.P.S.
SAMPLES E AND F
FIGURE 21

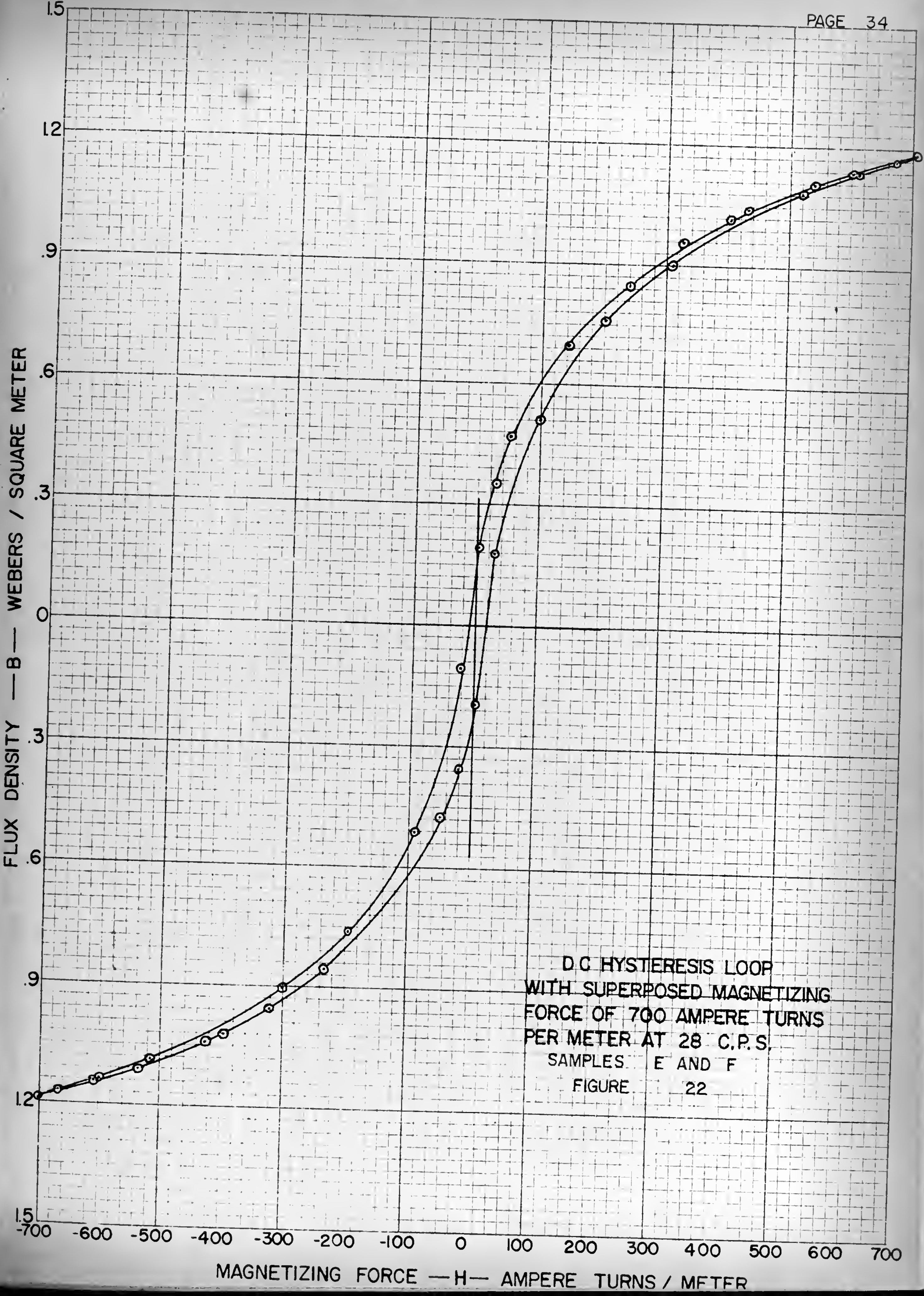

D C HYSTERESIS LOOP
WITH SUPERPOSED MAGNETIZING
FORCE OF 700 AMPERE TURNS
PER METER AT 28 C.P.S.
SAMPLES E AND F
FIGURE 22

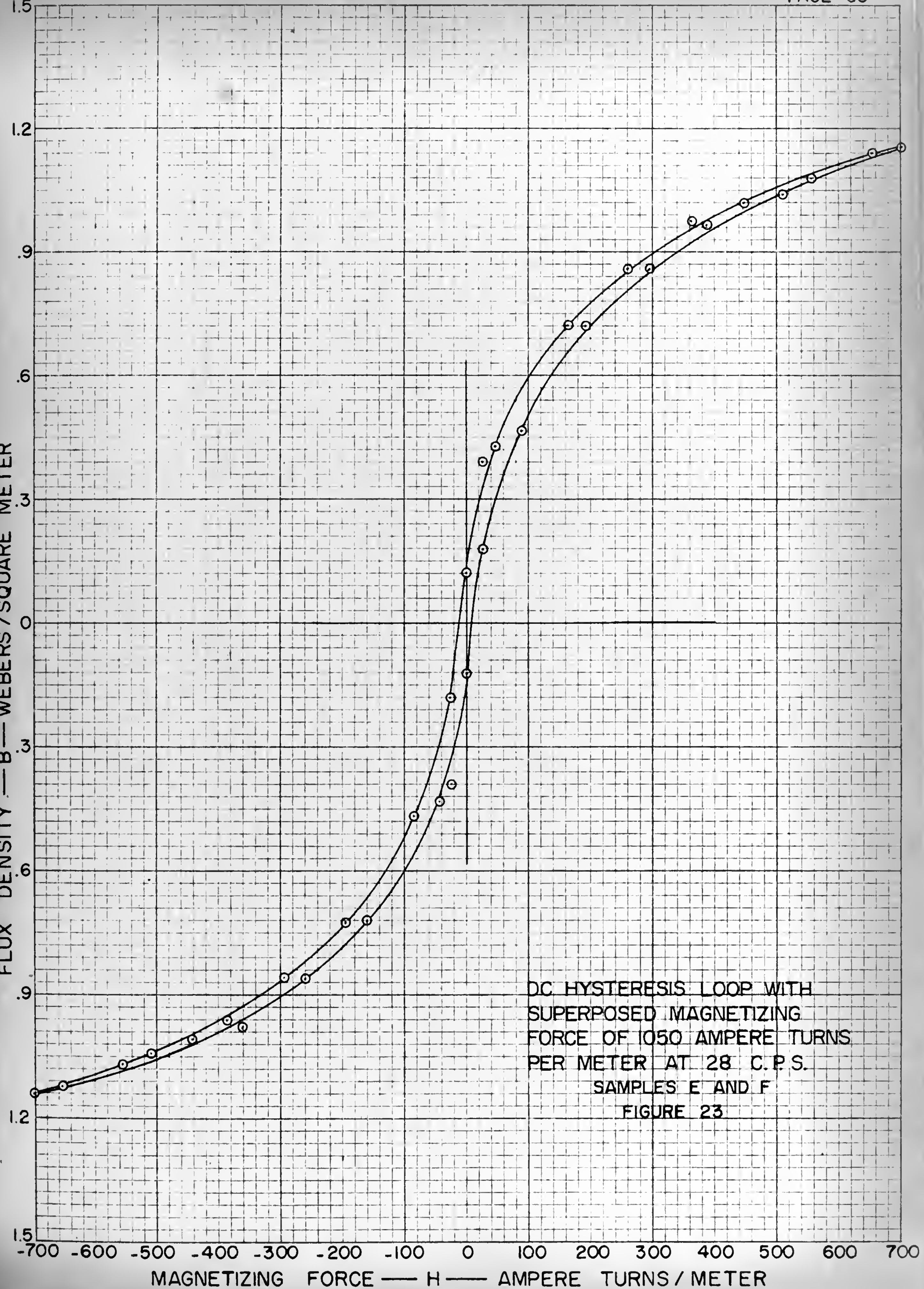

DC HYSTERESIS LOOP WITH
SUPERPOSED MAGNETIZING
FORCE OF 1050 AMPERE TURNS
PER METER AT 28 C.P.S.
SAMPLES E AND F
FIGURE 23

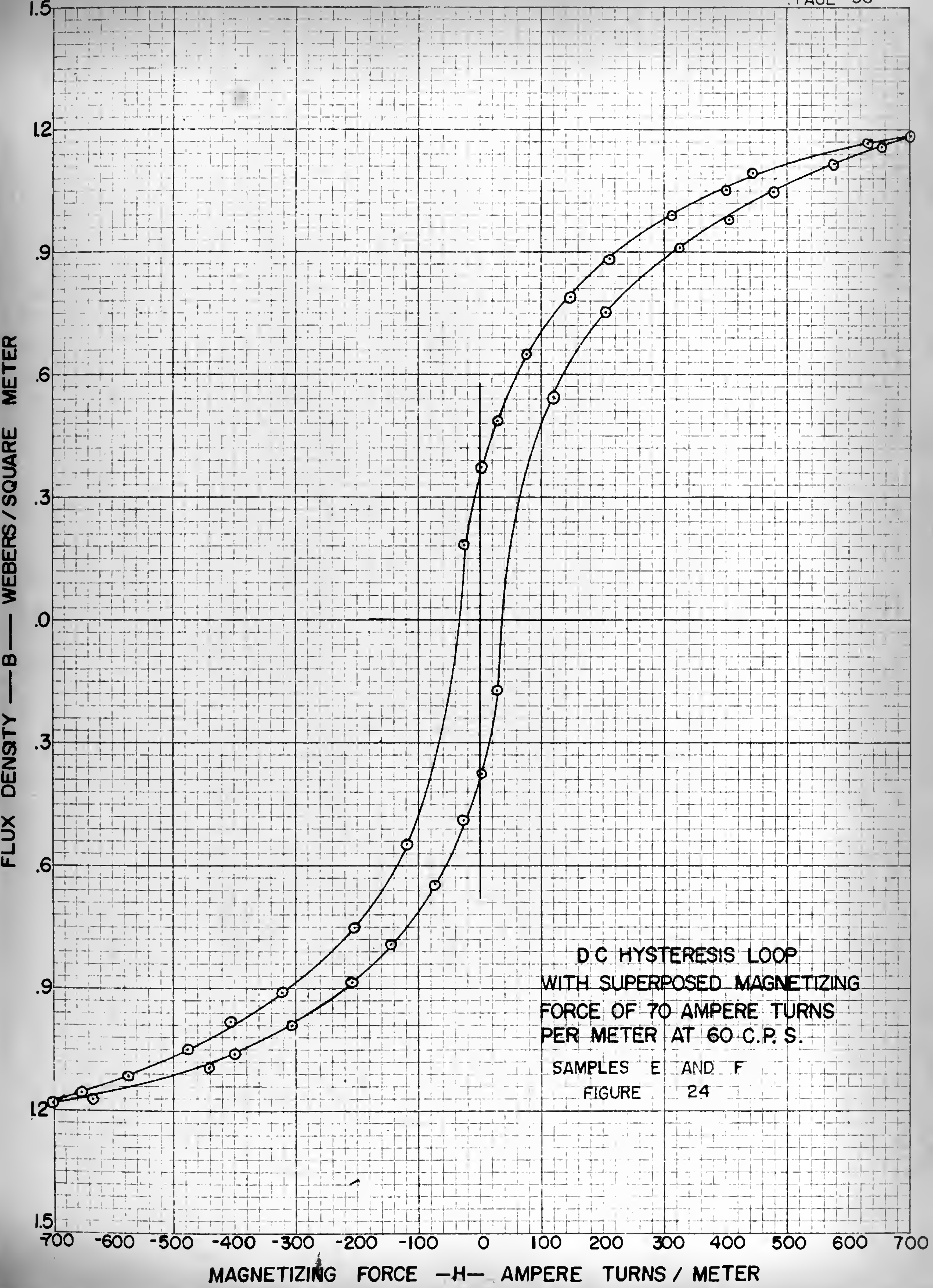

D C HYSTERESIS LOOP
WITH SUPERPOSED MAGNETIZING
FORCE OF 70 AMPERE TURNS
PER METER AT 60 C.P. S.

SAMPLES E AND F
FIGURE 24

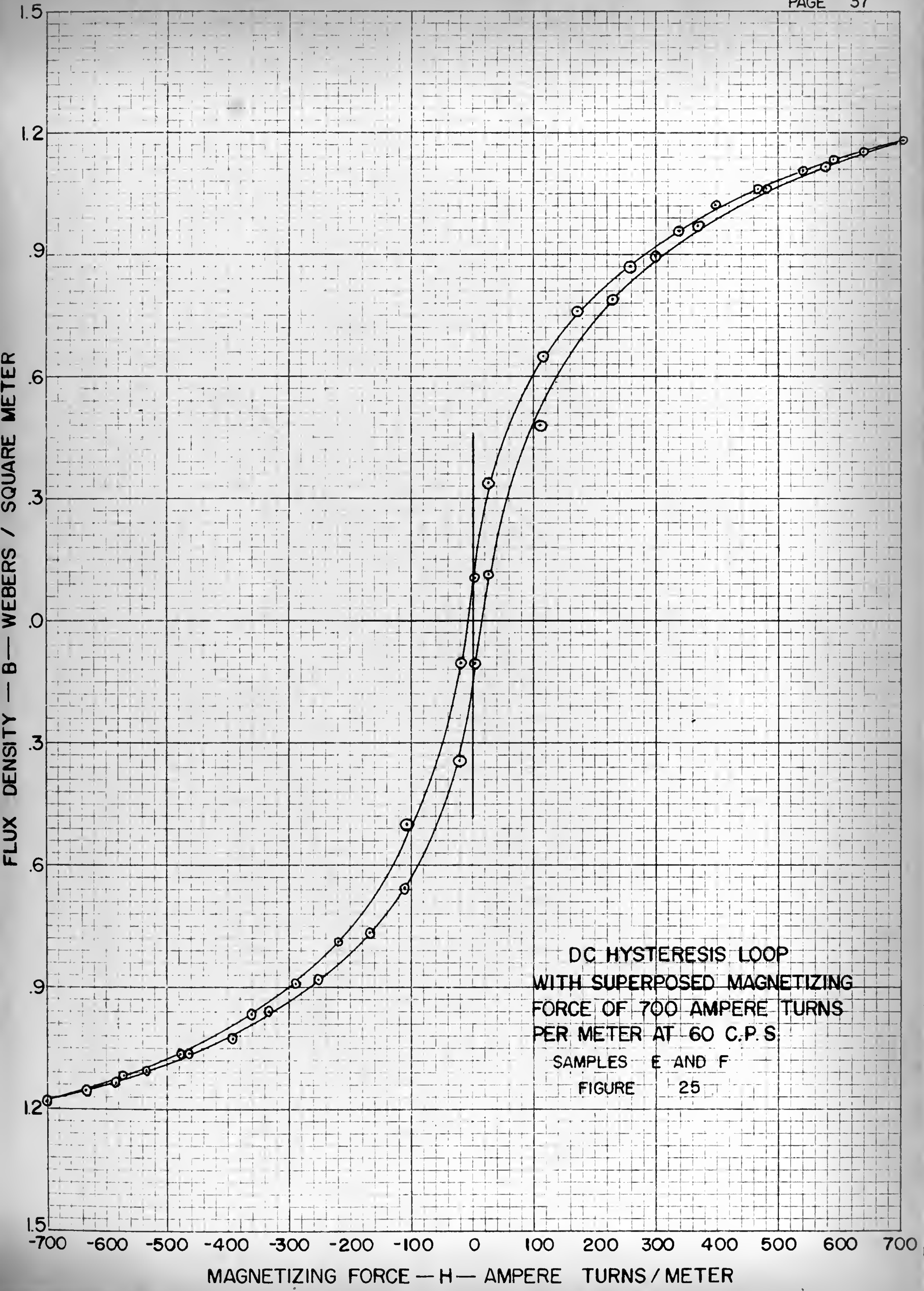

DC HYSTERESIS LOOP
WITH SUPERPOSED MAGNETIZING
FORCE OF 700 AMPERE TURNS
PER METER AT 60 C.P.S.
SAMPLES E AND F
FIGURE 25

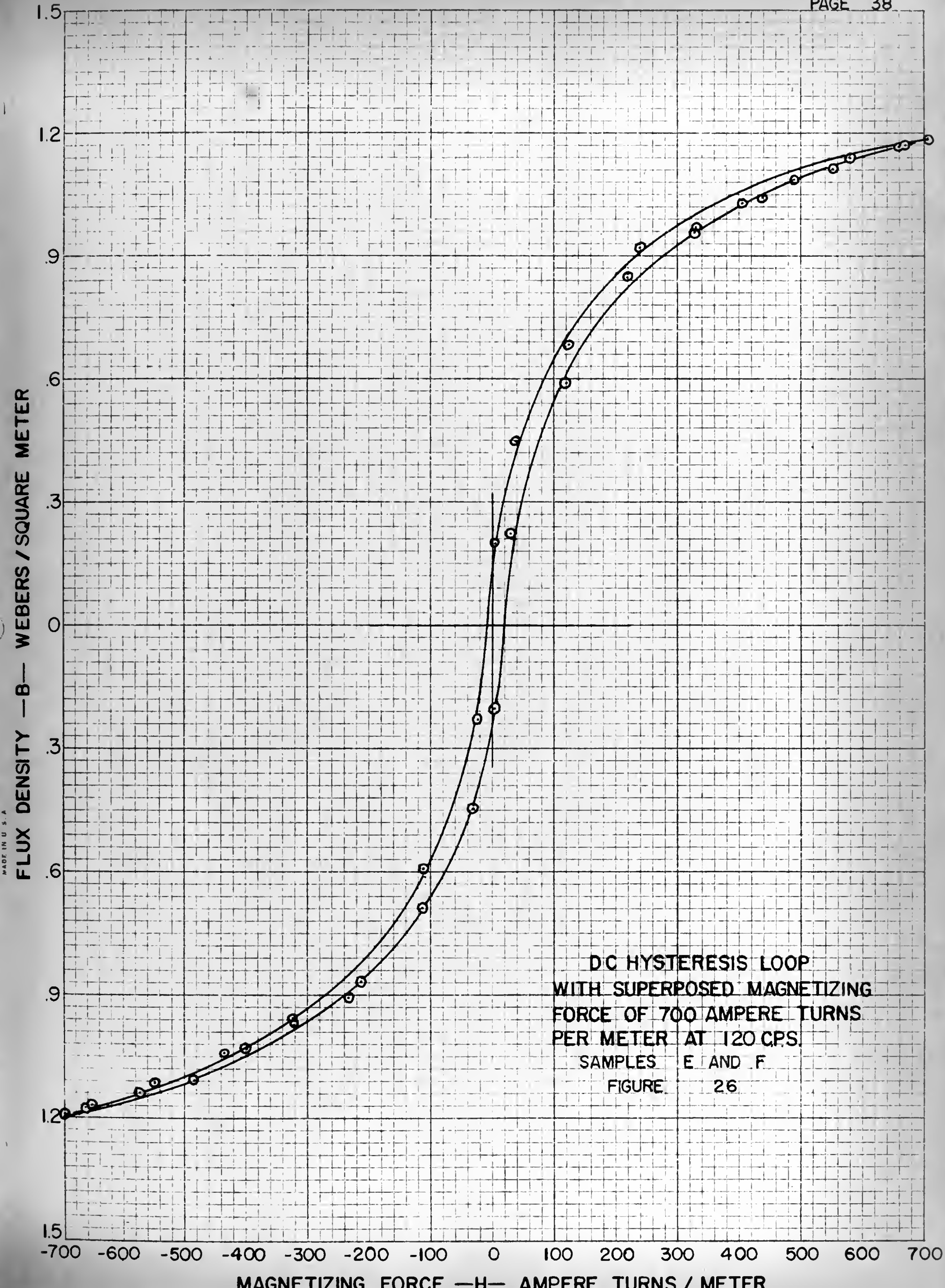

DC HYSTERESIS LOOP
WITH SUPERPOSED MAGNETIZING
FORCE OF 700 AMPERE TURNS
PER METER AT 120 C.P.S.
SAMPLES E AND F
FIGURE 26

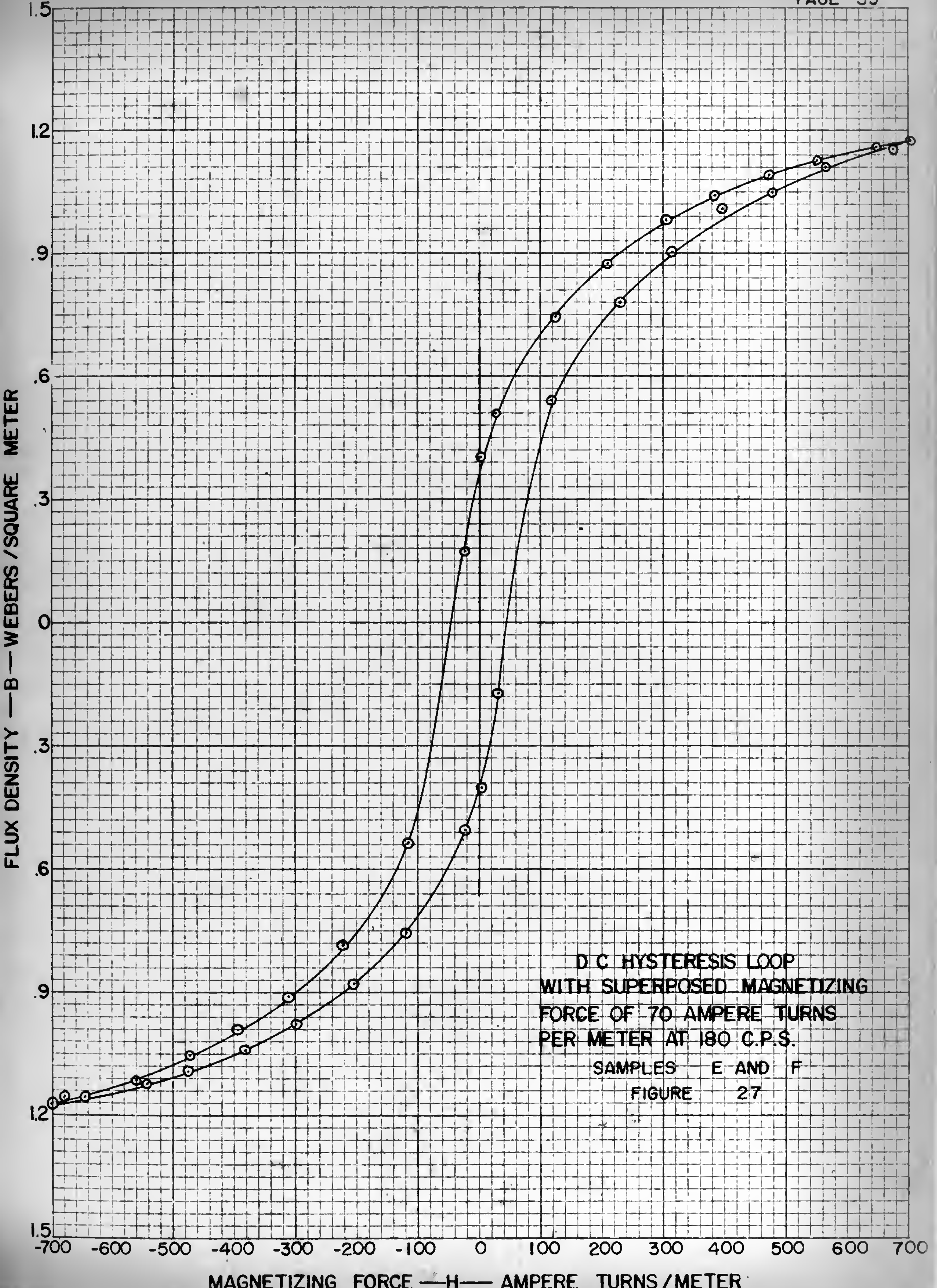

D C HYSTERESIS LOOP
WITH SUPERPOSED MAGNETIZING
FORCE OF 70 AMPERE TURNS
PER METER AT 180 C.P.S.
SAMPLES E AND F
FIGURE 27

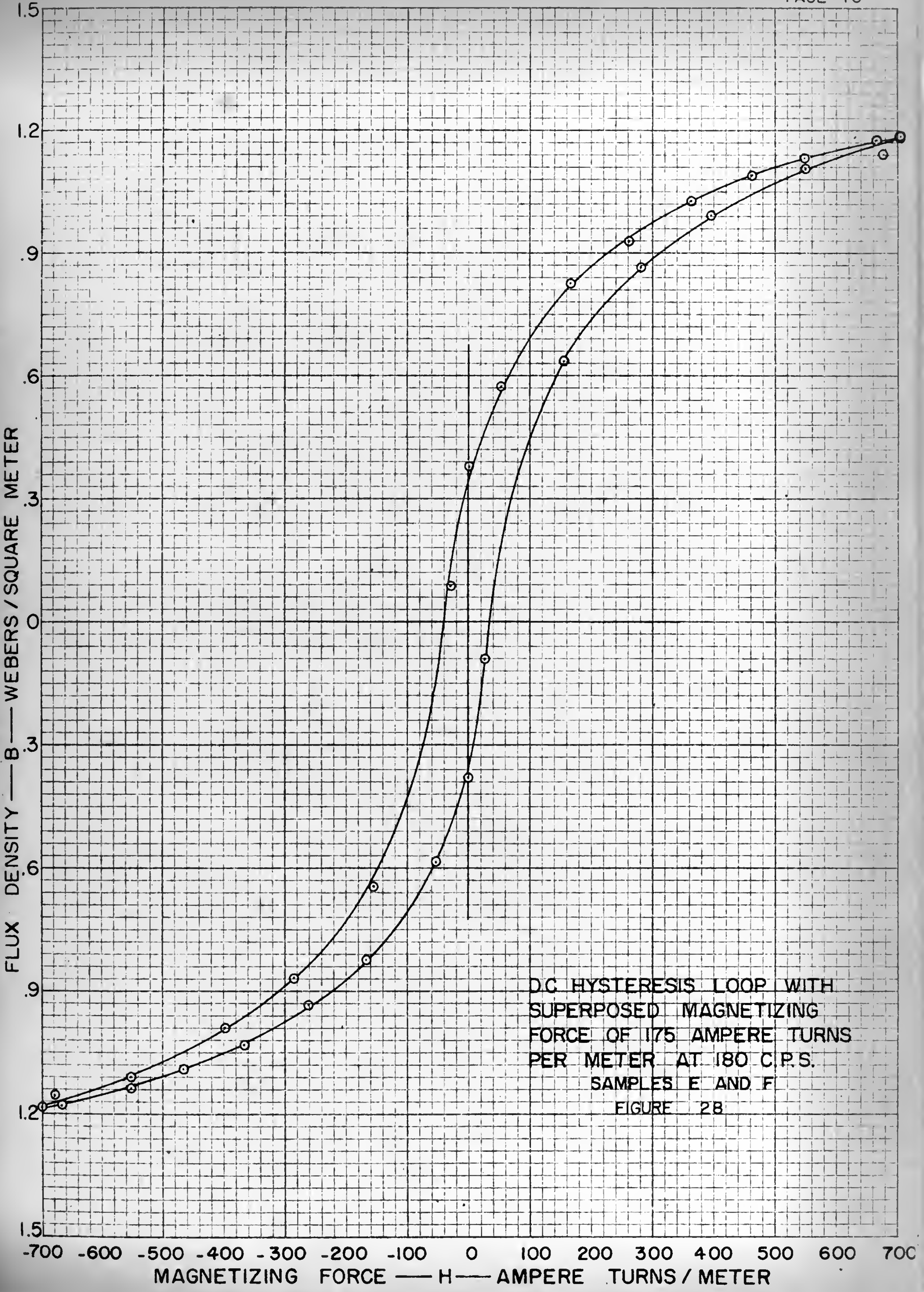

D.C HYSTERESIS LOOP WITH SUPERPOSED MAGNETIZING FORCE OF 175 AMPERE TURNS PER METER AT 180 C.P.S.

SAMPLES E AND F

FIGURE 28

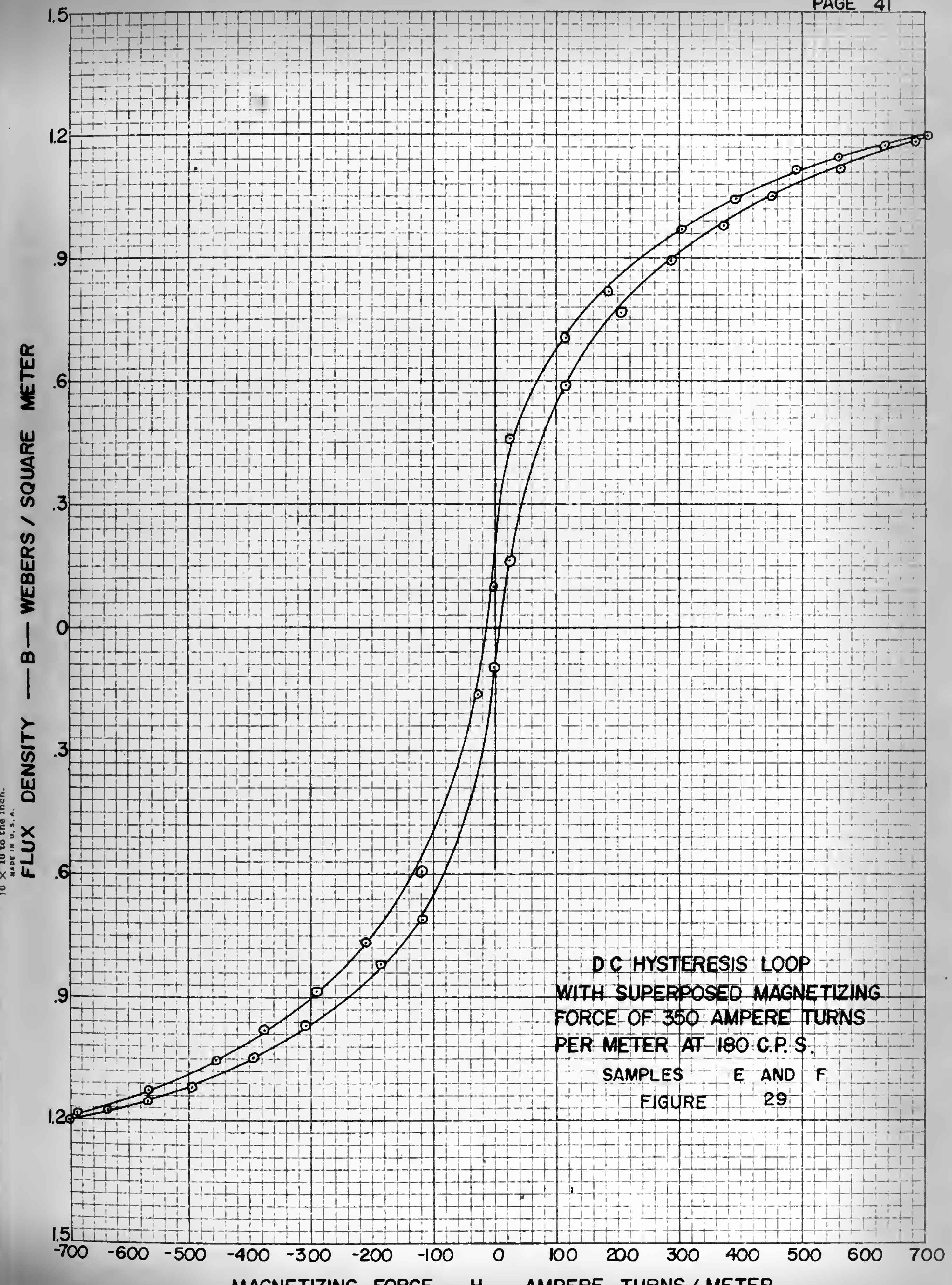

D C HYSTERESIS LOOP
WITH SUPERPOSED MAGNETIZING
FORCE OF 350 AMPERE TURNS
PER METER AT 180 C.P.S.
SAMPLES E AND F
FIGURE 29

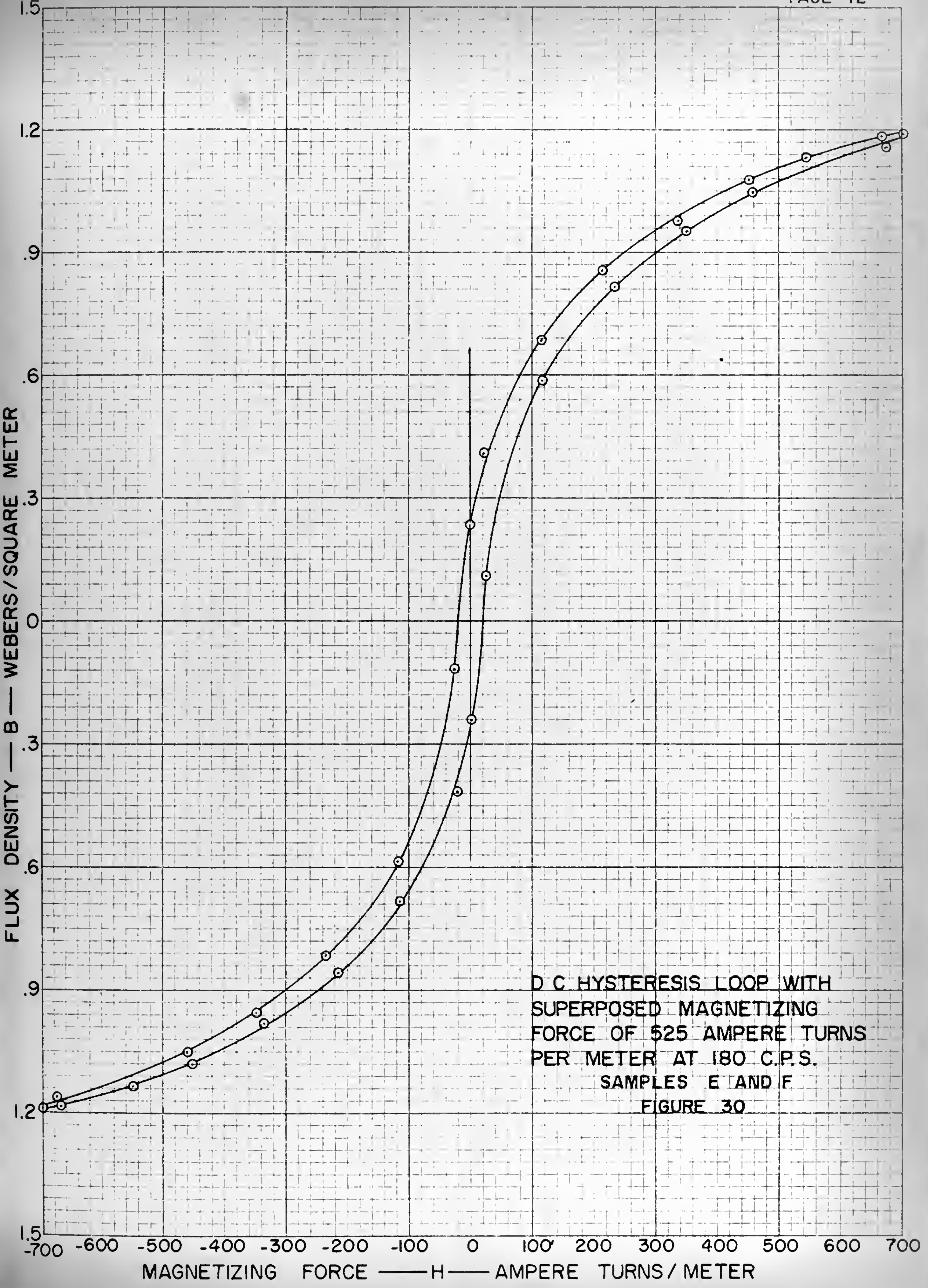

D C HYSTERESIS LOOP WITH
SUPERPOSED MAGNETIZING
FORCE OF 525 AMPERE TURNS
PER METER AT 180 C.P.S.
SAMPLES E AND F
FIGURE 30

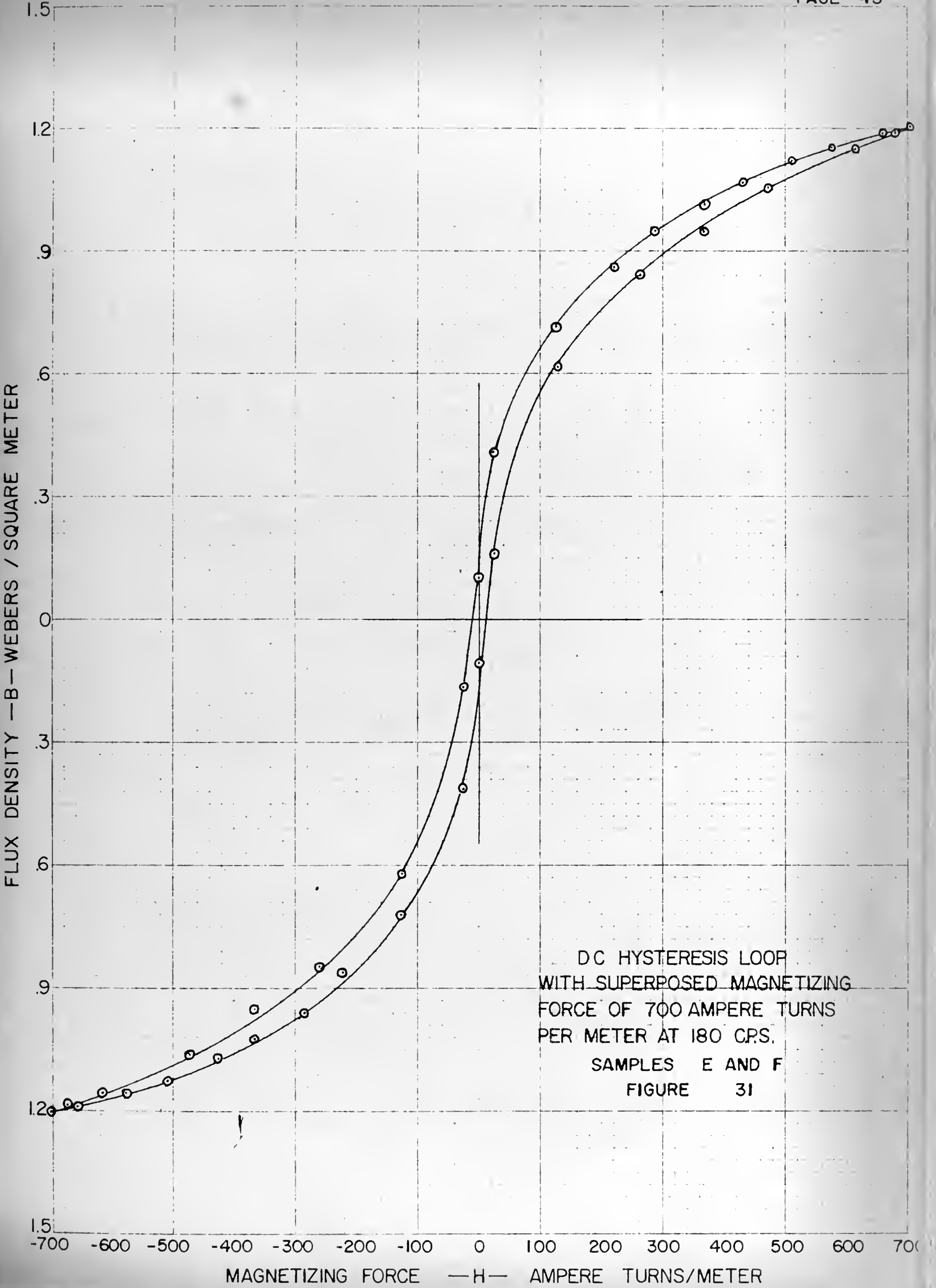

DC HYSTERESIS LOOP
WITH SUPERPOSED MAGNETIZING
FORCE OF 700 AMPERE TURNS
PER METER AT 180 CPS.
SAMPLES E AND F
FIGURE 31

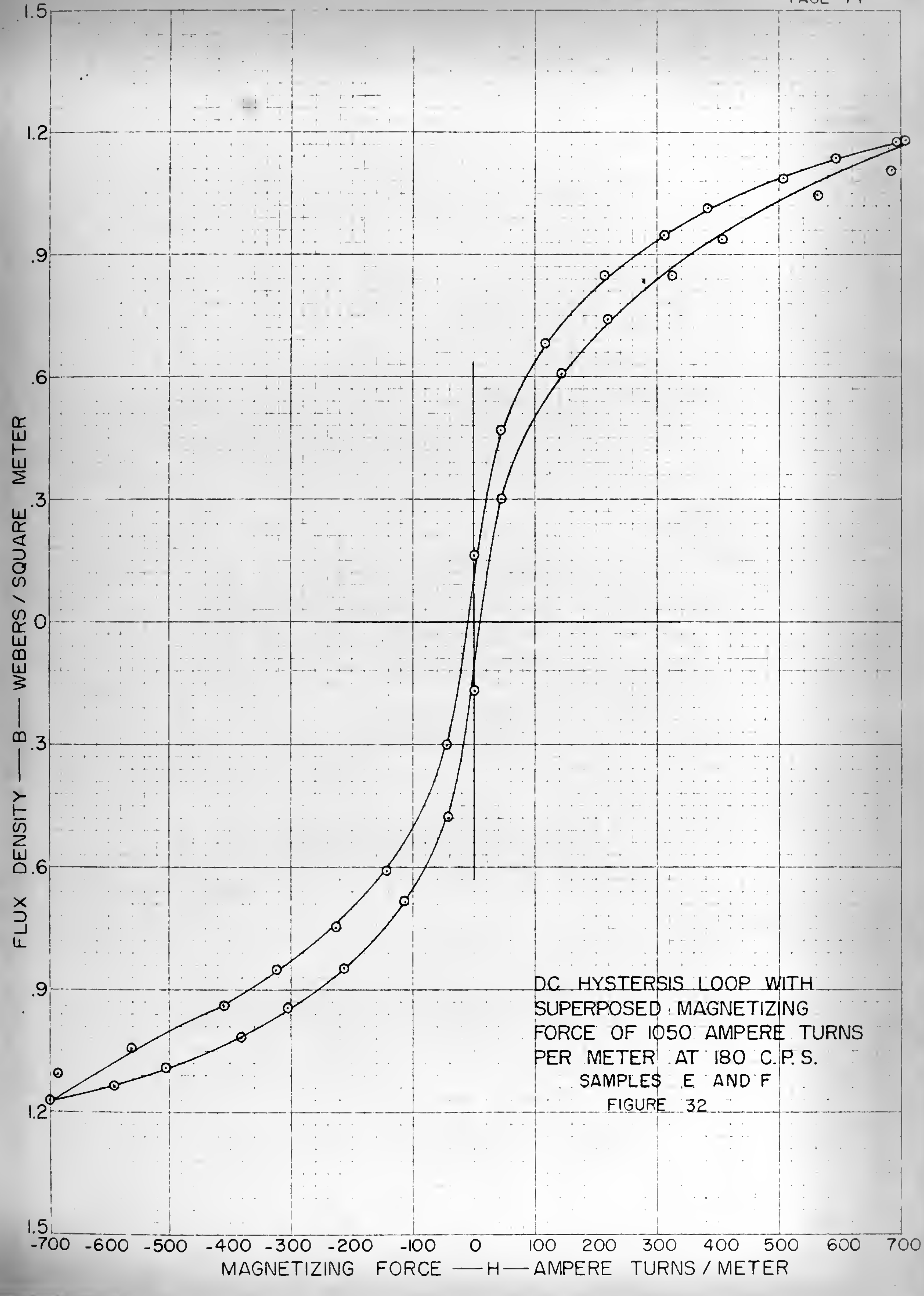

DC HYSTERSIS LOOP WITH
SUPERPOSED MAGNETIZING
FORCE OF 1050 AMPERE TURNS
PER METER AT 180 C.P.S.
SAMPLES E AND F
FIGURE 32

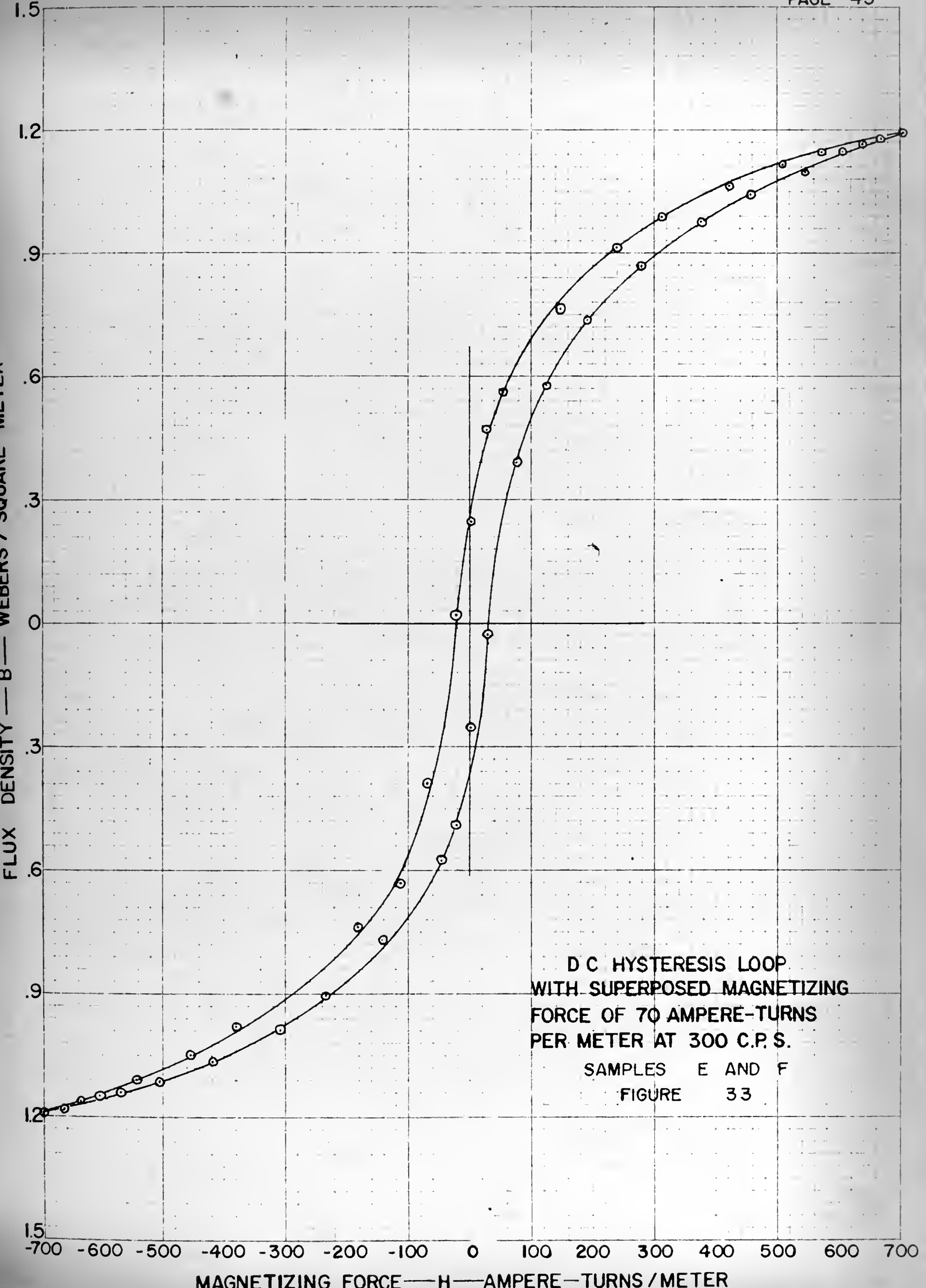

D C HYSTERESIS LOOP
WITH SUPERPOSED MAGNETIZING
FORCE OF 70 AMPERE-TURNS
PER METER AT 300 C.P.S.
SAMPLES E AND F
FIGURE 33

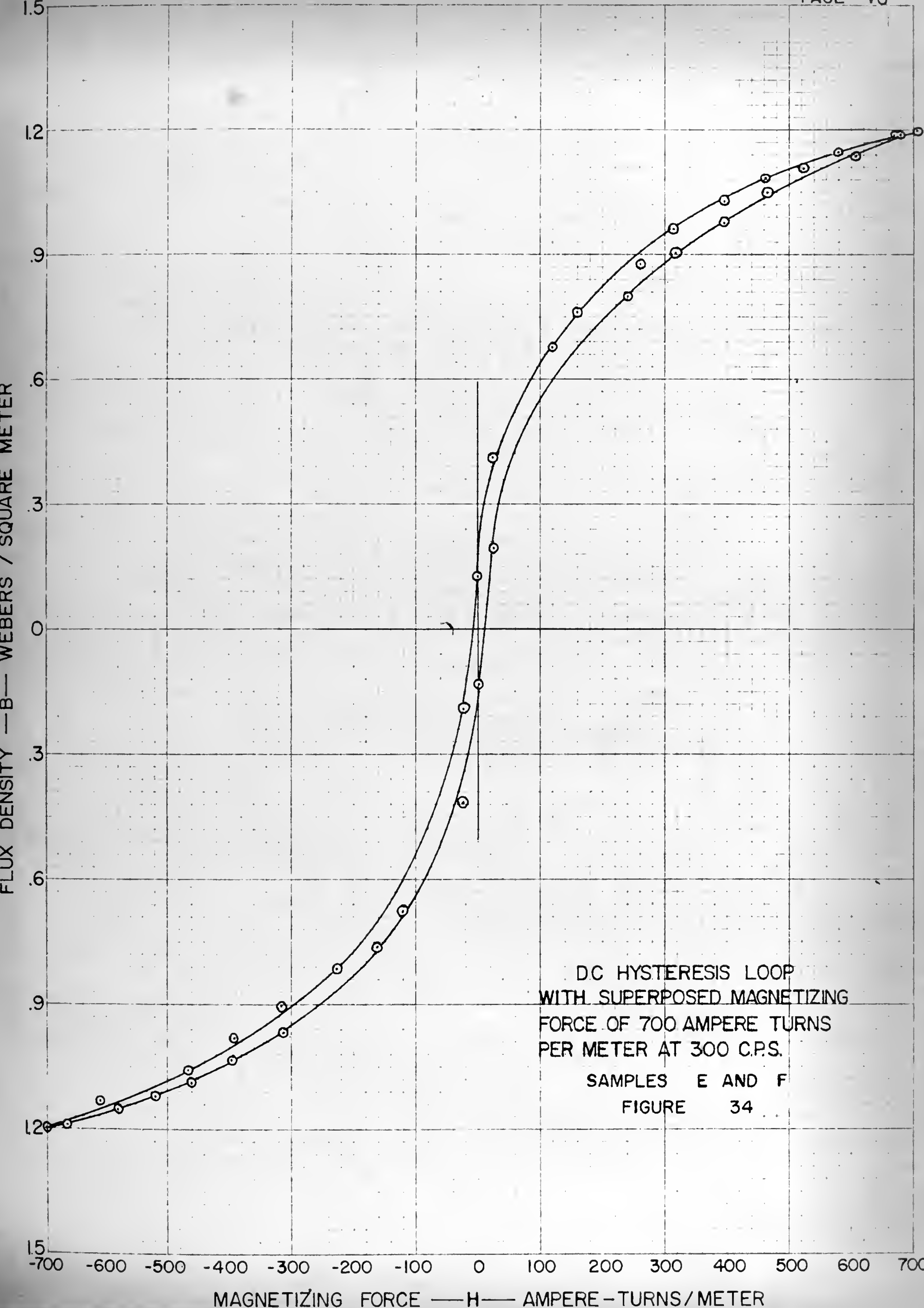

D.C HYSTERESIS LOOP
WITH SUPERPOSED MAGNETIZING
FORCE OF 700 AMPERE TURNS
PER METER AT 300 C.P.S.
SAMPLES E AND F
FIGURE 34

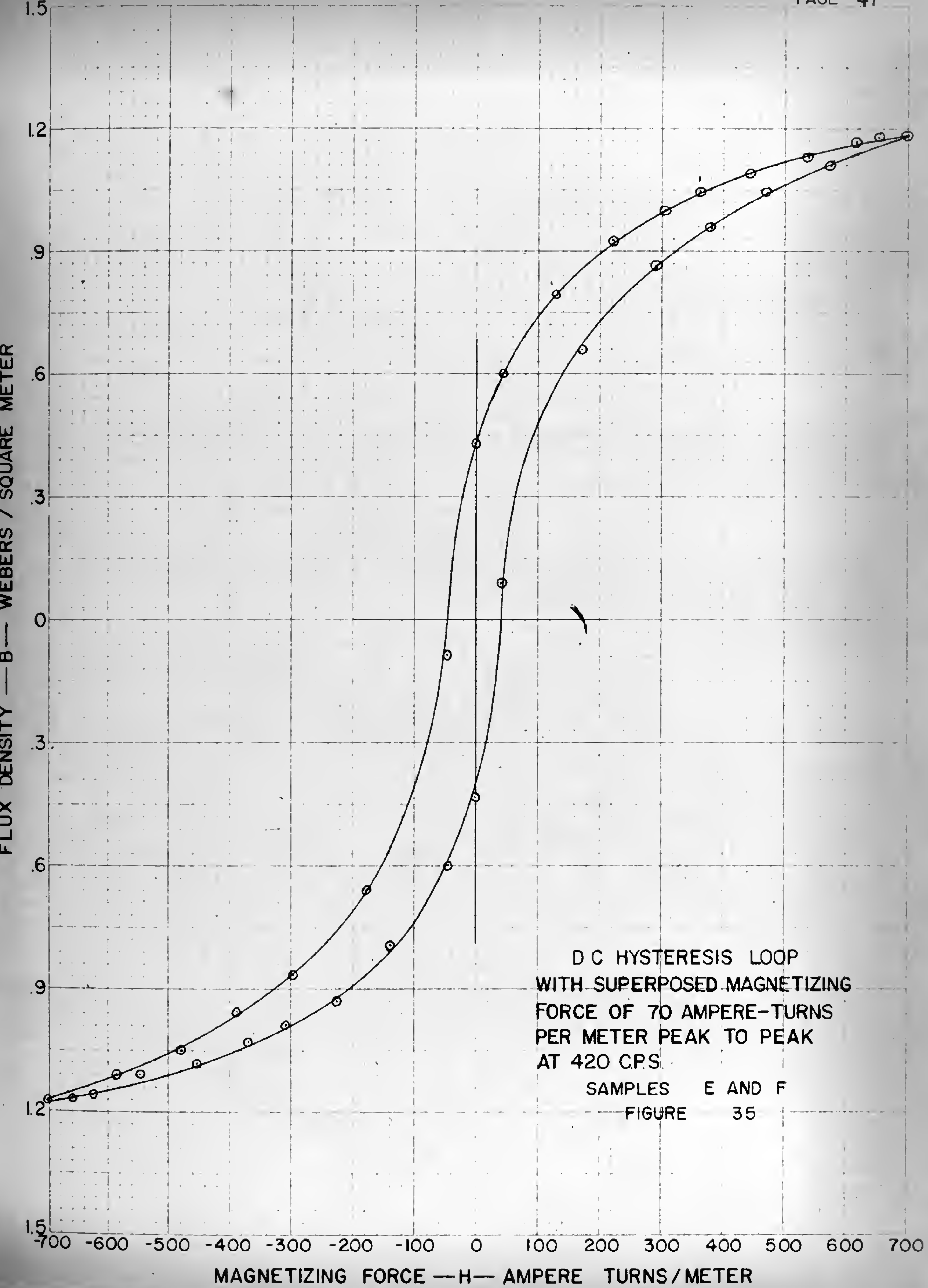

D C HYSTERESIS LOOP
WITH SUPERPOSED MAGNETIZING
FORCE OF 70 AMPERE-TURNS
PER METER PEAK TO PEAK
AT 420 C.P.S.

SAMPLES E AND F

FIGURE 35

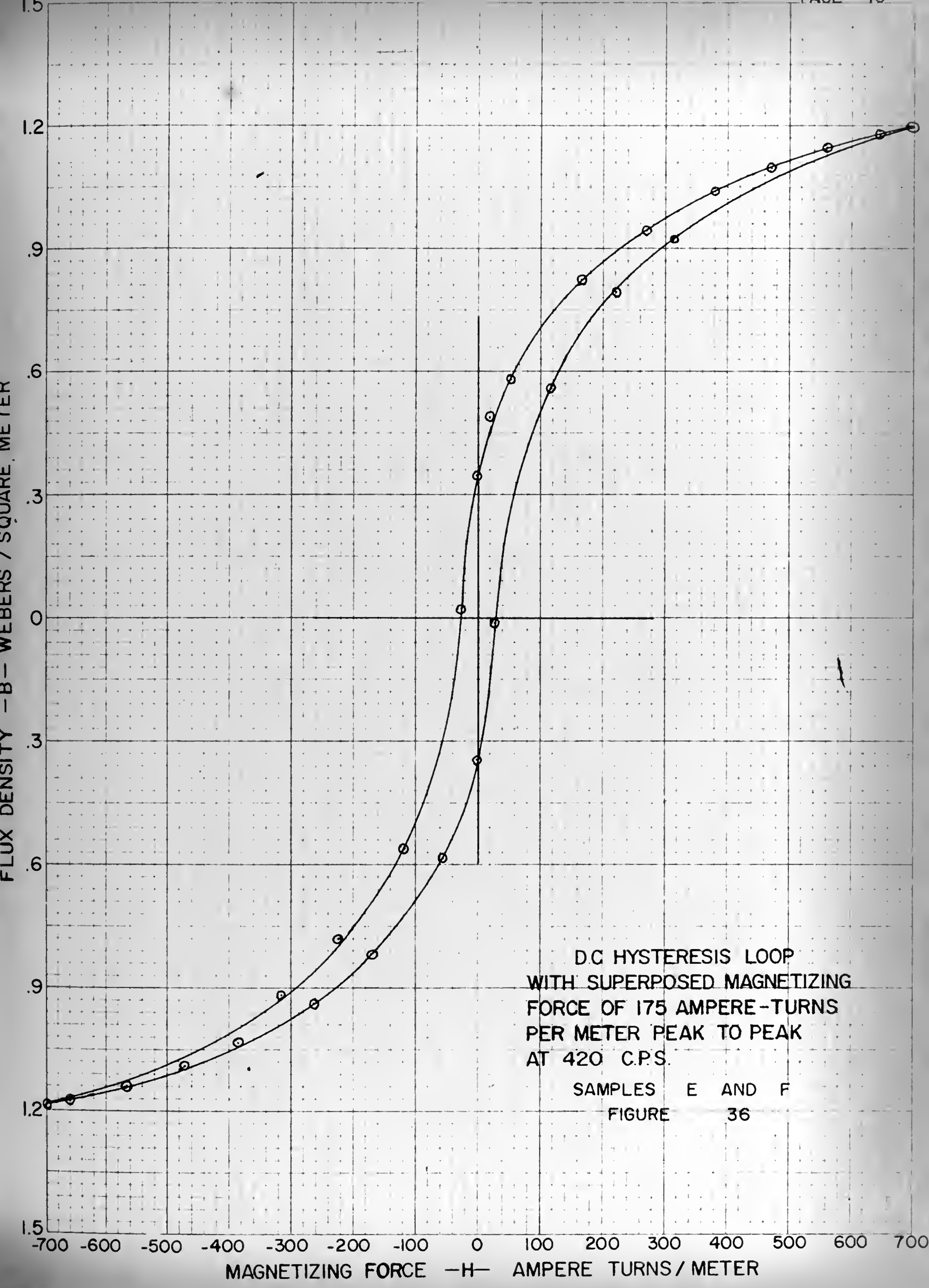

D.C HYSTERESIS LOOP
WITH SUPERPOSED MAGNETIZING
FORCE OF 175 AMPERE-TURNS
PER METER PEAK TO PEAK
AT 420 C.P.S.

SAMPLES E AND F

FIGURE 36

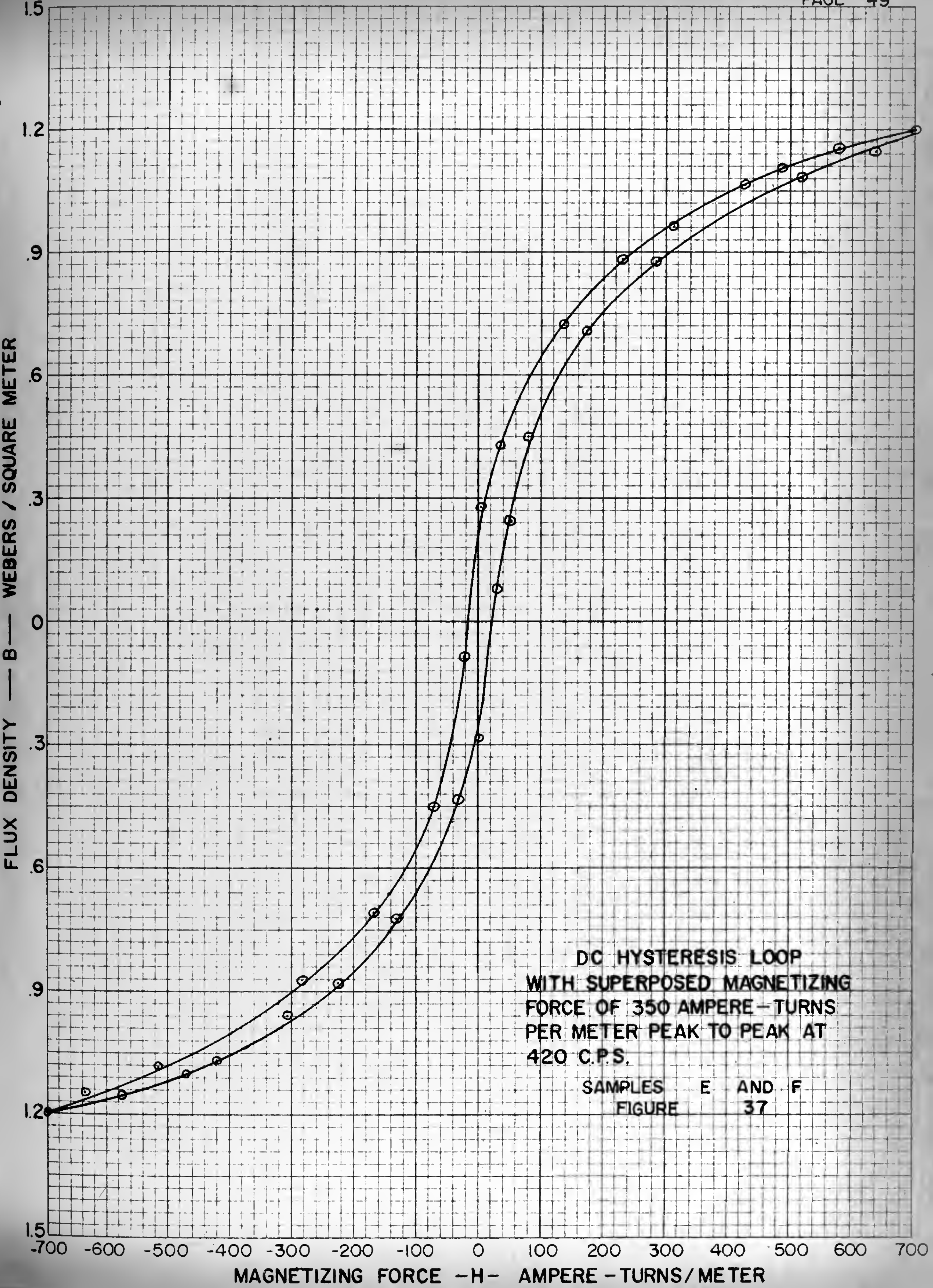

DC HYSTERESIS LOOP
WITH SUPERPOSED MAGNETIZING
FORCE OF 350 AMPERE-TURNS
PER METER PEAK TO PEAK AT
420 C.P.S.

SAMPLES E AND F
FIGURE 37

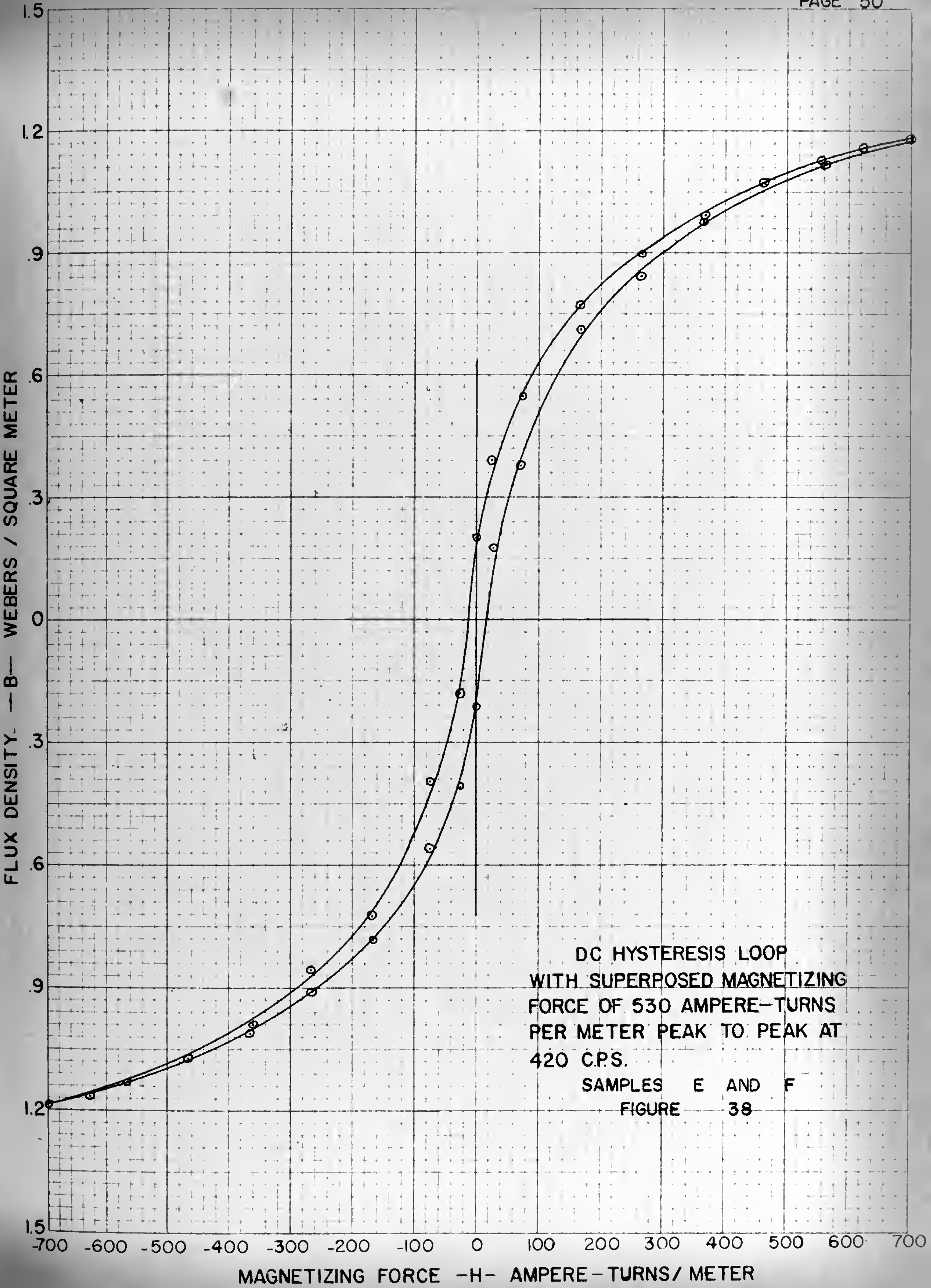

DC HYSTERESIS LOOP
WITH SUPERPOSED MAGNETIZING
FORCE OF 530 AMPERE–TURNS
PER METER PEAK TO PEAK AT
420 C.P.S.
SAMPLES E AND F
FIGURE 38

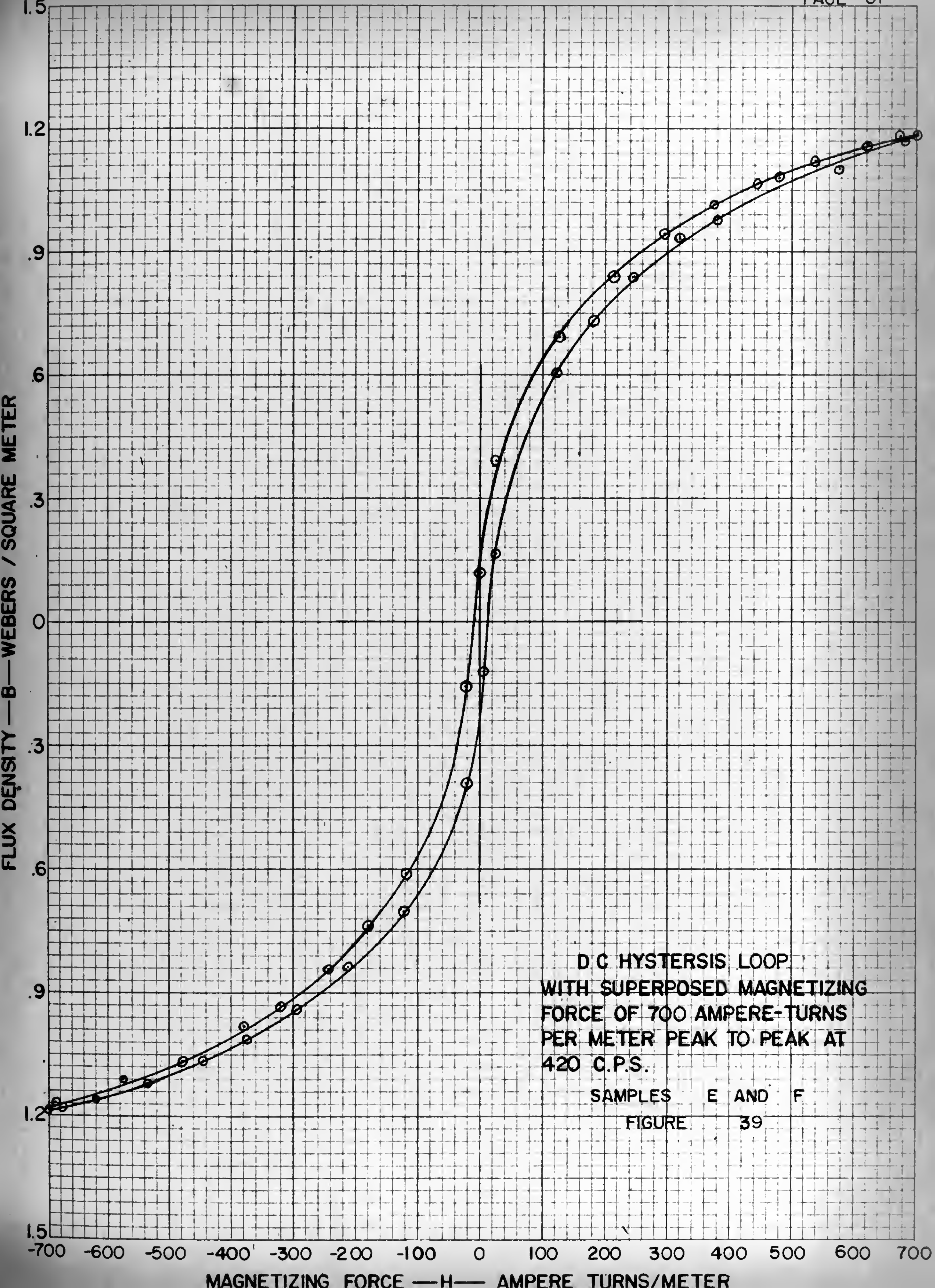

D C HYSTERSIS LOOP
WITH SUPERPOSED MAGNETIZING
FORCE OF 700 AMPERE-TURNS
PER METER PEAK TO PEAK AT
420 C.P.S.

SAMPLES E AND F

FIGURE 39

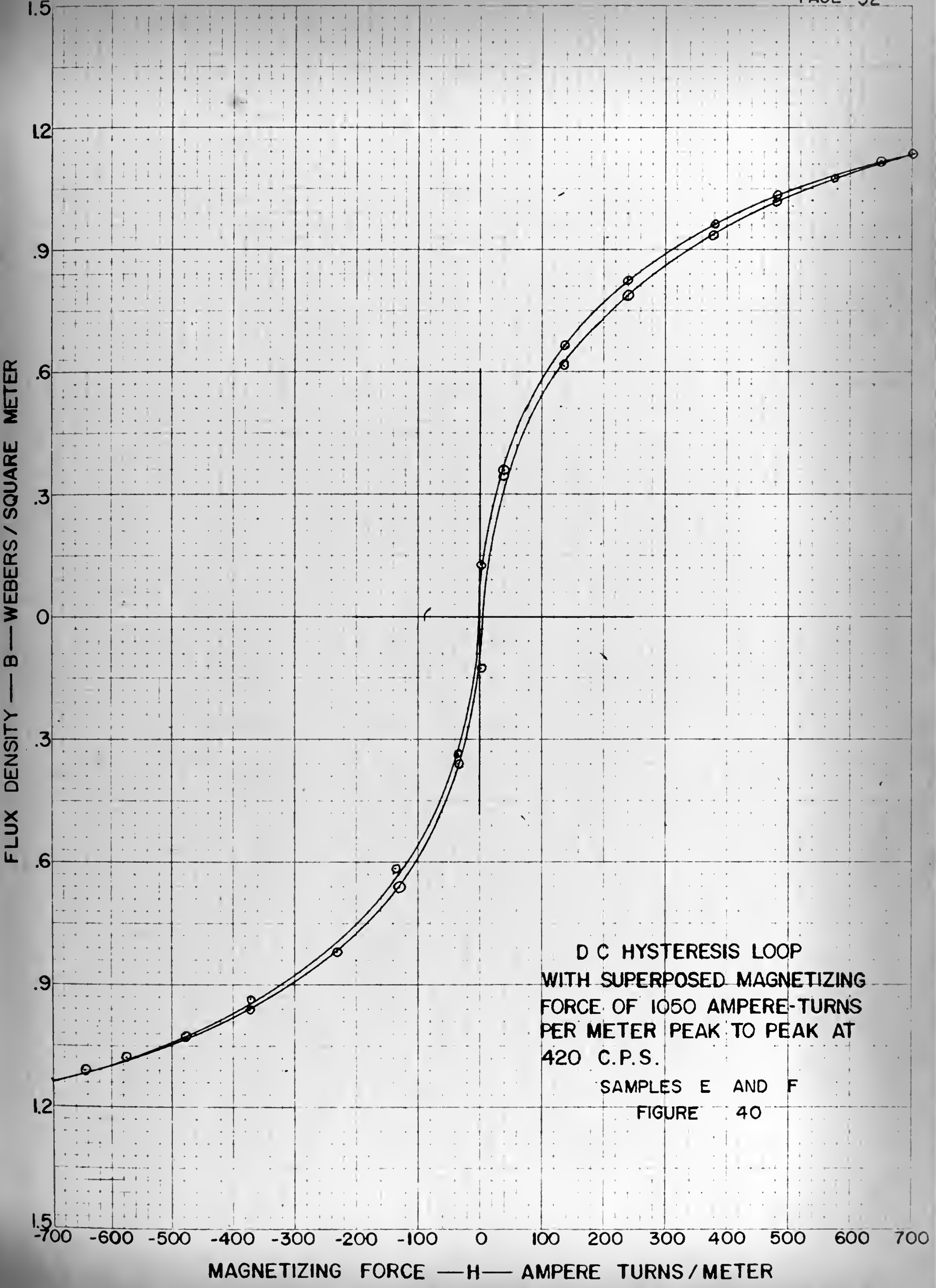

D C HYSTERESIS LOOP
WITH SUPERPOSED MAGNETIZING
FORCE OF 1050 AMPERE-TURNS
PER METER PEAK TO PEAK AT
420 C.P.S.

SAMPLES E AND F
FIGURE 40

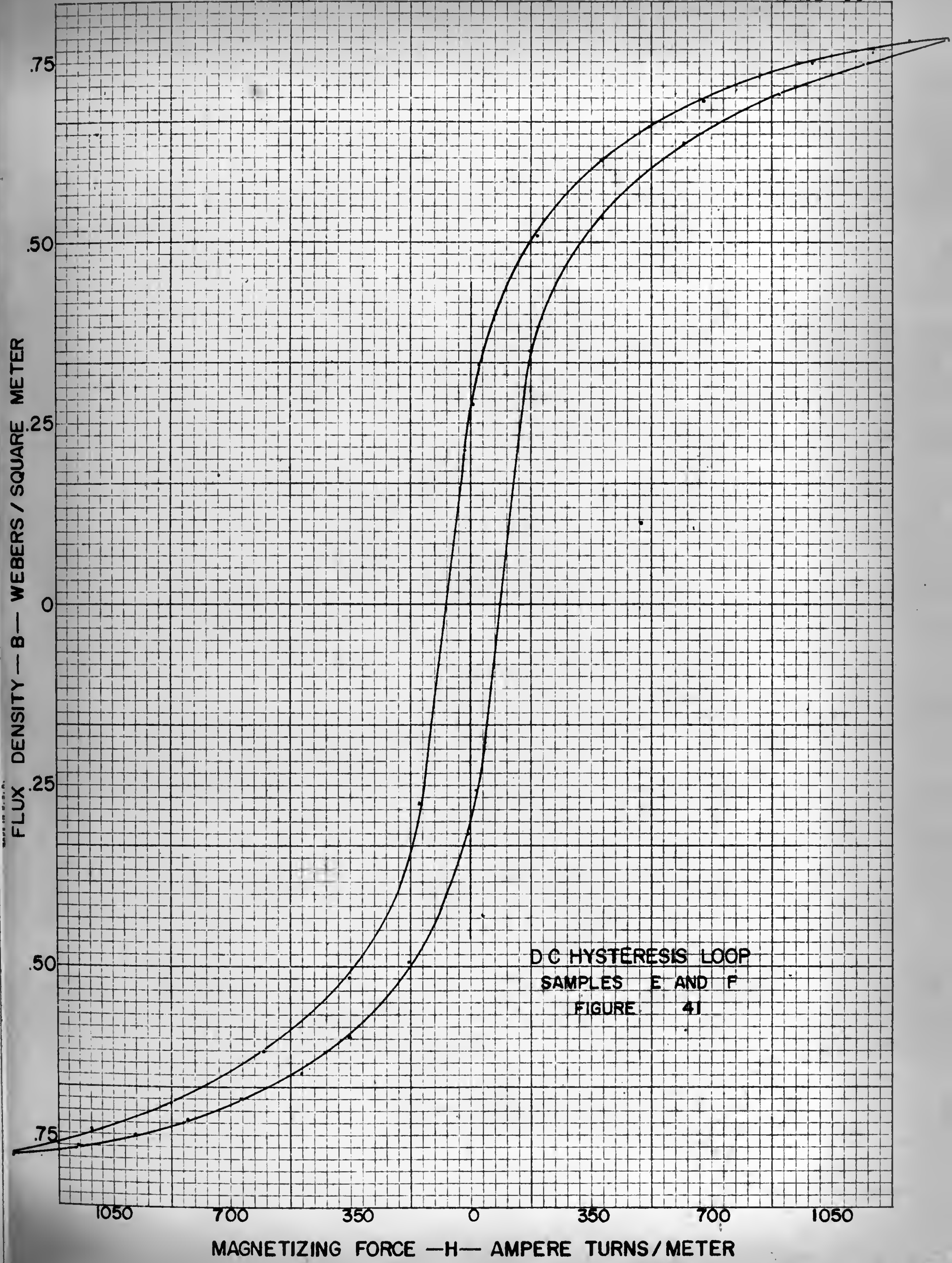

D C HYSTERESIS LOOP
SAMPLES E AND F
FIGURE 41

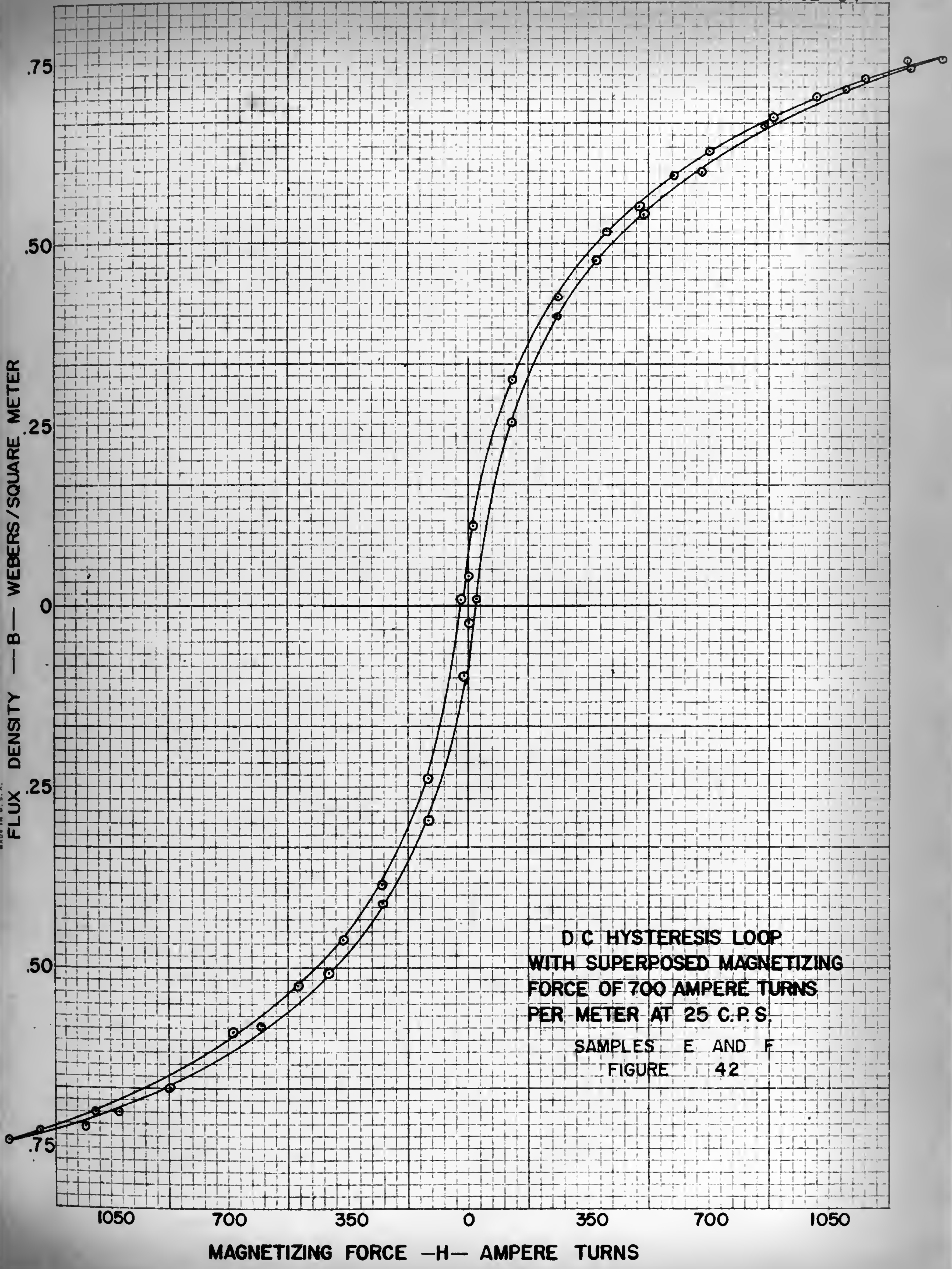

D C HYSTERESIS LOOP
WITH SUPERPOSED MAGNETIZING
FORCE OF 700 AMPERE TURNS
PER METER AT 25 C.P.S.

SAMPLES E AND F
FIGURE 42

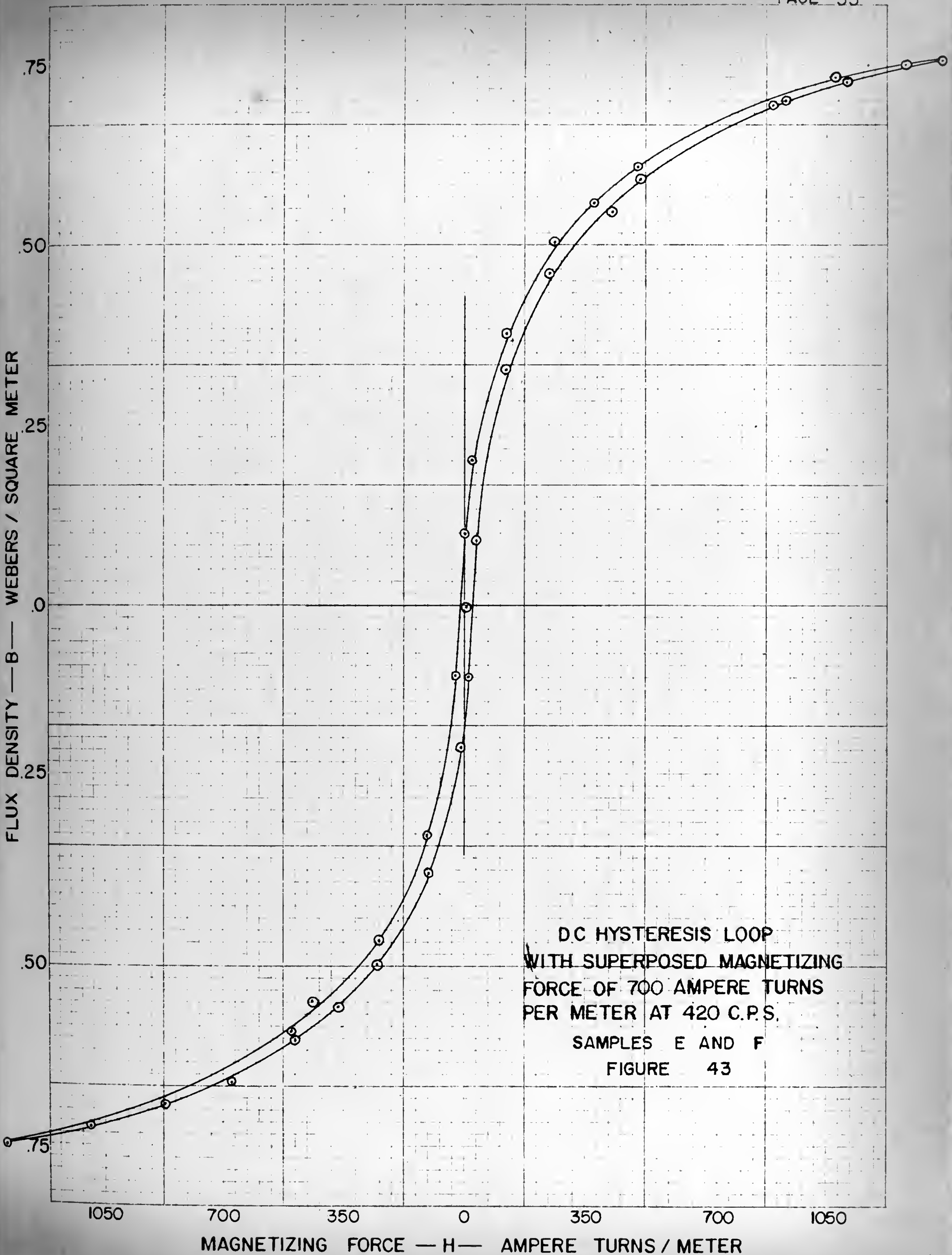

D.C HYSTERESIS LOOP
WITH SUPERPOSED MAGNETIZING
FORCE OF 700 AMPERE TURNS
PER METER AT 420 C.P.S.
SAMPLES E AND F
FIGURE 43

CHAPTER IV

FINDINGS AND CONCLUSIONS

The experimental work accomplished in this investigation was of an exploratory nature. It encompassed a study of the effect of a superposed alternating magnetizing field upon the hysteresis loop of magnetic materials. Two materials representative of modern commercial products were chosen to obtain these data. One core material was selected in the solid form; the other in a laminated form. (See Appendix A). Results were obtained for a range of values of amplitude and bias of varying alternating frequencies. Magnetization curves of samples were obtained for identification and matching of cores. A brief study of the effect of superposed alternating magnetizing field on the normal magnetization curves was undertaken at one frequency.

From the results of the investigation it was conclusively shown that the area of the D.C. hysteresis as obtained by ballistic methods decreases as the magnitude of the superposed alternating magnetizing field was increased. This was true for every frequency of superposed alternating magnetizing force tested. This is in agreement with the previous work by Fenzi and others. In accordance with the theory offered by Spooner the decrease in area of the hysteresis was not an indication that the actual hysteresis loss is decreased. The hysteresis loss of the magnetic material was only apparently decreased and may possibly be increased. This was not

verified in this investigation.

In the case of the laminated samples it was shown that, within the experimental accuracy of the work undertaken, the decrease in the area of the hysteresis loop was independent of the frequency of the superposed magnetizing force. For the tests on the solid cores the area was reduced inversely as the frequency of the superposed magnetizing field. The variation of the area with frequency in the tests using solid cores was probably due to the effect of eddy current shielding at the higher frequencies. This was substantiated somewhat by the fact that with the laminated cores the decrease in area was apparently independent of the frequency of the superposed bias.

The data obtained indicated that the point of maximum induction was markedly increased when an alternating bias was applied to the hysteresis loop. This increase in the induction of the core material was independent of both magnitude and frequency of the superposed magnetizing field for the solid and liminated cores. The increase in the point of maximum induction was much greater for the laminated cores.

Considering a series of tests at any frequency the data obtained for the laminated cores show that the slope of the hysteresis loops in the portions before and at the knee of the curve decreased as the magnitude of the superposed magnetizing force was increased. Considering the series of tests at a constant magnitude of superposed magnetizing force

of 700 ampere-turns per meter, there appears to be no change of the change of the slope of the hysteresis curves with a variation of the frequency of the bias.

In the study of the effect of varying the magnitude of an alternating superposed magnetizing force of 180 cycles per second upon the normal magnetization curve it was found that the initial permeability was first increased and then decreased as the magnitude of the bias was increased. The initial "bend" in the magnetization curve was removed. This was in agreement with previous work by Spooner(14) and others using a superposed magnetization force of 60 cycles per second. A marked decrease in permeability and induction was not obtained as was to be expected in light of the work of previous investigators at other frequencies. However, if higher value of superposed magnetizing force were used possibly the expected results would be obtained.

BIBLIOGRAPHY

1. Allegheny Ludlum Steel Corporation. Electrical Steel Sheets and Coiled Electrical Steel Strip, Technical Bulletin EM21, Allegheny Ludlum EM21 EDI 15M-348-GPC

2. Allegheny Ludlum Steel Corporation. Magnetic Materials, Allegheny Ludlum, 1947.

3. American Society for Testing Materials. A.S.T.M. Standards, A.S.T.M., 1949.

4. Ashworth, J.R. The Anhysteretic Magnetic Properties of Iron and Nickel, Philosophical Magazine, p. 357, Feb. 1954

5. Bozorth, Richard M. Ferromagnetism, 1st Edition. D.Van Nostrand Co., 1951

6. Boyajian, A. and Camilli, G. Orthomagnetic Bushing Current Transformer for Metering, AIEE Transactions, Vol. 64, pp. 137-140, and Discussion, pp. 427-428, 1945.

7. Dumont Laboratories. Dumont Oscillograph Record Camera, Type 296, Operating and Maintenance Manual, Dumont Laboratories Inc., 1951

8. Ewing, J.A. Magnetic Induction in Iron and Other Metals, 3rd Edition, D. Van Nostrand, 1900.

9. Gerosa, G.G. and Finzi, G. Rendiconti del R. Institute Lombardo, Vol. XXIV, fasc. x., April, 1891

10. Harris, F.K. Electrical Measurements, 1st Edition, Wiley & Sons, 1952

11. Lord, H.W. Dynamic Hysteresis Loop Measuring Equipment, AIEE No. 2, pp. 269-271, Sep., 1952

12. Niwa, Y. and Asami, Y. Magnetic Properties of Sheet Steel Under Superposed Alternating Field and Unsymmetrical Hysteresis Losses, Electrotechnical Laboratory, Report 124, Department of Communications, Tokyo, Japan.

13. Siskind, Phillip. A Permeability Analyzer for Magnetic Amplifier Cores, Communications and Electronics, AIEE No. 9, pp. 572-575, Nov., 1953

14. Spooner, Thomas, Properties and Testing of Magnetic Materials, 1st Edition, McGraw Hill, 1927.

15. Stout, Melville B., Basic Electrical Measurements, 1st Edition, Prentice-Hall, 1950.

APPENDIX A

DESCRIPTION OF SPECIMENS

In order to serve the purposes of this thesis the cores were to have identical electrical and magnetic characteristics. Hence several requirements had to be met by the two specimens:

1. Matched dimensionally.
2. Having same number of turns in primary, secondary, tertiary and additional windings.
3. Exciting winding should be capable of carrying up to 15 amperes of current.
4. Metallurgical composition and history to be the same.
5. Capable of approximating an infinite solenoid excited by a sheet of current.
6. Having magnetic characteristics generally independent of eddy current effects at frequencies up to 420 c.p.s.
7. Having magnetic characteristics generally independent of moderate temperature variations.
8. Be essentially free of capacitive coupling at frequencies up to 420 c.p.s.
9. Leakage flux to be negligible.

Although Camilli and Boyajian(6) believed that "reasonable care" in the selection and winding would insure experimenters of having matched specimens it was found that this task exceeded the capabilities of these experimenters and the facilities of this school. Not knowing what to expect from

failure to meet one or more of the requirements listed above the experimenters started with two mild steel solid specimens having specifications shown in Figure 44.

	A	B
Mean diameter:	4.406 in.	4.379 in.
Radial width:	1.19 in.	1.215 in.
Section:	.908 $in.^2$	.932 $in.^2$
Primary:	130 turns no. 17 wire	
Secondary:	10 turns no. 17 wire	

Figure 44. Specifications of Specimens A and B.

However, a cursory comparison of the magnetic properties of these cores (See Figure 45) showed that at the knee of the B-H curve the cores differed in flux by about 4% as measured by galvanometer. While this was a small difference it was decided to improve the specimens by giving the cores an annealing, cutting the cores on a lathe to more exact dimensions and rewinding the cores in an attempt to increase the number of turns-per-inch circumference.

The cores were each annealed by heating to 1550° F, holding at temperature for two hours, then furnace cooled in an air atmosphere. No packing was used to prevent scale formation.

The cores were relabeled C and D then cut on a lathe by Mr. A.J. White to the dimensions shown in Figure 46.

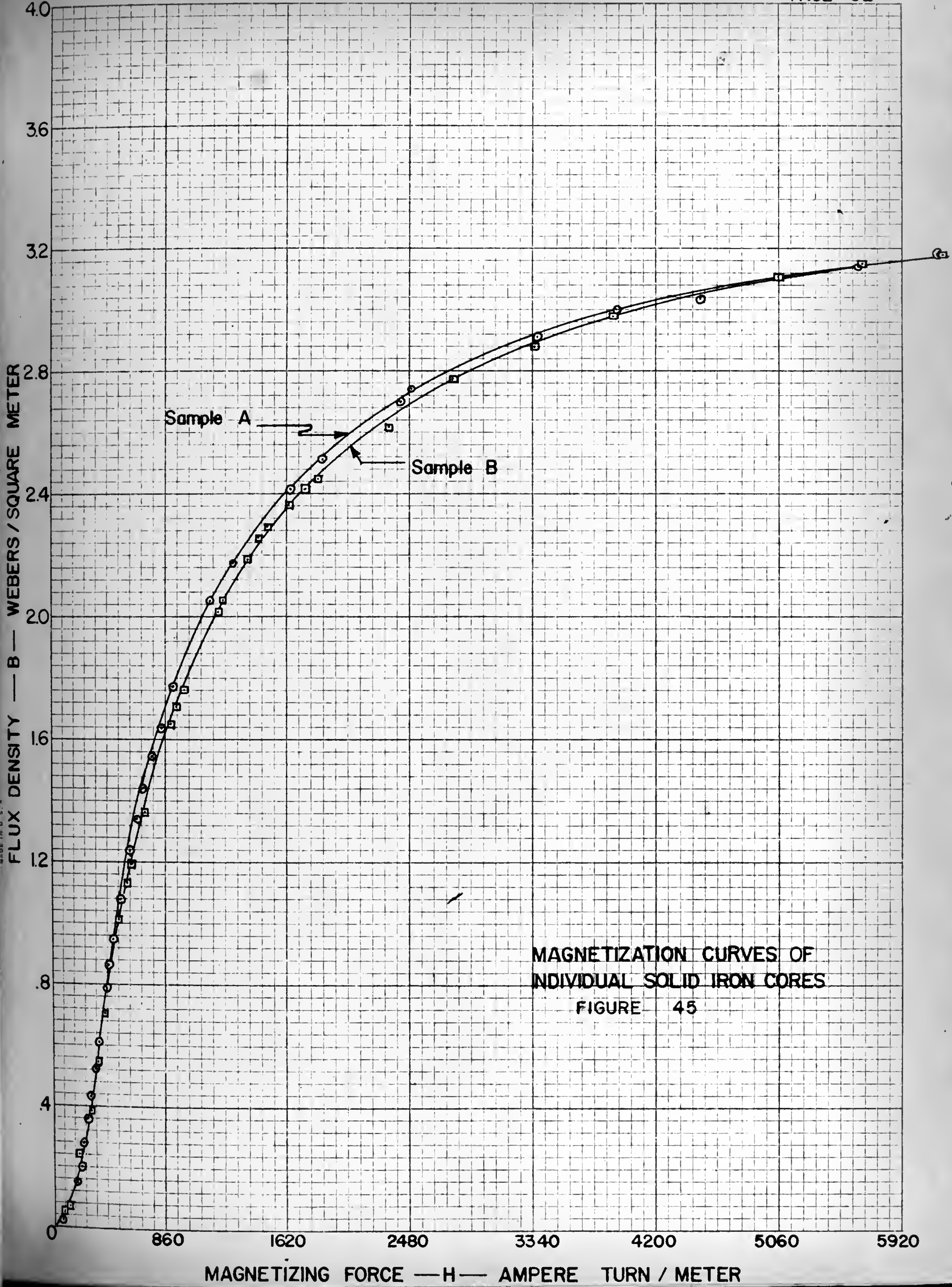

MAGNETIZATION CURVES OF
INDIVIDUAL SOLID IRON CORES

FIGURE 45

	Core C	Core D
Mean Diameter	4.408 in. or .1119 meters	4.409 in. or .1118 meters
Radial Width	1.149 in.	1.148 in.
Section	.809 sq. in. or 5.21x10-4 sq. meters	.809 sq. in. or 5.21x12-4 sq. meters
Thickness	.705 in.	.705 in.
Outer Diameter	5.557 in.	5.557 in.
Inner Diameter	3.259 in.	3.261 in.

Figure 46. Specifications of Specimens C and D.

A microscopic examination of the cores indicated the material to be a low carbon or mild steel.

The cores were weighed with the results shown in Figure 47.

	Core C	Core D
Weight	1436.2 grams	1435.7 grams
Volume	11.41 in. (187 cm)	11.41 in. (187 cm)
Specific Weight	7.68 g/cm	7.68 g/cm

Figure 47. Further Description of Cores C and D.

Rockwell B hardness was determined with the following results:

	Core	Core D
Hardness	Rockwell B 52.5 3.5	Rockwell B 51 1

These hardness variations indicated a variation in material. This was verified by the relative difficulty of cutting the material and by the appearance of the surface.

The cores were wrapped with a double layer of linen tape then a winding of 200 turns no. 17 varnish-insulated copper

wire. Another layer of linen tape was applied, then a 180 turn winding of no. 17 wire. Then 10 turns of varnish-insulated no. 25 copper wire was wound between the turns of the 180-turn winding. This winding extended for about half an inch circumference. Finally the specimens were wrapped with another layer of linen tape. Both cores were wound identically.

One major effect of electrical and magnetic mismatch of specimens is the appearance of an alternating voltage in the galvanometer circuit when alternating voltage is applied to either exciting windings, even though the A.C. windings are connected opposing and the pickup windings connected aiding. Hence the two cores C and D were compared on this basis. The results measured with a 60 cycle voltage applied to the 180 turn windings connected in opposition with respect to the 200 turn windings and the pickup windings are shown in Figure 48.

180 turn		200 turn		10 turn	
Volts RMS	Volts PK to PK	Volts RMS	Volts PK to PK	Volts RMS	Volts PK to PK
14.8	42	.14	.52	.005	.04
9.0	26	.09		.008	
6.0	17	.05	.20	.003	.02
For a single specimen					
C 7.6	22	6.9	20	.38	1.0
D 7.6	22	6.9	20	.38	1.0

Figure 48. Electrical Characteristics of Specimens C and D

It was not expected that the A.C. voltage applied to the 200-turn windings would exceed 10 volts RMS and that the milliwatts (less than 10) appearing in the galvanometer circuit would affect the galvanometer. The power generated in the galvanometer coil should be less than .045 microwatts. Also the 4.5 μamp A.C. current should not change the characteristics of the galvanometer. That these conclusions were perhaps not valid was indicated, when, on the first attempt to make measurements of the effect of a superposed 60 c.p.s. MMF on the static hysteresis loop, the galvanometer suspension was broken, possibly due to a burning.

Several attempts were then made to reduce the A.C. voltage in the galvanometer circuit by use of a band rejection filter, a capacitance shunt, and a balancing resistor on one of the A.C. exciting windings. For various reasons none of these were acceptable.

These difficulties indicated that even more carefully balanced specimens would have to be obtained.

The first several sets of readings were somewhat disappointing in that they showed very little effect on the static hysteresis loop of superposing an alternating MMF. A more careful analysis of the possible reasons brought out that eddy currents generated near the surface of the solid core by the alternating MMF might possibly shield the iron from the effect of the alternating MMF. See Spooner(14,p.98). That eddy

current effect was appreciable was determined by examining the dynamic hysteresis loop on a CRO and comparing it with the static loop. Although the CRO presentation was only roughly the true dynamic loop it was obvious to the experimenters that eddy currents were effecting considerably the experimental results.

The unanticipated adverse effects of magnetic dissimilarity of the cores and eddy current effects in the solid cores together with the desire to improve the mean diameter to radial width ratio persuaded the experimenters to procure new specimens.

An order was placed with TICE ELECTRIC COMPANY in Monterey, California for 300 laminations stamped from hot-rolled grain oriented 14 mil 4% silicon steel insulated sheets (Allegheny Ludlum Steel Corporation Transformer C type C-1 described in Allegheny Ludlum Technical Bulletin EM21). The dimensions to one-one hundredth were:

Outer Diameter	5.00 in.
Inner Diameter	4.25 in.

A total of five cores were prepared by selecting 27 laminations having a good coating of insulation, stacking them so that grain orientation was in the same direction for each lamination and wrapping hand-tight with a double layer of linen tape. Three pickup windings were wound on two of the cores. One 20-turn winding and one 30-turn winding each with varnish-insulated no. 25 copper wire were wound next to the

core. The 75-turn pickup winding using the same no. 25 wire was wound outside the linen tape protecting the outer exciting winding. The d.c. exciting winding consisted of 260 turns of varnish insulated no. 17 copper wire wound over the pickup windings. A single layer of linen tape protected these windings, then the a.c. exciting winding consisting of 260 turns of varnish insulated no. 17 copper wire. Another layer of linen tape protected this winding. On two specimens another pickup winding consisting of 75 turns of varnish insulated no. 25 copper wire was wound outside this layer of linen tape. This winding was applied after tests described below and because data taken with the galvanometer indicated more turns would be needed in the pickup winding.

In order to determine which combination of the four laminated cores would be most nearly balanced magnetically the method described by Siskind(13), was used. The circuit used is shown in Figure 49. For each combination an 8.0 amperes (RMS) 60 c.p.s. sine wave current was applied to the inner 260-turn winding. The 20-turn pickup windings were connected opposing with respect to the exciting winding and by means of a scale-calibrated CRO a Lissajous figure of "difference" voltage versus primary current (measured as voltage across a 0.5 ohm resistance) was presented. A VTVM was used to simultaneously measure the RMS value of voltage appearing across both pickup windings. The results are tabulated in Figure 50.

CIRCUIT FOR COMPARISON OF CORES

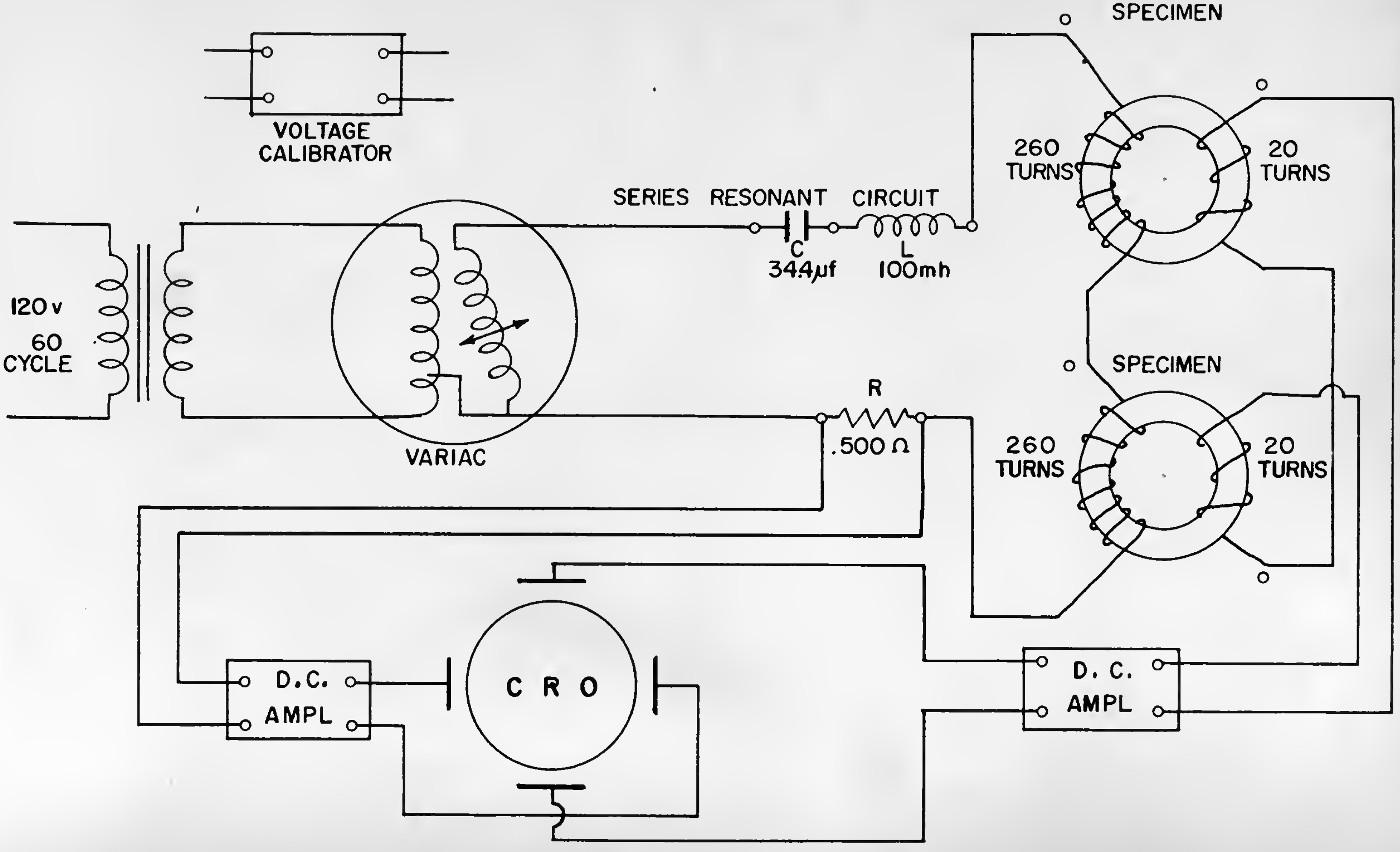

FIGURE 49

Cores	PEAK Value	RMS Value
1 and 2*	.35 v	.013 v
1 and 3	.72 v	- - -
1 and 4	1.03 v	.015 v
2 and 3	.23 v	.22 v
2 and 4	.96 v	.018 v
3 and 4	.93 v	.025 v

Figure 50. Comparison of Laminated Cores.

Using this test as a guide Cores 1 and 2 were selected and lettered Specimens E and F.

All static hysteresis loops were measured using the inner 260-turn winding as a D.C. exciting winding connected in series aiding for the two cores; the outer 260-turn winding as A.C. exciting winding connected in series opposition; and the outer 75-turn winding as a pickup or galvanometer winding connected in series aiding. Dynamic measurements were made using the inner 20-turn windings and the inner 260-turn windings. The 30-turn windings on these specimens were not used.

A summary description of these specimens is as follows:

CORE DESCRIPTION

Material: American Iron and Steel Institute designation M-19.

Diameters: Inner 4.25 in; Outer 5.00 in.

Thickness: .014 in. (29 gauge)

Insulation: Organic-annealed coating.

Iron energy loss: At 60 c.p.s. and 10 kilogauss: .72 watts/lb. and 15 kilogauss: 1.85 watts/lb.

---

*See photographs Figures 51 and 52.

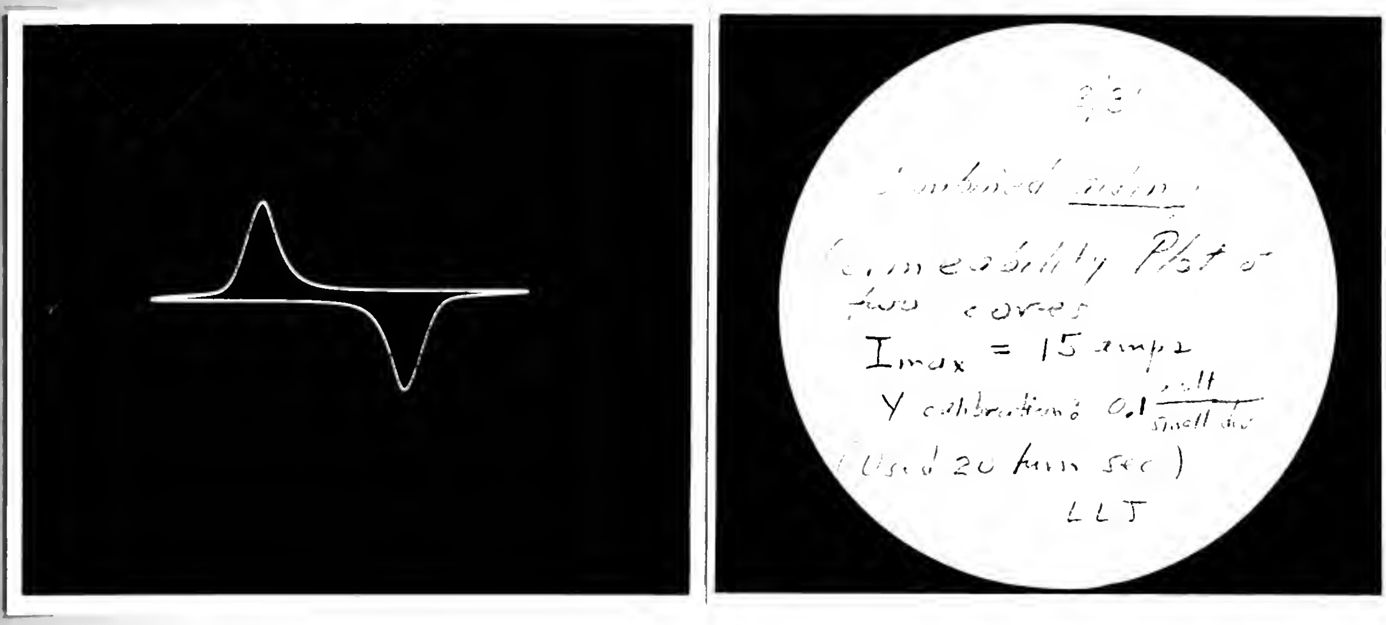

3/31

Combined aiding

Permeability Plot of two cores

I_{max} = 15 amps

Y calibration: 0.1 $\frac{\text{volt}}{\text{small div}}$

(Used 20 turn sec)

LLT

Figure 51

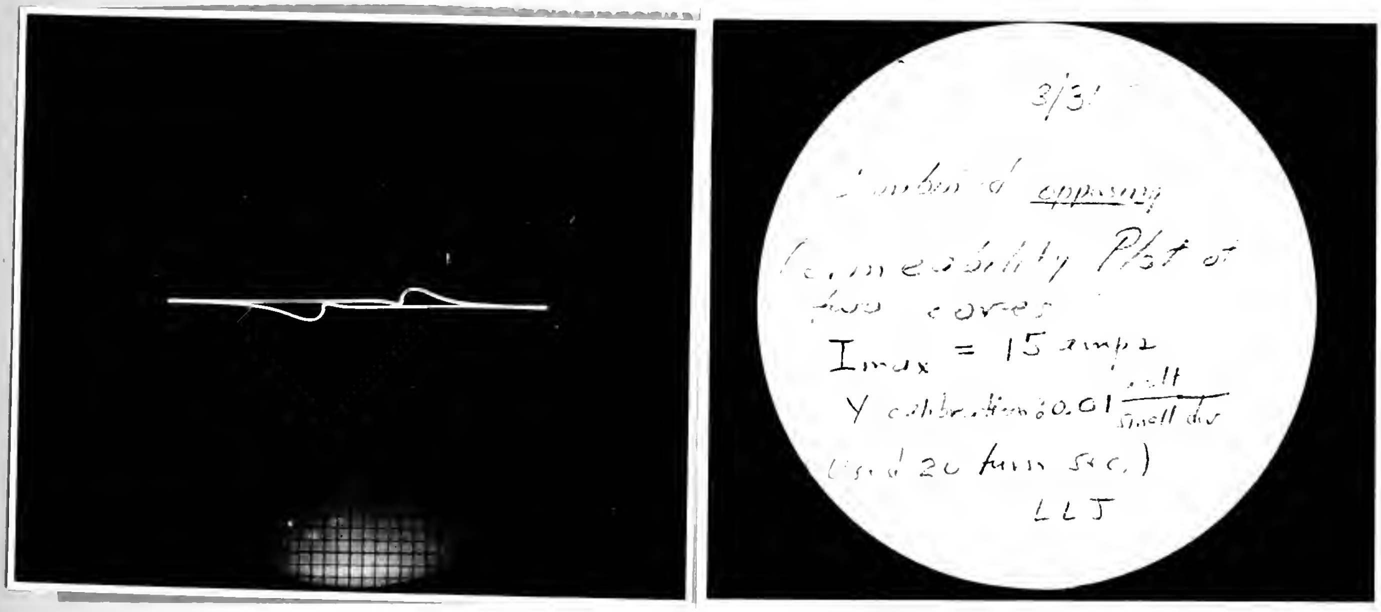

3/31

Combined opposing

Permeability Plot of two cores

I_{max} = 15 amps

Y calibration: 0.01 $\frac{\text{volt}}{\text{small div}}$

(Used 20 turn sec.)

LLT

Figure 52

Heat Treatment: Hot-rolled sheet worked by punching.

Maximum permeability: 8,000 at 6 kilogauss.

"Guaranteed" Flux Density at 10 oersteds: 12.7 to 13.8 kilogauss.

Measured Flux Density at 10 oersteds: 12 kilogauss.

Number of Laminations per Core: 27.

WINDINGS, INNER TO OUTER

1. Double layer linen insulating tape.

2.& 3. 20 turns insulating varnish coated no. 25 copper wire and 30 turns insulating varnish coated no. 25 copper wire.

4. 260 turns insulating varnish coated no. 17 copper wire.

5. Single layer linen insulating tape.

6. 260 turns insulating varnish coated no. 17 copper wire.

7. Single layer linen insulating tape.

8. 75 turns insulating varnish coated no. 17 copper wire.

9. Single layer linen tape over the 75 turn winding.

CALCULATED VALUES

Mean Diameter: 4.625 in.

Mean Diameter/Radial Width: 12.33 in.

Mean Magnetic Length: 14.51 in. or 0.3690 meters.

Correction Factor for Toroid: H_0/H_R 1.003 Spooner(14, p.295)

Section: 0.1418 sq. in. or 0.913×10^{-4} sq. meter

Exciting Winding Turn Density: 704 turns/meter

Pickup Winding Turns-Area Product: .00685 turns-sq. meter.

For further investigations even better specimens should be obtained. For example, factory prepared spiral-wound of ½ inch by two mil (.002 inch) moderate core loss steel in a ring about five inches in diameter and ½ x ½ section would be good cores. Several, perhaps five, of these should be procured and the best-matched two used.

APPENDIX B

USE OF GALVANOMETER

The galvanometer used in this study was a Leeds & Northrup DC Moving Coil Ballistic Galvanometer: List No. 2239-d, Flux-linkage Sensitivity 5.5 mm/weber; Period 19.6 second; CDRX 12,000 ohms; relative damping on open circuit .0309; relative damping with critical resistance 0.286; and internal (coil) resistance 2200 ohms. All constants were measured as described below.

The flux sensitivity was measured using a Standard Mutual Inductance described in detail in Figure 53. The secondary of the mutual inductance remained an integral part of the galvanometer circuit throughout the data-taking. On one occasion the suspension of the galvanometer was broken or burned out, possibly due to an overload of a.c. induced from the tertiary winding of the specimen. After Dr. C.H. Rothauge replaced this suspension, the galvanometer was recalibrated and this calibration periodically rechecked during the data-taking. The description herein is that of the galvanometer with replaced suspension. To facilitate periodic recalibration flux sensitivity was expressed as a ratio of primary current to millimeters deflection, these items being easily read. The effect of errors in the D.C. ammeter were reduced by using the same ammeter for calibrating the galvanometer and measuring the MMF applied to the specimen.

STANDARD SOLENOID WITH FIXED AND MOVABLE SECONDARIES

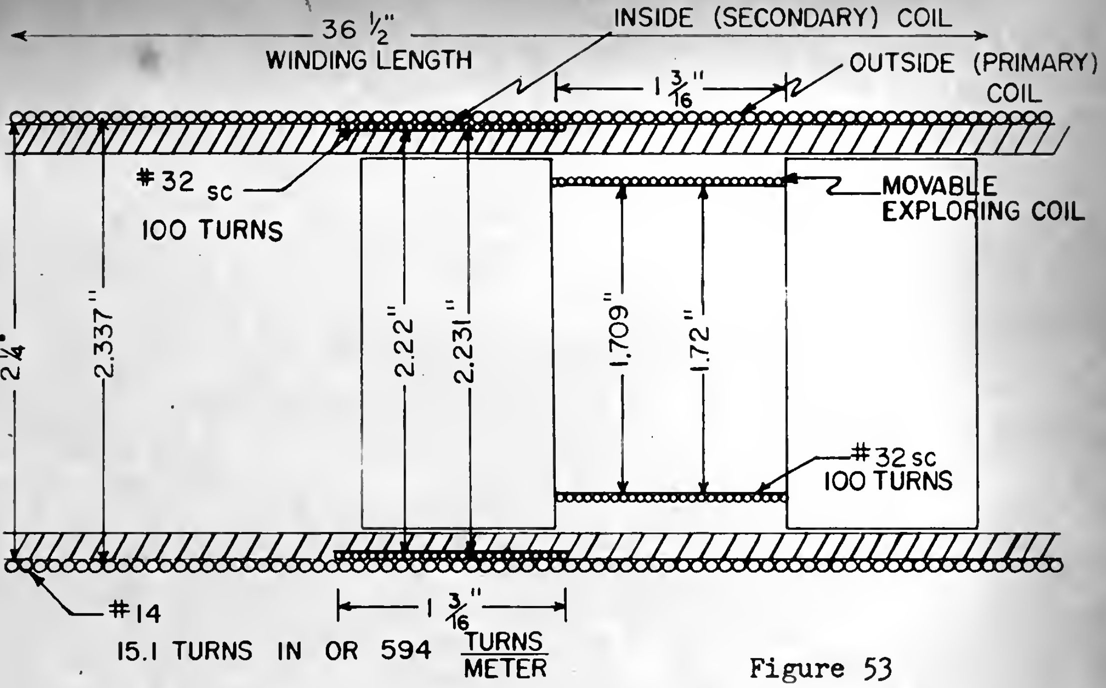

Figure 53

COMPUTED VALUES

Primary: H center $= .4\pi n I_{amp} = 7.47 n I_{amp}$ Gilberts/cm

B center $= 7.47 \times I_{amp} \times 10^{-4}$ Webers/ m^2

Area of Cross Section		Weber Turns
Inside (Secondary) Coil	$A = 8.03\pi \times 10^{-4}\ m^2$	$6\pi \times 10^{-5}$
Outside (Primary) Coil	$A = 8.79\pi \times 10^{-4}\ m^2$	$6.56\pi \times 10^{-5}$
Moveable Exploring Coil	$A = 4.77\pi \times 10^{-4}\ m^2$	$3.563\pi \times 10^{-5}$ at center

ELECTRICAL MEASUREMENTS

P Primary R = .88 ohms L = 1.08 mh

S_1 Inside Std. R = 9.94 " L = .57 nh

X Exploring Coil K = 8.5 ohms L = .38 mh

Mutual Inductances

P & S_1 $M = .19$ mh S_1 & X $M_{max} = .31$ mh

P & X $M_{max} = .11$ mh

BALLISTIC GALVANOMETER DETERMINATIONS List No. L&N 2239-D
Galvanometer Resistance 2130 ohms, CDRX 12000 ohms
Sensitivity .0018 Coulombs/cm

The period of the galvanometer was measured by deflecting the galvanometer with a small step-function D.C. current, opening the circuit and noting the times at maximum deflection.

The CDRX was approximated by using a Decade Resistance Box Type 1432-L No. 2992. Starting at 20,000 ohms successively smaller resistances were used until some value was obtained with which there was no detectable overshoot as the galvanometer returned to zero.

Relative damping was computed from

$$-\ln \frac{\theta_1 - \theta_F}{\theta_F} = \frac{\pi \gamma_1}{\sqrt{1-\gamma_1^2}}$$

$$-\ln \frac{\theta_2}{\theta_F} = \frac{\pi \gamma_0}{\sqrt{1-\gamma_0^2}}$$

and

$$\gamma_x = \frac{R_1}{R_x}(\gamma_1 - \gamma_0) + \gamma_0$$

$$R_1 = R_b + R_c + R_g$$

$$R_x = R_{leads} + R_g + R_{sec} + R_{c_{sec}}$$

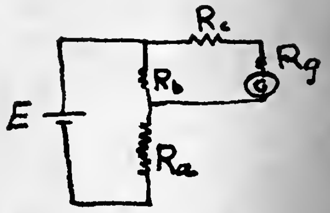

This procedure was taken from Harris(10, pp. 62-64).

The importance of high relative damping for making flux measurements is discussed by Harris(10,pp. 312-319). In particular, his equation for flux sensitivity:

$${}_{\gamma}S_{\phi_N} \triangleq \frac{{}_{\gamma}\theta_1}{\int e\,dt} = \left(\frac{\theta_F}{I_g}\right)\frac{2\pi}{T_0} \times \frac{1}{R_c} \times \frac{\gamma - \gamma_0}{1-\gamma_0} \cdot \frac{1}{2\gamma}$$

tends to show that as relative damping increases so also does flux sensitivity. In this equation:

θ is galvanometer deflection.

γ is relative damping, relative to critical damping.

$\left(\frac{\theta_F}{I_g}\right)$ is current sensitivity of the galvanometer, acting under the influence of a constant current Ig.

T_o is open circuit or free period.

R_c is the circuit resistance at critical damping (CDRX).

γ_o is open circuit relative damping, relative to critical damping.

Measurements were taken to determine flux sensitivity and the results are indicated below.

Ig of .1715 milliamps gave a steady state deflection of 66.8 mm. T_o was determined to be 19.58 sec. R_c (CDRX) was measured as 12,000. Open circuit relative damping was calculated to be .0309 and the actual relative damping with a circuit resistance of 2200 ohms was calculated to be 4.5. These figures give

$$\gamma S_{\phi_N} = \left(\frac{66.8}{171.5 \times 10^{-6}}\right) \times \frac{2\pi}{19.6} \times \frac{1}{12,000} \times \frac{4.5 - .031}{1 - .031} \times \frac{1}{2 \times 4.5} = 5.5 \frac{\text{mm}}{\text{weber}}$$

That this is the maximum which can be obtained without introducing a shunt resistor at the galvanometer terminals is readily apparent when it is observed that the external resistance for the galvanometer consisted of the ohmic resistance of the specimen secondaries, the lead resistance, and the resistance of the Standard Mutual Inductor secondary (9.94 ohms). This total resistance in series was roughly 15 ohms.

Referring to Figure 4, page 318, of Harris(10), it is seen that the relative flux sensitivity, actual to maximum, for the above values was about 94%. Since the addition of a

low resistance shunt to improve flux-linkage sensitivity by increasing relative damping could not improve the sensitivity appreciably but would decrease the deflection for a given impulse, no shunt was used.

The discussion above is based on the assumption that a simple instantaneous impulse was used. Actually, as may be seen by reference to Figures 54, 55 and 56, a double pulse was used. The two pulses were separated by as much as 15 milliseconds. In some cases the duration of the pulse was about 30 milliseconds. Figures 54, 55 and 56 are typical pulses. The double-pulse results when the exciting current is changed from −1 to 0 then from 0 to +1 in one throw of a DPDT switch.

That this double pulse is practically equivalent to a single instantaneous pulse when used with this galvanometer is evident from a study of Harris(10, pp. 321-326). The double impulse was considerably less than the time required for the galvanometer to reach maximum deflection (about one second).

In addition to increasing flux-linkage sensitivity the over-damping permitted faster readings due to the rapid deflection of the galvanometer. At the top of the swing the galvanometer tended also to "hold" which permitted somewhat more accurate readings. The elimination of shunt and series control resistances permitted a considerable reduction of thermal and contact emf effects.

Figure 54

3/24/54

Two pictures at
[illegible] voltage [illegible]
35mm Camera Settings:
① Bulb at f/11 X=15~/cm
② Bulb at f/11 X=15~/cm
③ Bulb at f/2.8 X=50~/cm

Y scale 5 ms/cm

Tektronix 512 Serial 2159
① $\Delta I = +1.0\alpha$ to $+0.5\alpha$
(2) $\Delta I = -1.0\alpha$ to $+1.0\alpha$
$\Delta I = -1.0\alpha$ to $+1.$ [illegible]

Figure 55

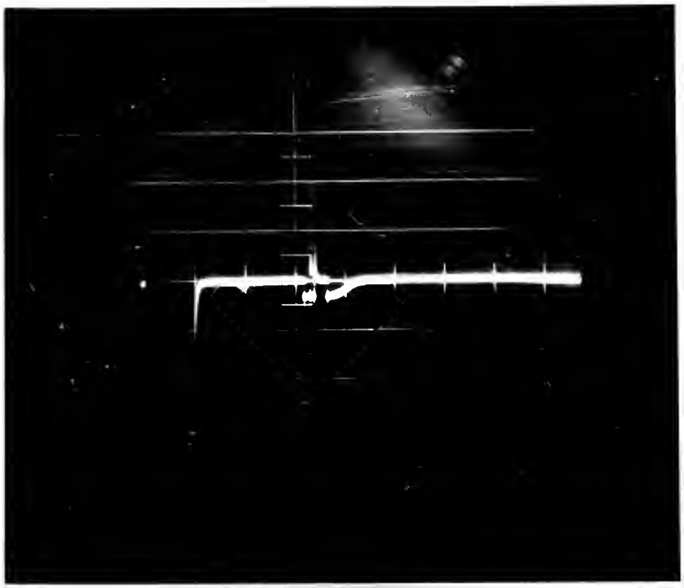

Figure 56

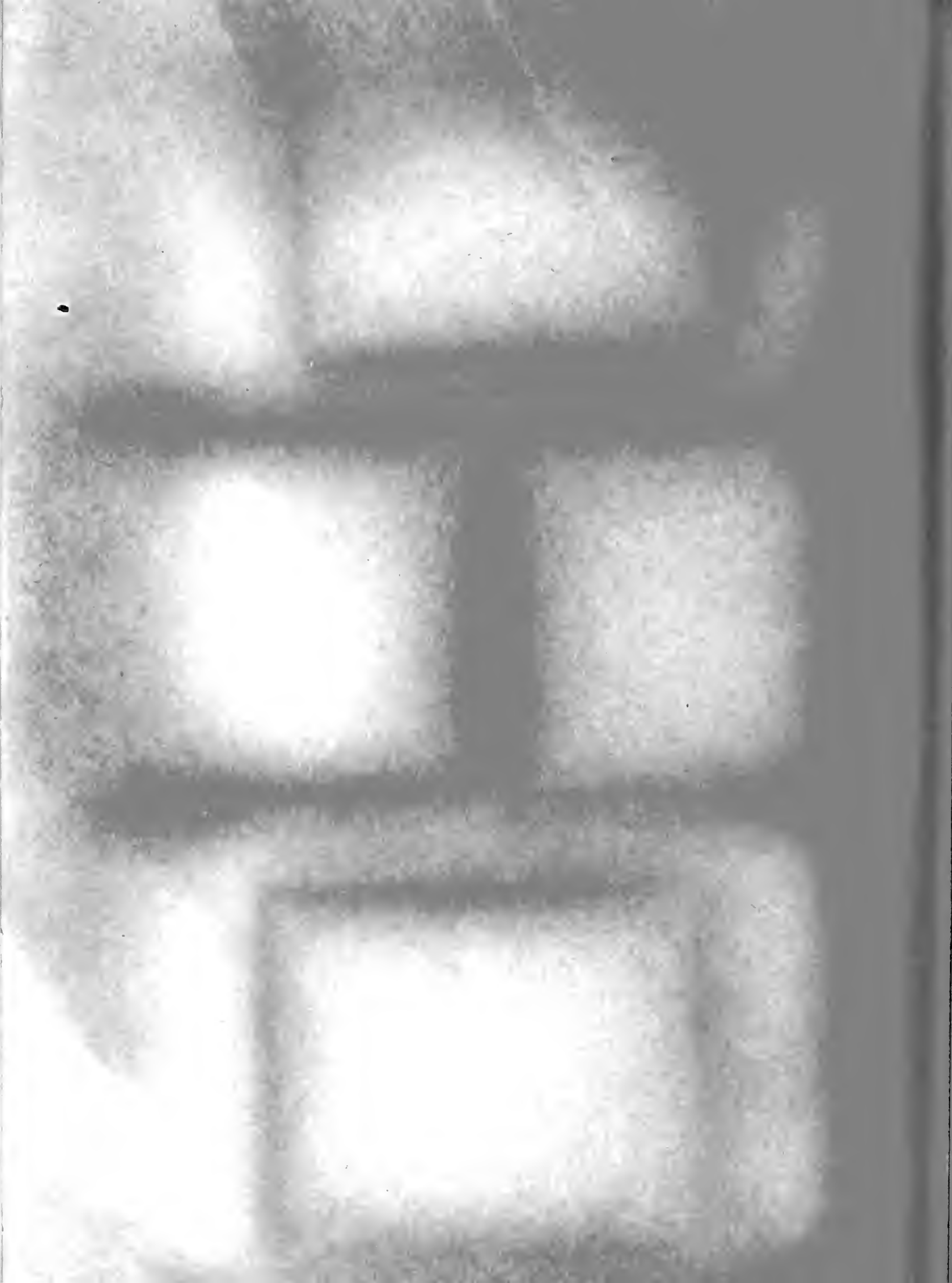

The calibration of the galvanometer was effected as analyzed below:

$$\theta_\phi = \int_{t_1}^{t_2} e\,dt$$

provided the duration of e is less than the time required for the galvanometer to reach the point of maximum deflection.

When

$$e_x = e_c$$

and

$$t_{x_2} - t_{x_1} = t_{c_2} - t_{c_1}$$

then

$$\theta_x = \theta_c$$

Now

$$e_x = -N_x \frac{d\Phi_x}{dt} = -N_x A_x \frac{dB_x}{dt}$$

and

$$e_c = -N_c \frac{d\Phi_c}{dt} = -N_c A_c \frac{dB_c}{dt}$$

Substituting

$$B_c = \mu_o \mu_r H_p = \mu_o \mu_r \frac{N_P I_P}{l_p}$$

Gives

$$e_c = -N_c A_c \mu_o \frac{d(\mu_r N_P I_P / l_P)}{dt}$$

and for the air cored Mutual Inductance Coil

$$\mu_r \doteq 1$$
$$N_P \neq f(t)$$
$$l_P \neq f(t)$$

Therefore

$$e_c = -\mu_o N_c A_c \left(\frac{N_P}{l_P}\right) \frac{dI_P}{dt}$$

Setting

$$e_x = e_c \frac{\Delta \theta_x}{\Delta \theta_c}$$

Then

$$-N_x A_x \frac{dB_x}{dt} = -N_c A_c \mu_0 \left(\frac{N_p}{\ell_p}\right) \frac{dI_p}{dt} \frac{\Delta \theta_x}{\Delta \theta_c}$$

$$dB_x = \frac{N_c A_c}{N_x A_x} \mu_0 \left(\frac{N_p}{\ell_p}\right) dI_p \frac{\Delta \theta_x}{\Delta \theta_c}$$

or

$$\Delta B_x = \left(\frac{N_c A_c}{N_x A_x}\right) (\mu_0) \left(\frac{N_p}{\ell_p}\right) \left(\frac{\Delta I_p}{\Delta \theta_c}\right) \Delta \theta_x$$

Now

$$\mu_0 = 4\pi \times 10^{-7}$$

$N_c A_c = .0803\pi$ turn-m^2

$N_x A_x = .00685$ turn-m^2 (Specimens E and F)

$\frac{N_p}{\ell_p} = 594$ turns/meter

Hence

$$\Delta B_x = \left(\frac{.0803\pi}{N_x A_x}\right) (4\pi \times 10^{-7}) (594) \left(\frac{\Delta I_p}{\Delta \theta_c}\right) \Delta \theta_x$$

$$= \frac{1.872 \times 10^{-4}}{N_x A_x} \left(\frac{\Delta I_p}{\Delta \theta_c}\right) \Delta \theta_x$$

$$\Delta B_x = .02750 \left(\frac{\Delta I_p}{\Delta \theta_c}\right) \Delta \theta_x$$

$\frac{\Delta I_p}{\Delta \theta_c}$ was determined from a calibration test to be .6054 amperes/mm as may be seen from Figure 57.

Hence

$$\Delta B_x = .0275 \times .6054 \ \Delta \theta_x = .0166 \ \Delta \theta_x$$

With two cores in series

$$\Delta B_{x_{each}} = \frac{1}{2} \Delta B_x = 8.32 \cdot 10^{-3} \Delta \theta_x \ \frac{\text{webers}}{\text{m}^2}$$

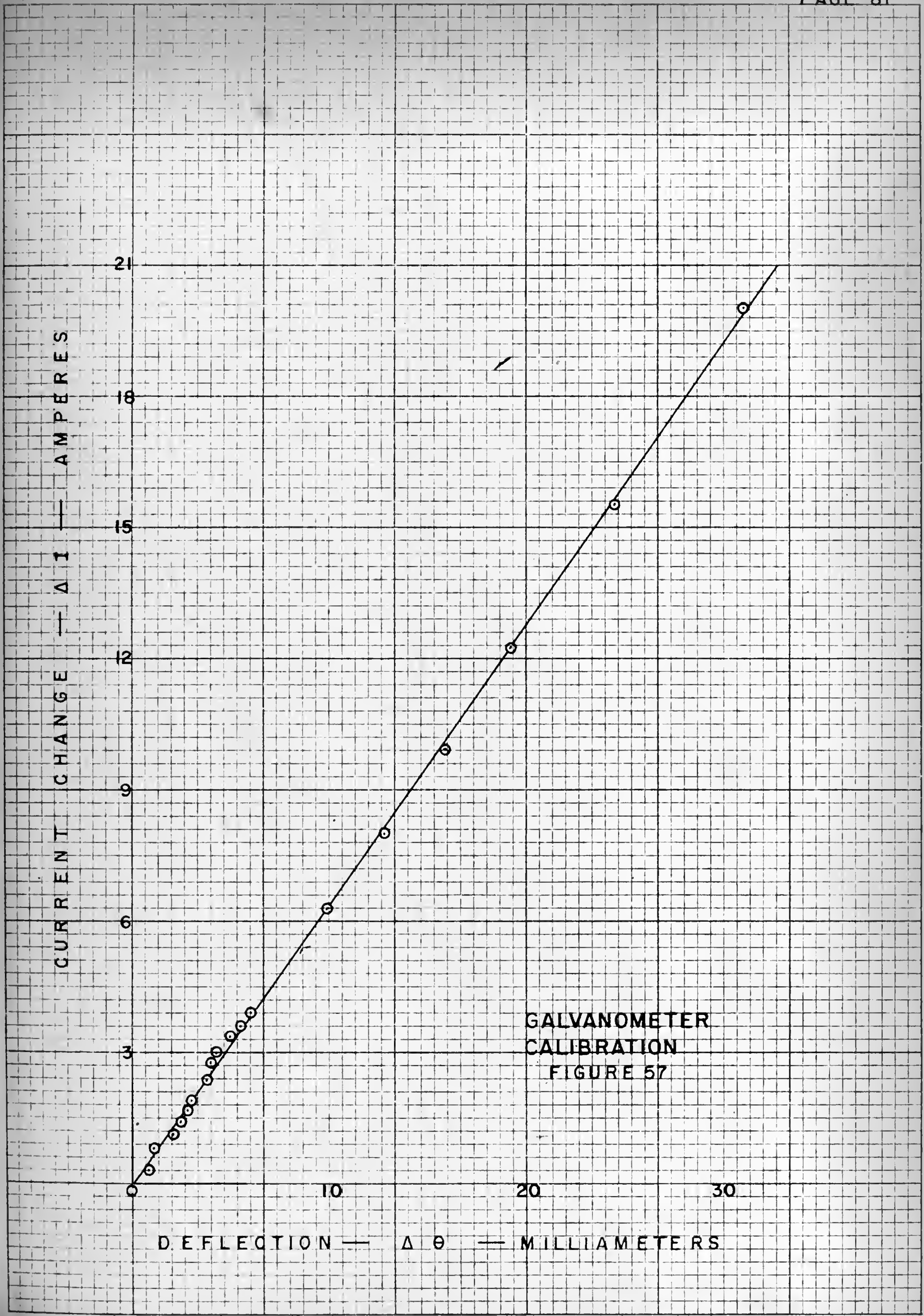

GALVANOMETER CALIBRATION
FIGURE 57

APPENDIX C

CIRCUITS AND LAYOUTS

Photographs of the layouts used are Figures 58, 59 and 60. Figure 58 shows the D.C. layout for taking data for hysteresis loops as seen from the operator's position. Under the table is shown part of one of the generators of the Harmonic Generator set, a General Electric Company set number 83, driven by a variable speed D.C. motor and having six generators: a 5KVA fundamental, a 2KVA 2nd harmonic, a 2KVA 3rd harmonic, a 1KVA 5th harmonic, and a 1KVA 7th harmonic. On the near left table is shown one of the General Radio V20 HM 230v, 8 amp, Variacs used to control A.C. exciting current. The standard resistance of .100 ohm and the DuMont Type 304H CRO with a DuMont Type 264-B Voltage Calibrator are not shown. These were used to measure maximum values of A.C. exciting current from which was calculated the maximum applied alternating magnetizing force. On the center table is shown a Weston A.C. ammeter for monitoring A.C. current in the position normally used. The center board on which are mounted the switches and junctions required for control of the D.C. exciting current was constructed by C.E. Baker, EM2, USN, and E.T. Kozol, IC3, USN, in accordance with a sketch prepared by the authors. On the right near edge is the Weston Model 45 2-ampere D.C. ammeter, serial 24667, used to measure values of D.C. magnetizing current. Other D.C. ammeters used were also Weston Model 45 ammeters. These

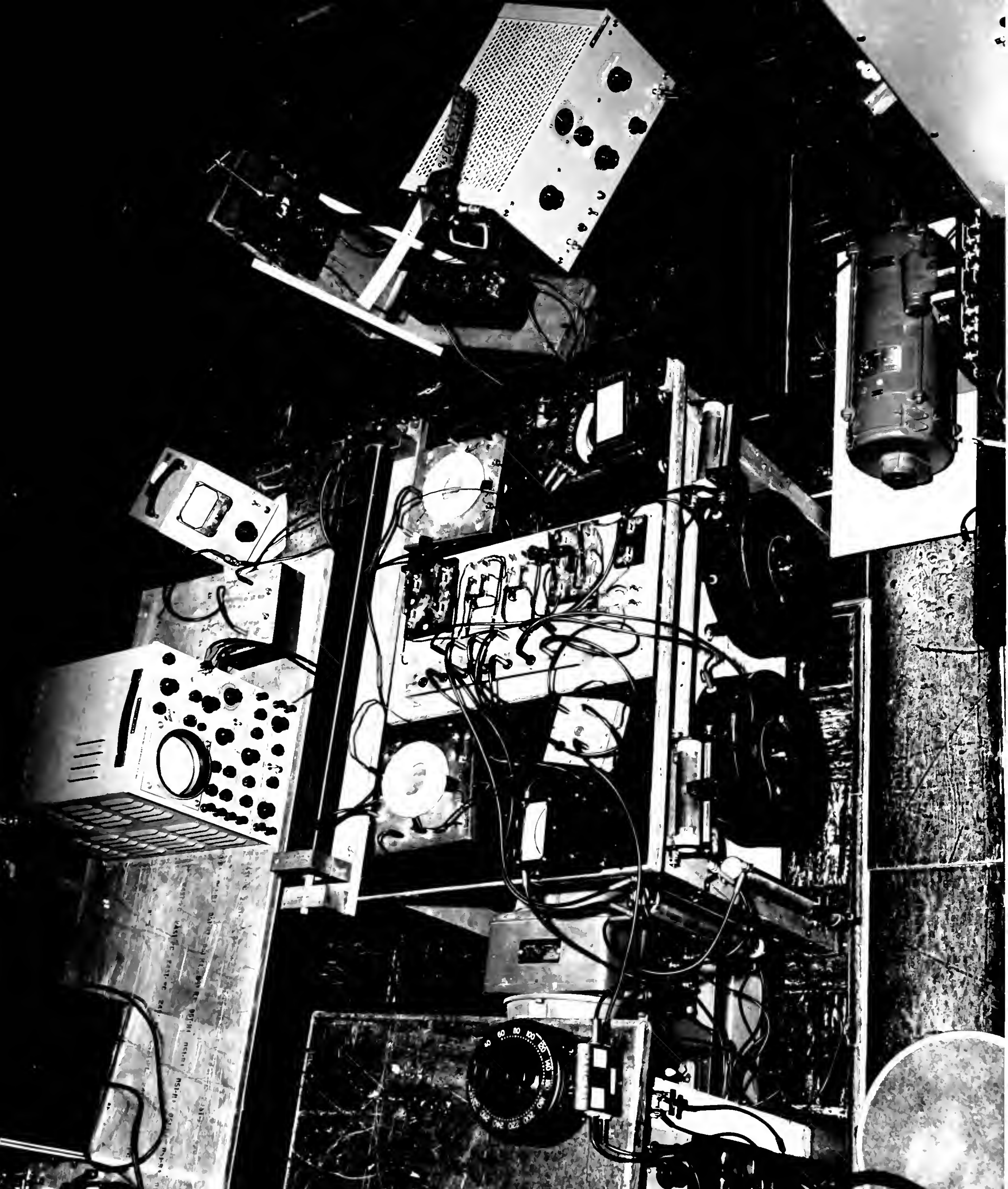

FIGURE 58

PHOTOGRAPH OF LAYOUT FOR
OBTAINING STATIC HYSTERESIS LOOPS

were a 1-ampere meter, serial 30016, and a 5-ampere meter (for calibration purposes), serial 29558. The very back of this table holds the Calibration Mutual Inductor described in Appendix B, Figure 53. The two white rings seen are specimens C and D. The table in the background holds one Tektronix CRO's used and one of the VTVM's used to check the galvanometer circuit for an excess of A.C. voltage, as discussed in Appendix B. On the right and on a separate table to avoid the vibration experienced on the center table and to avoid the possibility of error by stray flux sets the Leed & Northrup Type 2239-D galvanometer. On the galvanometer stand is the General Radio Company. Decade Resistor Type 1432-L, Serial 2992, set at 12,000 ohms and used as a CDRX for the galvanometer. Not clearly shown but setting between the D.C. ammeter and the right-hand specimen are the two L&N copper contact DPDT switches used in the galvanometer circuit. Mounted on the front of the center table are the two pairs of resistors, the right pair being R1 and the left pair being R2, used in the D.C. exciting current circuit. The two slide-wire resistance shown mounted vertically at the left leg of this table were used when larger values of current were required for calibration. Two items shown but not used are the Hewlett-Packard Function Generator to the right of the galvanometer and the General Electric Amplidyne Generator on the floor to the right.

Figure 59 shows the layout used for making dynamic measurements. Under the table to the right may be seen the

FIGURE 59

PHOTOGRAPH OF LAYOUT
FOR DYNAMIC MEASUREMENTS

Westinghouse Electric Company Signal Corps type TR 6 B 3-KVA 60 c.p.s. Isolation Transformer used to supply the five-outlet panel attached to the table. This panel then supplied all the equipment shown, except the D.C. Power Packs, and permitted grounding all equipment to a common ground. The grey box on the floor next to the Isolation Transformer is a Sorensen Regulator Model 1000, Serial 451, used to supply power to the two DuMont Type 304H CRO's shown on the table. This Regulator served to reduce the drift of the trace caused by fluctuations of CRO supply voltage. On the floor to the left of the Regulator is seen the elements of the series-resonant circuit used to obtain sine wave exciting current to excite the specimens for various tests. It consists of a bank of Westinghouse Inerteen Capacitors, Style 1491080C, 3 phase, 2-KVAR, 60 c.p.s. 460v ratings. Four of these elements gave 34.4 mf of capacitance. Three of the cylindrical air-cored inductors rated at 35 mh each were used to give about 100 mh of inductance. On the far right may be seen the General Radio Wave Analyzer GR 736-A Serial 1492 used to determine the purity of sine wave currents and voltages.

Figure 60 is a closer view of the central components of Figure 59. In it may be seen the two D.C. power packes used to furnish power to the Boeing D.C. amplifier used in the Integrator (just to the left of the lower CRO). Behind the power packs to the left is one of the VTVM's used to determine RMS voltages in various parts of the circuit. Under the Boeing

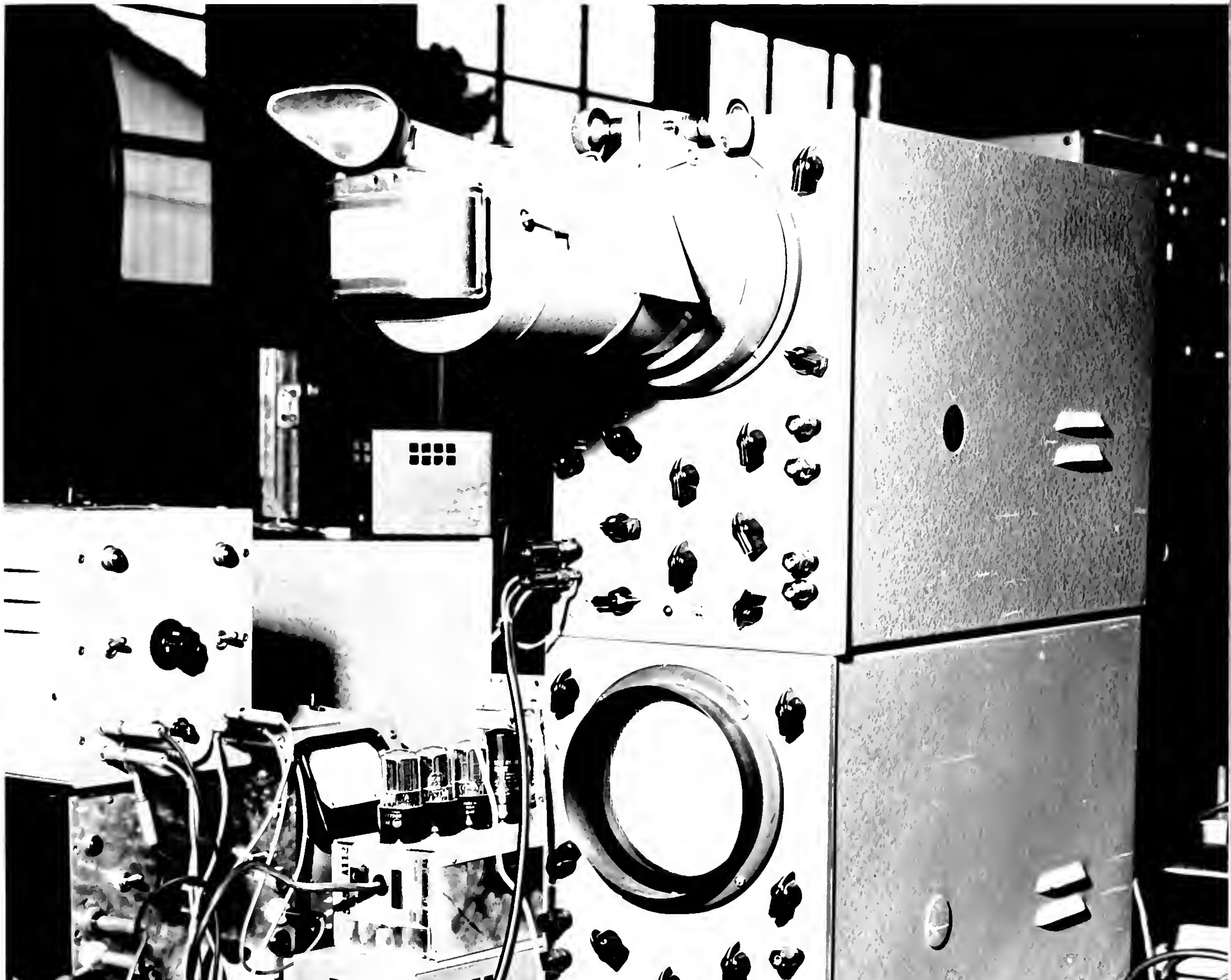

FIGURE 60
DETAILED PHOTOGRAPH OF
LAYOUT FOR DYNAMIC MEASUREMENTS

Amplifier (the device showing all the tubes) is the DuMont Voltage Calibrator Type 264-B, Serial 3350, used to calibrate the CRO's as described in Appendix D. The bottom DuMont type 304-H CRO shown was used only for its D.C. vertical-axis amplifier. The input to this amplifier was from a .500 ohm nichrome wire resistance mounted under the table; the high currents passing through this resistance caused it to get dangerously hot. The output from this amplifier was connected at the rear of the CRO to the horizontal-axis plates of the top CRO. The top CRO, Serial 7860, was used extensively in the taking of data for the dynamic testing portion of this thesis. The camera seen attached to the top CRO is the 35mm camera discussed in Appendix E. Exciting current control was accomplished by use of the Variac seen at the right of the picture. The Weston Model 433 5/20/50 A.C. ammeter seen was used to insure that too high currents were not used.

The various circuits used are shown in Figures 61, 62, 63 and 64. The galvanometer circuit, the use of which is comprehensively discussed in Appendix B, is shown in Figure 61. All connections are copper-to-copper except for the connections to the terminals of the galvanometer itself. No thermal or contact emf's could be detected, however, in this circuit. Note that the calibration circuit was connected for use by throwing the selector switch, S3.

Figure 62 is the circuit used for applying D.C. to the

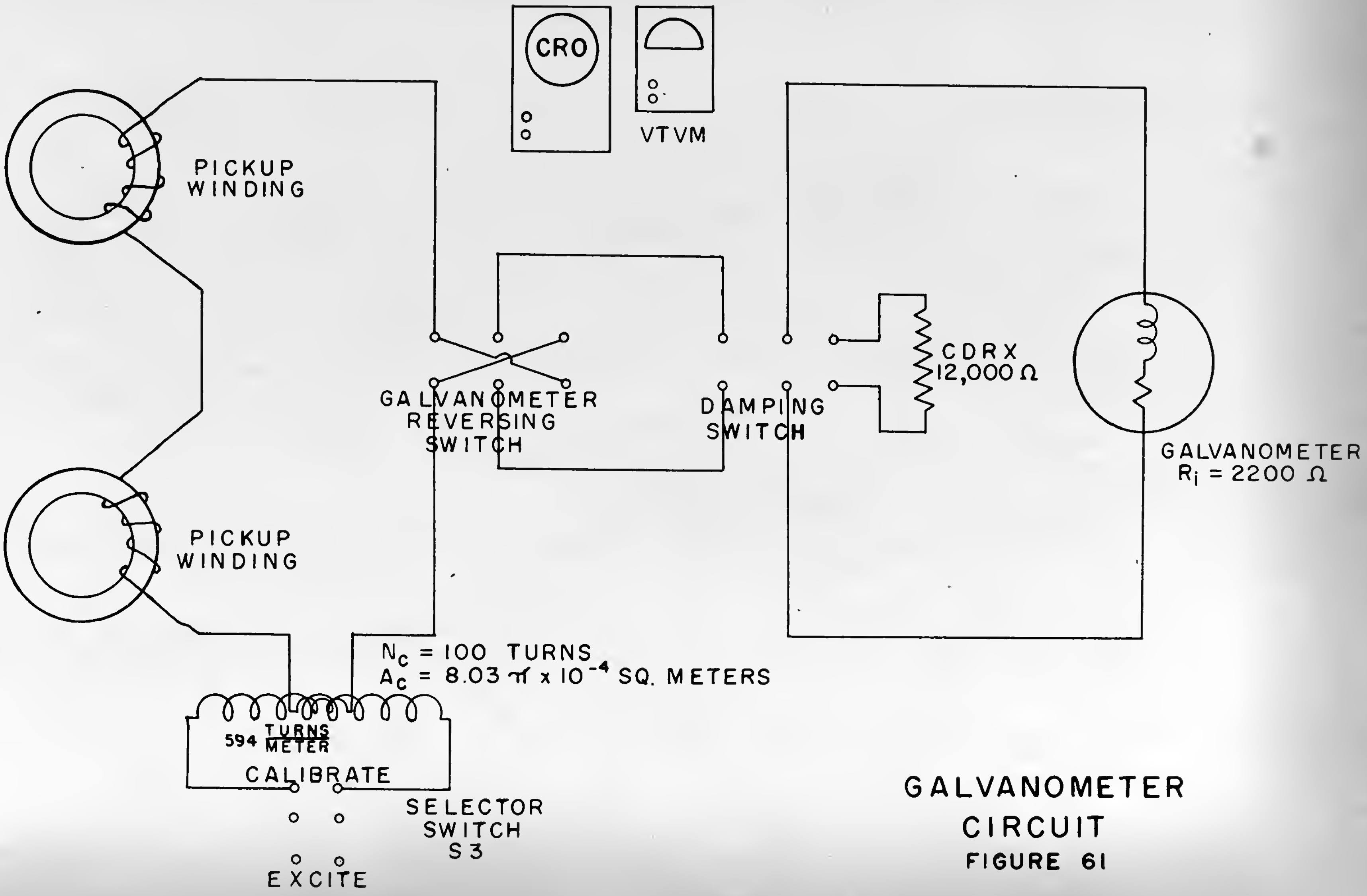

GALVANOMETER CIRCUIT
FIGURE 61

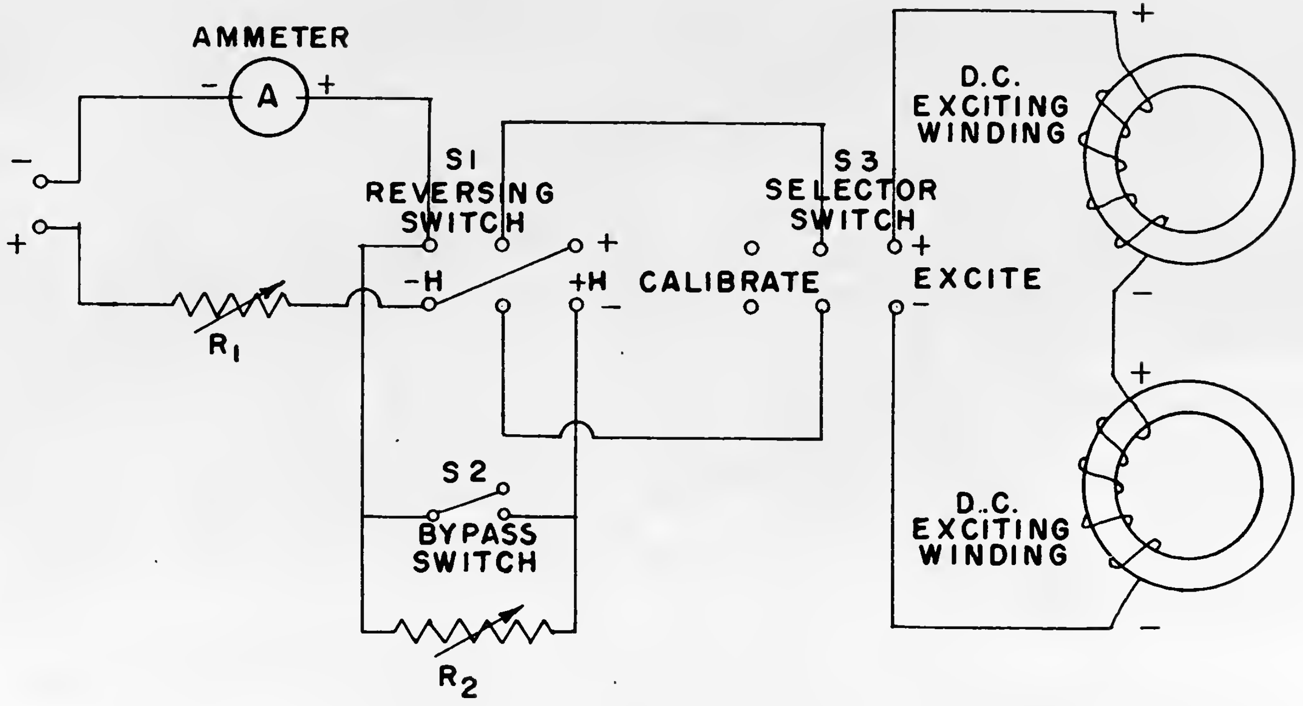

D.C. CIRCUIT

FIGURE 62

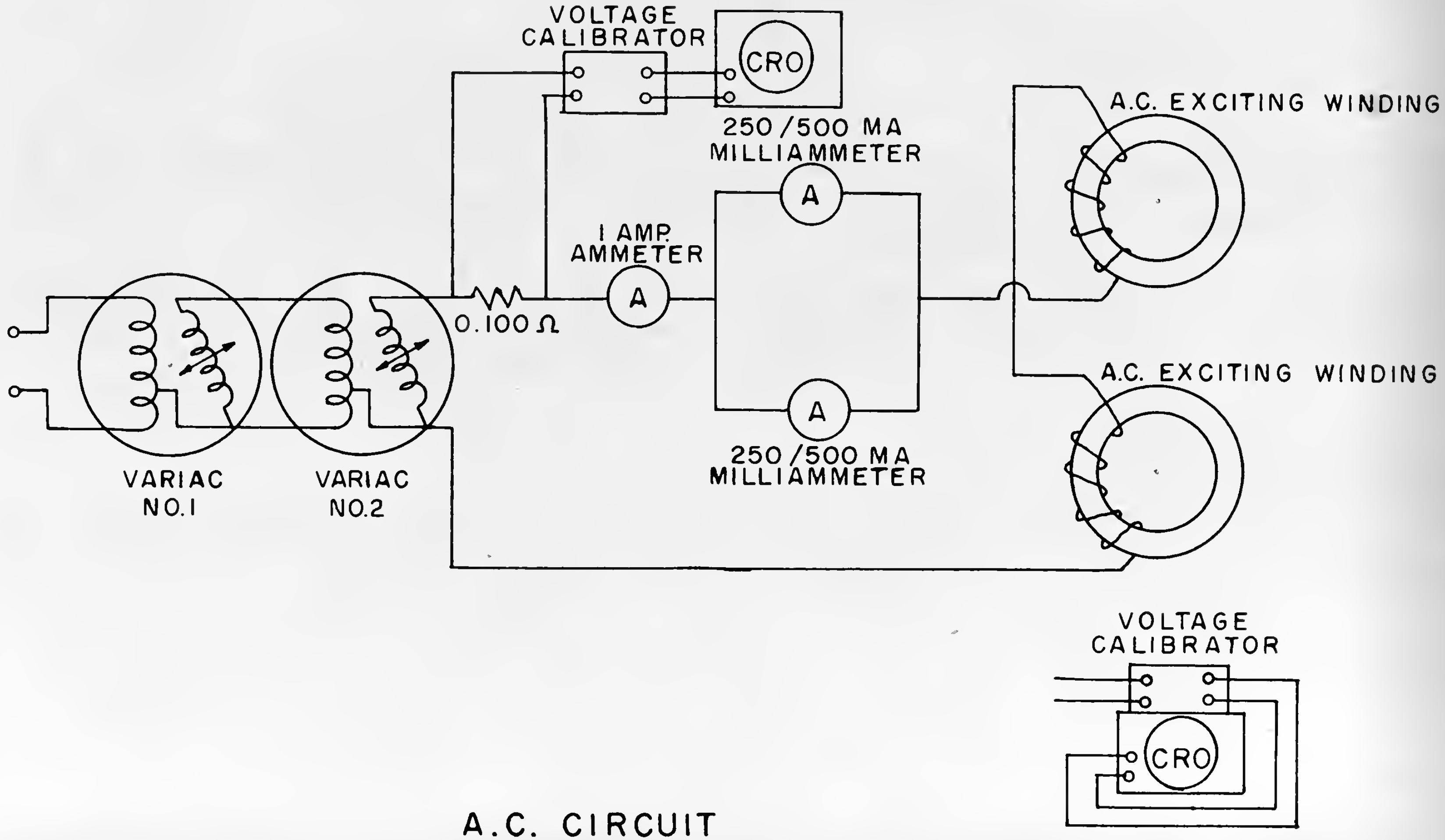

A.C. CIRCUIT

FIGURE 63

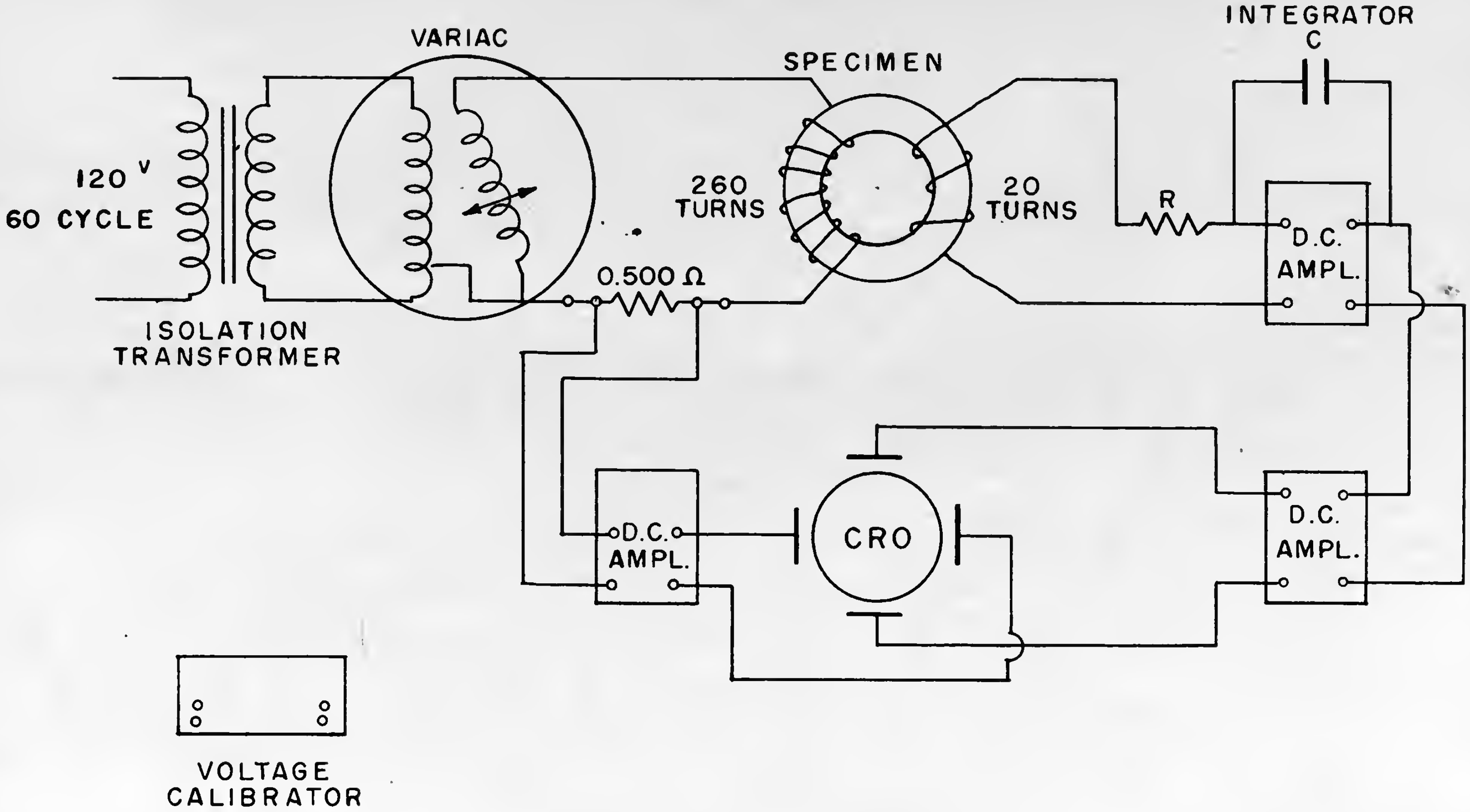

CIRCUIT FOR
DYNAMIC HYSTERESIS
LOOP

FIGURE 64

D.C. exciting windings and for accomplishing the control described in Appendix B. The D.C. current source was a Western Electric 6.75 KW D.C. generator, Type M5, Serial 384099, rated for 255 ampere at 1200 RPM.

As can be seen in Figure 63 the A.C. exciting current was supplied through two Variacs. The distortion introduced by these Variacs was negligible, as was determined by a thorough test conducted with the Wave Analyzer. Even at low currents at 300 c.p.s. no appreciable distortion which could be attributed to this use of the Variacs could be detected. Although three ammeters are shown in the A.C. circuit, these were not used for primary measurement of applied A.C. current. Since the maximum alternating magnetizing force and the wave shape were the items of interest in this experiment, the .100 ohm resistor, the Voltage Calibrator, and the CRO served as the primary means of measuring and observing this current.

The 60 c.p.s. hysteresis loops obtained were taken by means of the circuit shown in Figure 64. Another way of obtaining a "hysteresis loop" was to integrate the very peaked voltage appearing when a sine wave exciting current was used to excite the primary of the specimen. This integrated voltage was shown together with this sine wave current. Figure 74 of Appendix E shows the result, and according to Lord(11) this cannot be the true hysteresis loop for reasons he gives. The circuit to obtain these figures, less the integrator, is similar to that shown in Figure 49. The value of "R" used in the Integrator was the 1.00 megohm input resistor of the Boeing

Analog Computer amplifier, while the feed-back capacitor used was .00263 microfarad in value.

Not shown in these figures for the reasons that results obtained were unsatisfactory and of no added value to this thesis is the Pulse Generator built by these investigators according to a wiring diagram given in Siskind(13). This Pulse Generator works very well, but due to other difficulties and to lack of time to correct them was never used in this work. The original intent was to apply the output of this Pulse Generator to the Z-axis of the CRO. This would serve to make a spot on the trace of the Lissajous figure. By calibrating or by other means the horizontal position of this spot could be made to give quite accurate readings on the X-axis of the CRO. The position of the spot was moved by means of a phase shifting synchro which fed into the input of the Pulse Generator.

Discussed in Appendix D is an Integrator built by these investigators according to a wiring diagram presented also by Siskind. This figure is not presented here, either, since results obtained using this integrator were disappointing and since a much better integrator; namely, the Boeing Analog Computer, was available to these investigators.

APPENDIX D

ASSOCIATED EQUIPMENT

CATHODE RAY OSCILLOGRAPHS (CRO)

Three types of CRO's were used during this investigation: the DUMONT TYPE 304H, the TEKTRONIX TYPE 512, and the TEKTRONIX TYPE 511 AD.

Some various uses to which these CRO's were put are listed below:

1. Present Lissajous figures of hysteresis loops, differential permeability plots, and difference voltage plots.
2. Determine peak values of currents and voltages.
3. Observe A.C. voltage appearing in galvanometer circuits.
4. Record pulse shape in galvanometer circuit.
5. As D.C. amplifiers.
6. To aid in selecting matched specimens.
7. To determine distortion limits of wave forms, visible deviation from a sine wave being taken as 2% distortion.
8. Calibrate phase shift dials on Harmonic Generator.

Except for items 1 and 5 these uses are mentioned elsewhere in some detail.

Hoping to avoid the phase distortion effects discussed by LORD(11) these experimenters, with the technical assis-

tance of Harmony MINOR, arranged for the X amplifier and the Y amplifier (MMF and Flux Density scales respectively) to be the same type amplifier, namely, the vertical amplifier of the DUMONT 304H CRO. All other inputs of the cathode ray tube were disconnected and these amplifiers connected to the vertical and horizontal deflection plates.

Due to lack of time no effort was made to determine the phase shift characteristics of these amplifiers nor their frequency response characteristics. It was thought that to a first approximation these effects would be negligible.

Another effect which should be considered is the fact that the vertical and horizontal deflection plates are at different positions along the cathode ray tube. The relative position of these plates may or may not have some effect on the distortion of the Lissajous figure. The TEKTRONIX CRO's proved unsatisfactory for taking dynamic hysteresis loops because the grid presentation was unstable and because the horizontal volts/cm amplification was not adequate. However, a better CRO than the available DUMONT 304H is to be preferred.

APPENDIX E

DYNAMIC TESTING

This appendix is devoted to the presentation of the meager results obtained by these experimenters in the attempt to extend this study to a consideration of what happens when a higher frequency is superposed on the A.C. hysteresis loop. It was hoped that this problem could be attacked from the standpoint of the effect on the differential permeability curve (as approximated by Figure 73) on superposing an alternating magnetizing force. It was decided that specimens much more carefully matched than were the ones available to these investigators would have to be obtained and that much greater refinements to the method of obtaining a Lissajous figure of the differential permeability loop than presented by Siskind(13) would have to be developed. Although this was perhaps the more interesting part of the thesis, lack of time to accomplish the necessary refinements forced the omission of this portion.

Figure 65 is simply a photograph of a series of Lissajous figures which approximate successive hysteresis loops taken at 60 c.p.s. It is included only for the purpose of showing what can be done using the DuMont CRO and CRO Record Camera in this connection. Notice that apparently the successive presentations shifted to the left between each exposure.

Figure 65

Series of 60 Cycle Hysteresis Loops

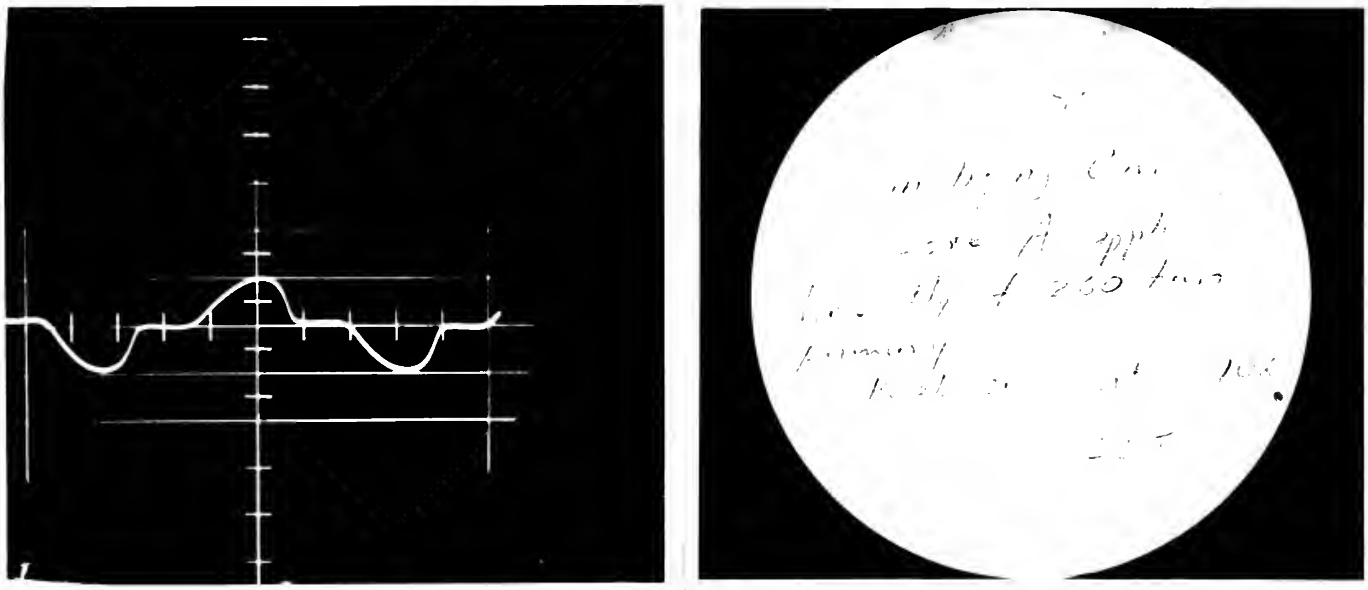

[illegible] Current

[illegible] Applied

[illegible] of 250 turn

primary

Peak [illegible] 10a

[illegible]

Figure 66

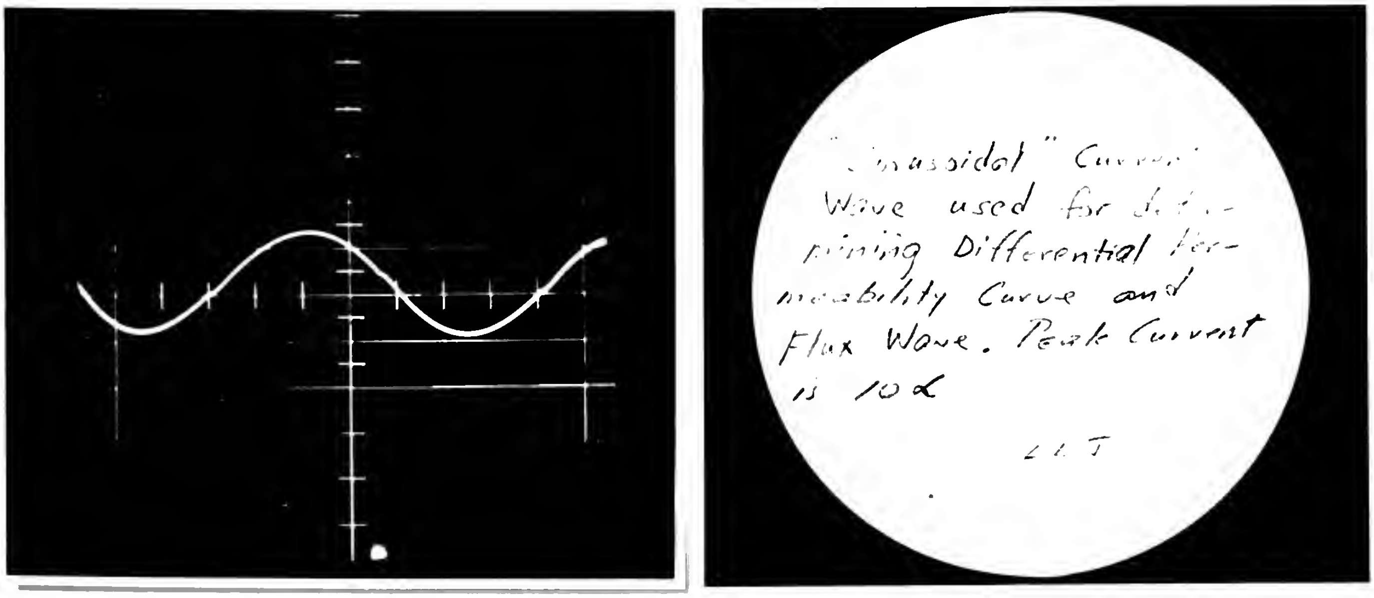

"Sinusoidal" Current Wave used for determining Differential Permeability Curve and Flux Wave. Peak Current is 10a

LLT

Figure 67

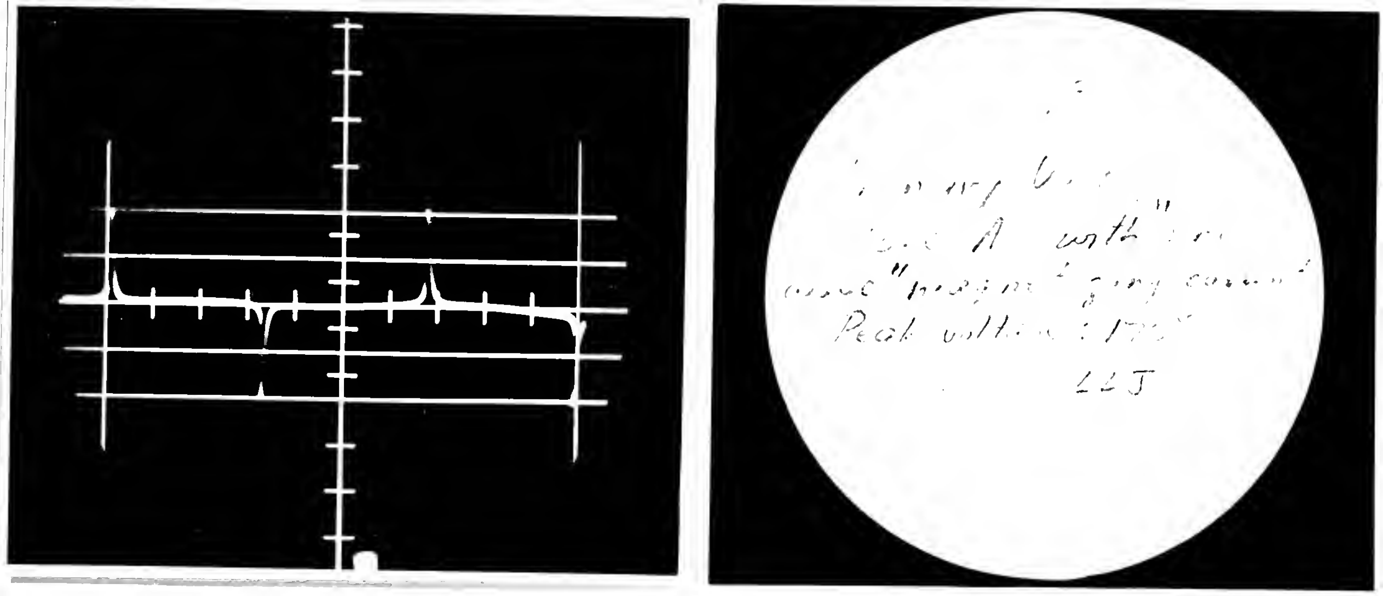

[illegible] A with [illegible]
[illegible] "[illegible]" [illegible]
Peak voltage: 17[illegible]
LLJ

Figure 68

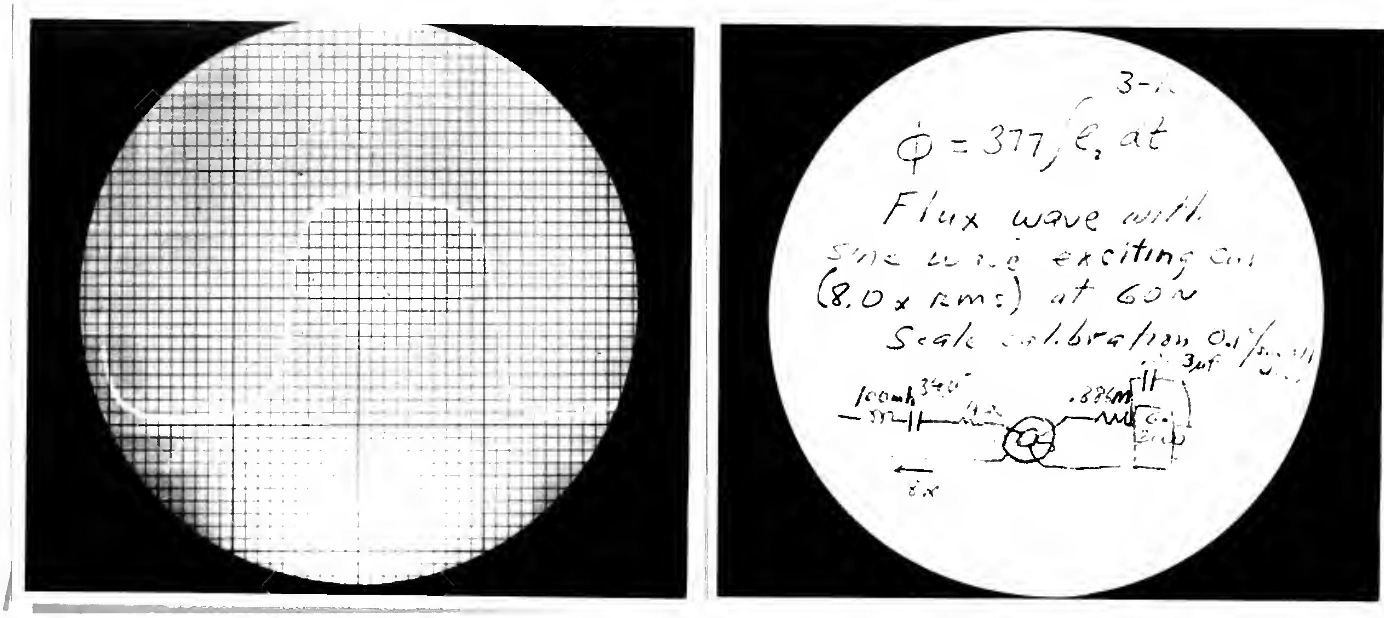

3-[illegible]

$\Phi = 377\int e_2\, dt$

Flux wave with
sine wave exciting current
(8.0 ma rms) at 60~
Scale calibration 0.1 [illegible]

Figure 69

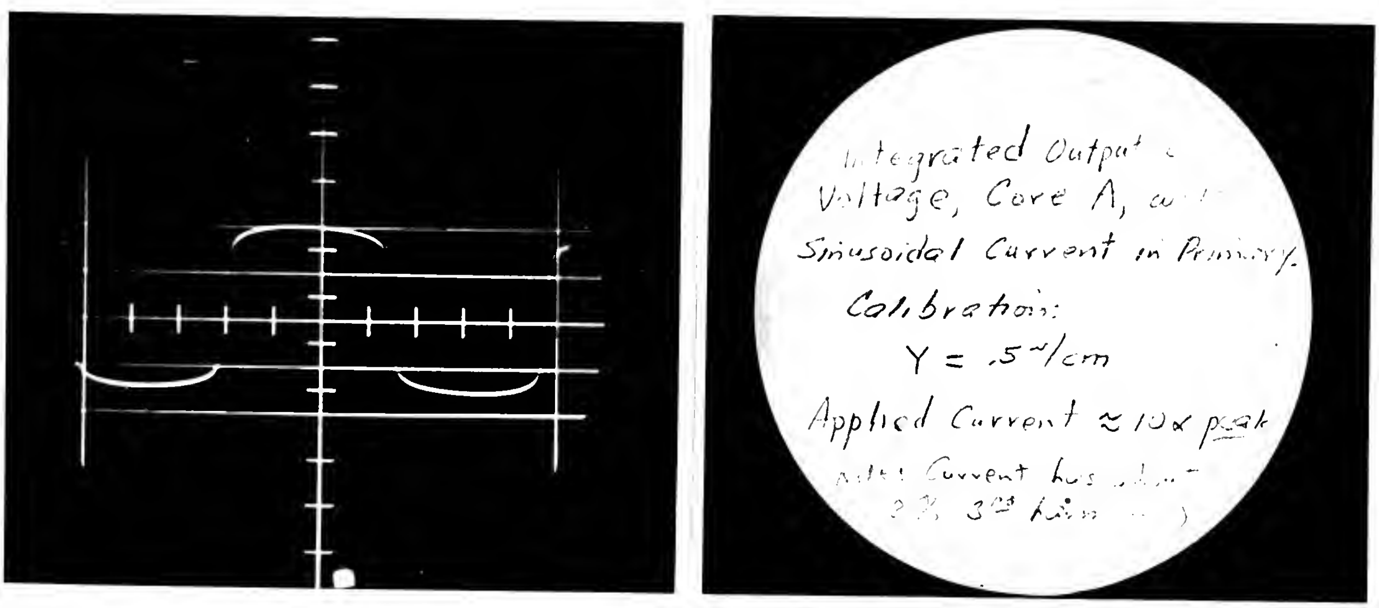

Integrated Output
Voltage, Core A, with
Sinusoidal Current in Primary.
Calibration:
Y = .5~/cm
Applied Current ≈ 10ma peak
(Note: Current has about
2% 3rd harm[illegible])

Figure 70

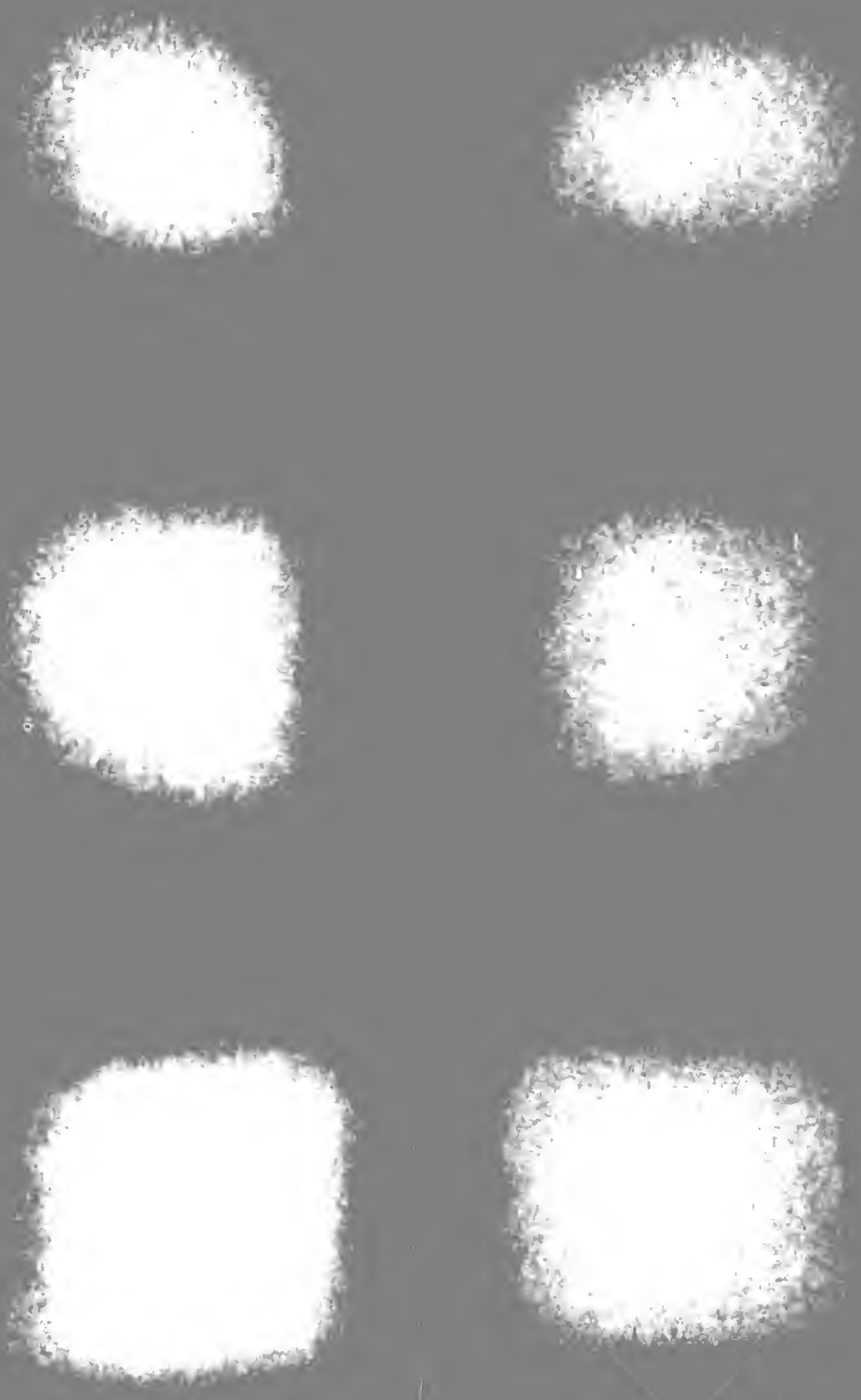

The succeeding Figures, 66 through 70, tell a story the background of which may be found in Siskind(13) and Lord(11). When a sine wave voltage is applied to the primary of Specimen E, the resultant current is that shown in Figure 66. However, when this current is filtered through a series-resonant circuit, resonant at 60 c.p.s. in this case, the current is that shown in Figure 67. The slight harmonic seen in this wave was determined to be primarily a third of about 2% value. This is contrary to what was expected from a consideration of Siskind(13). The voltage associated with this current is that shown by Figure 68. This same voltage, reduced in magnitude, appeared in the secondary. Integration of this voltage gives the flux wave shown in Figures 69 and 70. The difference between these waves is that they were taken using two different CRO's. Figure 70, was taken using a DuMont CRO, while Figure 69 was taken using a Tektronix CRO.

When the highly peaked output voltage shown in Figure 68 is plotted on the CRO against the sine wave current of Figure 67, the resulting Lissajous figure resulting is similar to what Siskind (13) refers to as a differential permeability curve (see Figure 73). That this is not the case here can be appreciated by a reference to Siskind's derivation of the differential permeability curve. The applied current must be a sine wave of such a magnitude that the iron is fully saturated within a few degrees of the zero crossing of the axis of the sine wave current. Figure 67 shows that here such is not

the case.

Plotting the flux wave of Figure 69 against the sine wave current of Figure 67 gives what appears to be the hysteresis loop (at 60 c.p.s.) of this specimen, Figure 74. But Figure 75 shows another Lissajous figure of the same specimen, and this apparent hysteresis loop is different from that of Figure 74. The presentation of Figure 75 was obtained by applying a sine wave voltage to the specimen, integrating the sine wave voltage output (60 c.p.s.), and plotting this against the normal magnetizing current similar to that of Figure 66. According to Lord(11) the Lissajous figure of Figure 74 is the one in error. This may be due to the eddy current effects of the higher harmonics of flux operating in the core when the sine wave current is used. A further study of Lord(11) indicates that not even Figure 75 is the true hysteresis loop of the specimen, since these experimenters did not take the pains indicated by Lord that are necessary to insure a true hysteresis loop.

The following sections deal with the theory of electronic integration, the use of an amplifier constructed by these investigators, and means of calibrating a DuMont Type 304-H CRO for magnetizing force (H) and flux density (B) readings.

Integration -- Theory

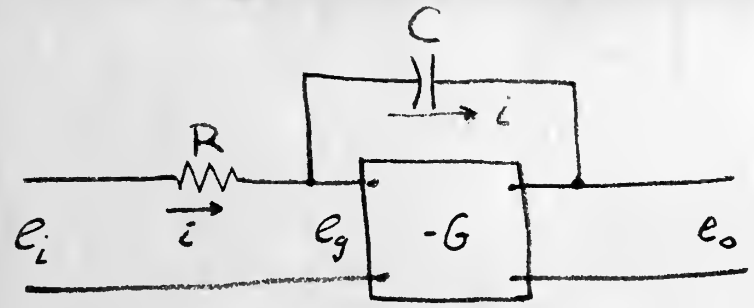

It is assumed that since the input to the amplifier is a vacuum tube no current will flow at Eg.

It is also assumed that a phase inversion occurs in the amplifier, so that gain, G, is negative.

By definition

1. $$-G \triangleq \frac{e_o}{e_g}$$

Also

2. $$e_i = iR + e_g$$

3. $$e_g = e_o + i\frac{1}{j\omega C}$$

Substituting for eg

4. $$e_i = iR - \frac{e_o}{G}$$

5. $$-\frac{e_o}{G} = e_o + i\frac{1}{j\omega C}$$

6. $$i = -e_o\frac{j\omega C(1+G)}{G}$$

7. $$e_i = -e_o \frac{j\omega RC(1+G)}{G} - \frac{e_o}{G}$$

8. $$\frac{e_o}{e_i} = \frac{-G}{j\omega RC(1+G) + 1}$$

9. $$= -\left(\frac{G}{1+G}\right) \frac{1}{j\omega RC + \frac{1}{1+G}}$$

10. $$= -\frac{G}{(1+G)RC} \frac{1}{j\omega + \frac{1}{(1+G)RC}}$$

In the usual form this equation is

$$KG \triangleq \frac{e_o(s)}{e_i(s)} = -\frac{G}{1+G}\left[\frac{1}{s\tau + \frac{1}{1+G}}\right]$$

For large values of G (values of about 2000 were actually used):

$$KG \doteq -\frac{1}{s\tau}$$

which is the equation for pure integration.

However Lord(11) observes that the amplifier must not be permitted to introduce phase shift into the circuit, otherwise the Lissajous figure to represent, say, a dynamic hysteresis loop will be in error.

Integrator -- Construction

The integrator is described by Siskind(13) as a Miller effect integrator. It uses two pentodes, both 7G7, although 6AH6, 7V7, 7H7, 7C7 and many other sharp-cut-off pentodes could be used. One criterion in the application is high gain. The 7G7 has an approximate plate resistance of 0.8 Megohn and a gm of 4500 micromhos, giving a product of 3600.

The amplifier is a "starved pentode" feeding a cathode follower. The pentode is "starved" by working it into a very high plate load, 11½ megohms. This permits realization of the high gain feature of the pentode as a class A1 amplifier. The output of this stage feeds into the second stage which is connected as a cathode follower. Although this reduces the overall gain such an arrangement is necessary to enable one to handle the RC feedback loop for various values of C and R without overloading the amplifier. Also, with this arrangement oscillation difficulties are considerably reduced. The effect is high gain with one phase inversion.

The gain of this amplifier was measured with no feedback and a 60 c.p.s. input signal. For an input signal of 10 millivolts the output was 26 volts giving a gain of 2600. Increasing the input signal resulted in saturation with a maximum output voltage of 86 volts.

Values of R and C were determined by three criteria:

1. No attenuation for 60 c.p.s., hence

$$RC = \frac{1}{\omega} = \frac{1}{377} = 2.66 \text{ millisecs}$$

2. Grid voltage is to be less than 10 millivolts.

Since

$$e_g = e_i - iR$$

$$R = \frac{e_i}{i} - \frac{e_g}{i}$$

This indicates a large value of R for a moderate value of e_i and a small value of i. Hence a 1.25 megohm (variable) resistence was used.

3. Very little load may be drawn from the secondary winding on the toroid. This also indicates a high value for the input R.

For convenience a C of about .003 microfarads was used and R was adjusted until, with a pure sine wave voltage input of 10 volts peak to peak, no attenuation and no distortion was detectable with the CRO. Grid voltage was measured with a VTVM and found to be 5 millivolts RMS, or for a sine wave, 14 millivolts peak-to-peak. This means a gain at 60 c.p.s. of more than 700.

Fidelity of integration was determined by the use of the Square Wave Generator and a Dumont Electronic Switch. When the square wave was fed into the integrator, a triangular wave was the integrated output. As nearly as could be determined by use of the electronic switch this integration was true and complete.

Later developments and a reference to Lord(11) convinced these experimenters that this simple integrator was

insufficient for our purposes. An unexplained loop appeared in the saturated ends of the hysteresis loops. Upon a suggestion from Dr. Allen E. VIVELL the possibility of phase shift distortion was considered. To check this idea a three phase synchro phase shifter was used to replace the sine wave H voltage. The magnitude of this voltage was matched with the magnitude of the actual e_H voltage by means of a slide wire rheostat. When the phase of this e_H voltage was shifted it became readily apparent that the loop effect was actually due to phase shift in the system. Since the integrator discussed herein was an RC coupled device it immediately became suspect.

A study of Lord(11) convinced the experimenters that sub-harmonic phase distortion was also an important effect. Inasmuch as the integrator discussed herein is not a D.C. amplifier, hence would not amplify subharmonics with the desired fidelity, it was decided to abandon this device in favor of a BOEING D.C. AMPLIFIER taken from the BOEING ANALOG COMPUTER MODEL 6568.

Calibration of CRO for Hysteresis Measurements

$$\mathcal{H} = \frac{N_1 i}{l_m} \quad \frac{\text{amp-turns}}{\text{meter}}$$

$$i = \frac{e}{R} \quad \text{amps}$$

$$k \triangleq \frac{e}{d} \quad \frac{\text{volts}}{\text{small division}}$$

$$\therefore \mathcal{H} = \frac{N_1}{l_m R} k\, d \quad \frac{\text{amp-turns}}{\text{meter}}$$

If 260 turns (primary winding)

.369 meters (mean magnetic path)

0.500 ohms (resistance in series with primary winding).

$$\mathcal{H} = 1408\, k \cdot d \quad \frac{\text{amp-turns}}{\text{meter}}$$

Using the Dumont Voltage Calibrator Type 264 B Serial 3175 to set values of k the results in Figure 71 are obtained

H	units	k	scale selector	dial
100d	amp-turns meter	.071	D.C. 10	$45\frac{1}{2}$
17.70d	oersteds	.0565	D.C. 10	53
2d	amp-turns in	.0560	D.C. 10	55

Figure 71: H Calibration of CRO

For flux density calibration

$$e_{sec} = -N_{sec}\frac{d\phi}{dt}$$

$$\phi = -\frac{1}{N_{sec}}\int e_{sec}\,dt$$

$$B \triangleq \frac{\phi}{A_{iron}} = -\frac{1}{N_{sec}A_{iron}}\int e_{sec}\,dt$$

But the integrator gives

$$e_{out} \doteq -\frac{1}{RC}\int e_{in}\,dt$$

with only one specimen

$$e_{sec} = e_{in}$$

Hence

$$B = \frac{RC}{N_{sec}A_{iron}}\,e_o$$

Defining

$$k \triangleq \frac{e_o}{d}\ \frac{\text{volts}}{\text{small division}}$$

$$B = \frac{RC}{N_{sec}A_{iron}} \times k\cdot d$$

Where

$R =$ 1 megohm (input resistance to amplifier)

$C =$ .00263 microfarads (feedback capacitance for integrator)

$A_{iron} =$ .914 x 10^{-4} sq. meters (area of section of specimen)

$N_{sec} =$ 20 turns (on secondary of specimen)

Then

$$B = 1.440\,kd\ \frac{\text{webers}}{m^2}$$

Using the Dumont Voltage Calibrator Type 264B Serial 3175 to set values of k the results in Figure 72 obtained for the Dumont CRO Type 304 H Serial 7538.

B	units	k	scale selector	dial
0.1 d	webers m	.0696	D.C. 10	90
d	kilogauss	.0696	D.C. 10	90
100 d	kilolines in	0.1077	D.C. 10	54½

Figure 72. B calibration of CRO

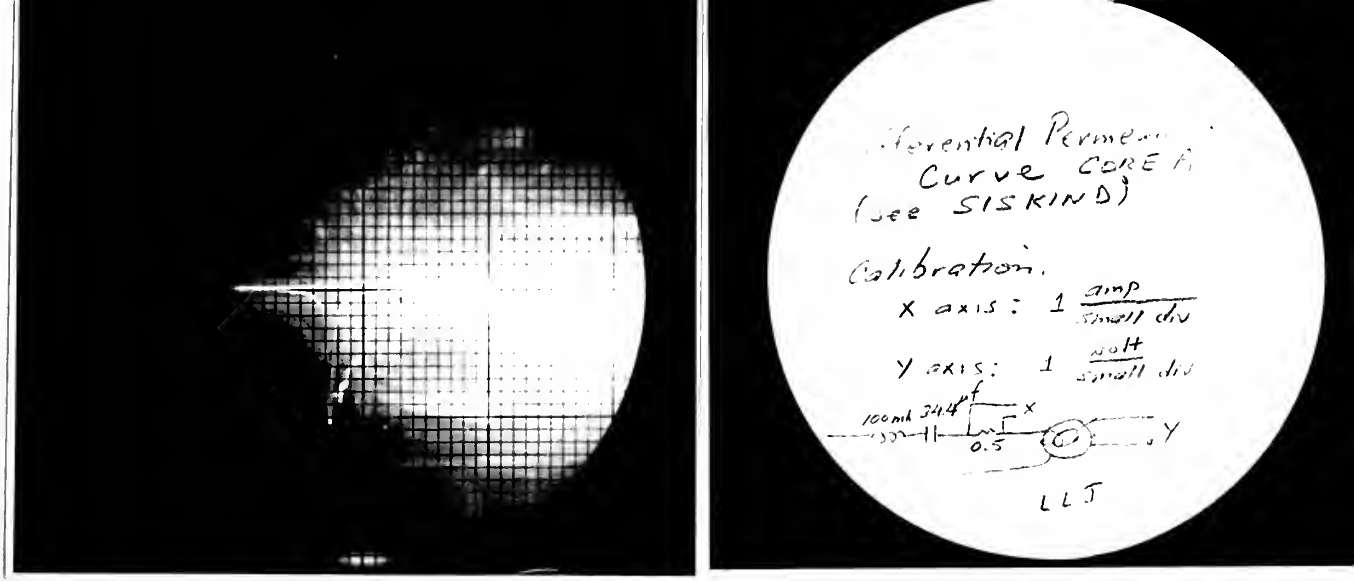

Figure 73

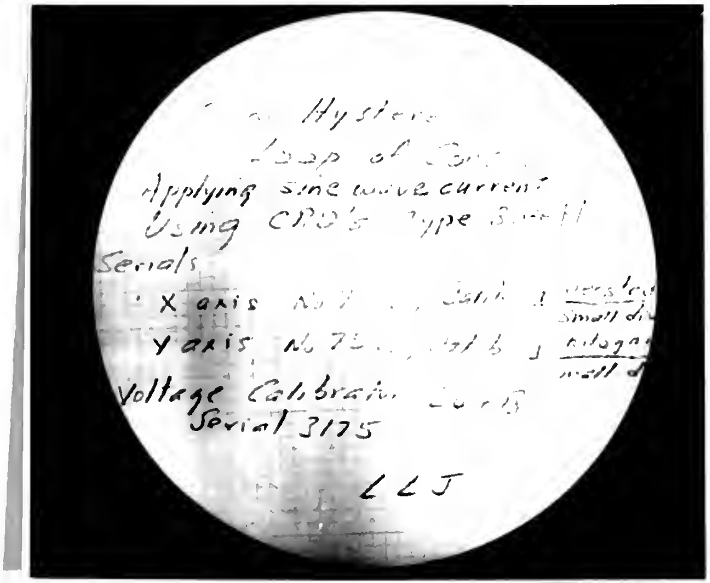

Figure 74

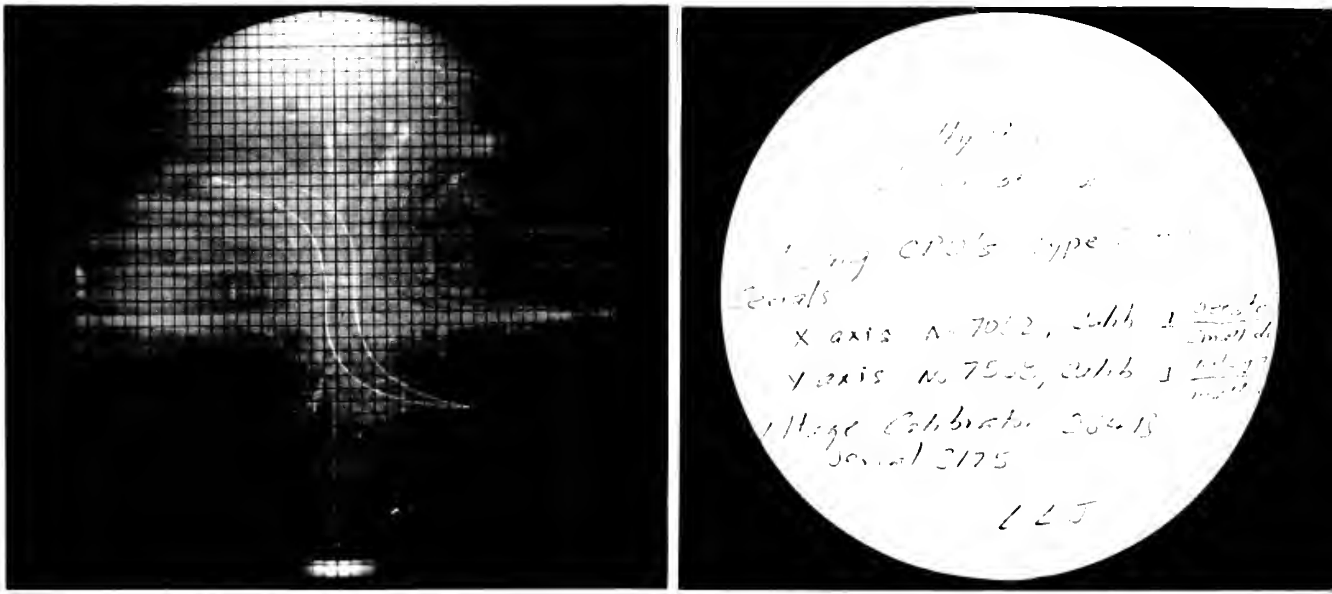

Figure 75

APPENDIX F

USE OF 35mm CAMERA

Description:

(See manufacturer's instruction pamphlet(7) for DUMONT OSCILLOGRAPHIC RECORD CAMERA Type 296, Serial 6x98.)

Film:

35mm Linagraph Ortho film was used throughout and more is available from Photography Shop. This film is loaded by operator in a darkroom, either in a cartridge provided or directly into camera. Care must be taken to wind spool so that the short projection engages rewind spindle, otherwise, the back of the camera cannot be replaced. After loading wind off three exposures if cartridge is used. This insures that fogged film, if any, will not be used for recording data.

Use with Dumont CRO Type 304 H: Serial 7538

1. Set trace intensity for sharpest focus. This is about half the maximum intensity.

2. Camera settings f/2.8 at 1/25 and f/5.6 at 1/10 were used with satisfactory results to record a 60 c.p.s. signal. For signals which retrace less frequently more time should be allowed.

3. To obtain a superimposed grid, turn Y-amplifier to off, set X-amplifier for a two-inch trace, turn intensity to maximum and move trace off the scope so that the reflected glow of trace is about centered on the scope. Leaving camera

in place with same settings as for signal, snap the shutter ten to fifteen times.

4. Wind to next exposure.

Use with TEKTRONIX CRO Type 512: Serial 3304

This long-persistence scope was used for single-trace triggered impulse (transients).

1. Mount camera barrel locking ring so that the slot on the ring (for tightening) does not coincide with slot inconveniently provided at top of scope mounting ring. Otherwise a clouded exposure will reult.

2. Set intensity for optimum focus. This occurs at about two-thirds the maximum intensity.

3. Set f/2.8 with time on BULB and apply the transient.

4. To obtain grid turn GRID ILLUMINATION to maximum, then back off ¼ turn to prevent blanking the transient trace. Turn trace intensity to minimum. Expose (at f/5.6 on BULB) for about two seconds.

5. With this scope and camera the grid and transient can be recorded simultaneously, provided TRACE STABILITY and TRIGGER AMPLITUDE are carefully adjusted so that an unwanted retrace does not occur during the time (about two seconds) allowed for the grid to make an impression on the film.

6. Wind to next exposure.

Use with TEKTRONIX CRO Type 511AD: Serial 3312

1. Take care that a light leak does not occur through

tightening slot on locking ring and the slot at top of mounting ring of this scope.

2. Set GRID ILLUMINATION to maximum and back off ¼ turn.

3. Adjust intensity for optimum focus. Set focus dials.

4. Set camera at f/5.6 at 1/10 and mount on barrel.

5. Snap shutter to obtain trace.

6. Turn trace intensity to minimum and snap shutter four more times to obtain grid.

7. Wind to next exposure.

Use with Data Monitor:

1. Record data on monitor using ordinary black lead pencil.

2. Remove camera and barrel from locking ring, place over data and snap. Use same camera settings as for scope; that is, f/5.6 at 1/10.

3. Wind to next exposure.

4. It is possible to superimpose data on trace with fairly good results. However more experience is required to insure consistently good results using this technique.

Developing Film:

1. Carefully rinse developing tank, thermometer, measuring flask and beakers to remove all traces of hypo from equipment that will hold developing solution.

2. Prepare half-strength developing solution by using twelve ounces DEKAL 12 solution and twelve ounces of cold

water. Insert thermometer and set aside in beaker.

3. Pour twentyfour ounces of hypo fixer.

4. Clear a working place and lay out spool, tank, and top of developing tank in preparation for loading tank in the dark. If inexperienced in winding on developing tank spool, practice using on old roll of 35mm film until you can do it with your eyes shut.

5. Turn out all lights, open camera, wind film on spool, put spool in tank, and put top on tank, closing it securely. Lights may now be turned on.

6. Check temperatures of developing solution and set timer for <u>five minutes for 68° F. or six and one half for 60° F</u>.

7. Pour in developer and start timer. Every minute agitate solution by spinning the spool with shaft provided.

8. At end of developing time pour out developer. Rinse the film by filling and emptying tank once with cold water.

9. Immediately pour in fixer (hypo) and fix for 12 to 15 minutes. Agitate every minute or so.

10. At end of fixing time pour out fixer and commence rinsing by running cold water into tank. Rinse for 15 to 20 minutes. After about 1 minute of rinsing the top may be removed from tank and the film inspected.

11. <u>Carefully rinse</u> all equipment used and replace in storage provided.

12. During rinsing time film cartridge and camera may be reloaded. This must be done in complete darkness since LINAGRAPH ORTHO is very sensitive film.

13. After rinsing hang film up in warm freely ventilated location, being careful that emulsified side will not be scratched. A soft blotter can be used to wipe off excess water. Film will dry in two to four hours.

Making Prints:

1. Rinse trays, measuring flasks, beakers, handling tongs, and stirrers to avoid polluting developer with fixer.

2. Prepare one-third strength developing solution using 8 ounces DEKAL 12 solution and 16 ozs. cold water. Pour into one-quart developing tray.

3. Fill second developing tray with cold fresh water.

4. Fill third developing tray with hypo fixer.

5. Prepare enlarger by setting desired print size (usually 3 x 4 inch exposed area on 4 x 5 paper with ½ inch border is very satisfactory). Set frame (usually ½ inch). Cut photographic paper to size (8 x 10 inch sheet cut into quarters). For enlarging, F3 paper is satisfactory for these exposures.

6. Exposure time and enlarger aperture settings for F3 paper and two feet away will be about f/11 at 10 seconds. These vary with the enlarger, but in any event should be adjusted so that <u>developing time is 1 to 1½ minutes</u>. Adjust

by using small test sheets, perhaps 1 x 4, cut from one piece of paper.

7. Develop paper 1 to 1½ minutes, rinse in water, and fix for 10 to 20 minutes.

8. Wash prints for 15 to 20 minutes in running water.

9. Dip prints in anti-curl solution, if available, lay face down on glossing sheet, roll water out using absorbent roller and put in warm place to dry. When prints dry off the sheet, they are done.

10. Carefully rinse and put away all equipment used for developing.

APPENDIX G

ORIGINAL DATA

The original laboratory data sheets for the experimental tests conducted in conjunction with this thesis are included in this appendix in the order indicated below:

A. Solid Cores

No.	Curve	Sample	Max. DC magnetizing force AT/m	Max. AC magnetizing force AT/m	Frequency of AC magnetizing force
1	Magnetization	C	8000	-	-
2	"	D	"	-	-
3	"	C&D	1150	-	-
4	Hysteresis	C	"	-	-
5	"	D	"	-	-
6	"	C&D	"	-	-
7	"	"	"	810	12
8	"	"	"	"	60
9	"	"	"	"	180
10	"	"	"	"	300
11	"	"	"	"	420
12	"	"	"	1620	"

B. Laminated Cores

No.	Curve	Sample	Max. DC magnetizing force AT/m	Max. AC magnetizing force AT/m	Frequency of AC magnetizing force
1	Magnetization	E&F	750	-	-
2	"	"	3500	-	-
3	"	"	750	70	180
4	"	"	"	175	"
5	"	"	"	350	"
6	"	"	"	700	"

7	Hysteresis	E&F	700	-	-
8	"	"	"	70	28
9	"	"	"	175	"
10	"	"	"	350	"
11	"	"	"	700	"
12	"	"	"	1050	"
13	"	"	"	70	60
14	"	"	"	700	"
15	"	"	"	"	120
16	"	"	"	70	180
17	"	"	"	175	"
18	"	"	"	350	"
19	"	"	"	520	"
20	"	"	"	700	"
21	"	"	"	1050	"
22	"	"	"	70	300
23	"	"	"	700	"
24	"	"	"	70	420
25	"	"	"	175	"
26	"	"	"	350	"
27	"	"	"	525	"
28	"	"	"	700	"
29	"	"	"	1050	"
30	"	"	1400	-	-
31	"	"	"	700	25
32	"	"	"	"	420

C. Calibration

1 Calibration of galvanometer.

2 Determination of period of galvanometer.

3 Harmonic analysis of applied voltage.

H	I	Io	Lf	Def	B	I	Do	Df	Def	H	B
			cm			1.240	0	10.46		6[illegible]	[illegible]
[illegible]	.028	[illegible]	0.17	0.16	[illegible]	1.254	0	10.68		[illegible]	[illegible]
3[illegible]	.059	0	[illegible]	.65	[illegible]	1.266	0	10.71		[illegible]	[illegible]
[illegible]	[illegible]	0	.72	[illegible]	[illegible]	[illegible]	0	10.88		[illegible]	[illegible]
[illegible]	.142	0	1.61	1.61	[illegible]	[illegible]	0	11.02		846	[illegible]
[illegible]	.181	0	[illegible]		[illegible]	[illegible]	[illegible]	11.18		[illegible]	[illegible]
[illegible]	[illegible]	0	3.66		[illegible]	1.65[illegible]	$.02^{E}$	11.32	11.30	[illegible]	[illegible]
[illegible]	[illegible]	0	[illegible]		[illegible]	[illegible]	[illegible]	11.56	11.54	[illegible]	[illegible]
[illegible]	.305	0	[illegible]		[illegible]	[illegible]	[illegible]	[illegible]	[illegible]	[illegible]	[illegible]
[illegible]	[illegible]	0	[illegible]		[illegible]	[illegible]	[illegible]	[illegible]	11.63	[illegible]	[illegible]
[illegible]	.421	0	6.72		[illegible]	[illegible]	[illegible]	11.75	11.24	[illegible]	[illegible]
	.482	[illegible]	[illegible]		[illegible]						
[illegible]	.521	[illegible]	[illegible]		[illegible]						
[illegible]	.562	0	[illegible]		[illegible]						
[illegible]	.640	0	[illegible]		[illegible]						
[illegible]	.624	0	7.60		[illegible]						
[illegible]	.721	0	[illegible]		[illegible]						
[illegible]	.823	0	[illegible]		[illegible]						
[illegible]	.869	0	[illegible]								
[illegible]	.901	0	[illegible]		[illegible]						
[illegible]	.942	0	[illegible]		[illegible]						
[illegible]	1.005	0	[illegible]		[illegible]						
	1.058	0	[illegible]								
[illegible]	1.090	0	10.15		[illegible]						
[illegible]	1.160	0	10.35								

I ∆ 10

[illegible] .0025

+ 21667

Mag Curve S-pl #C 10-5-54

amp	H	B	mm	mm	mm	I								H	B	H	B
I			Do	Df	Def	I	Do	Df	Def	I	Do	Df B	Def				
.02	11.3	.0018	0	1.8^{E}	1.8	.52	$.1^{F}$	76.8	76.1	1.16	$.2^{R}$	103.2	103.4	297	.0758	661	.103
.04	22.8	.0023		2.3	2.3	.54	$.2^{F}$	76.8	77.0	1.20		104.2	104.4	308	.0766	685	.1012
.06	34.3	.0039		3.0	39	.56	$.2^{R}$	78.8	79.0	1.24		105.2	105.4	[illegible]	[illegible]	707	.105
.08	45.7	.0052		5.2	5.2	.58	$.2^{F}$	79.9	80.1	1.28		106.0	126.2	331	.0797	730	.1058
.10	57.2	.0080		8.0	8.0	.60	$.2^{R}$	81.0	81.2	1.38		107.2	107.4	342	.0808	759	.107
.12	68.6	.0112		11.2	11.2	.62	$.2^{R}$	81.8	82.0	1.36		108.0	108.2	354	.0816	775	.108
.14	80.0	.0157		15.7	15.7	.64	$.2^{R}$	83.8	84.0	1.40		108.8	109.0	366	.0836	799	.1084
.16	91.5	.0209		21.0	21.0	.66	$.2^{R}$	84.8	85.0	1.44		109.3	109.5	376	.0846	821	.109
.18	102.8	.0260		26.2	26.2	.68	$.2^{R}$	86.0	86.2	1.48		110.8	111.0	388	.0858	845	.1105
.20	114.1	.0314	$.2^{E}$	31.8	31.6	.70	$.2^{0}$	86.8	87.0	1.52		112.0	112.2	400	.0866	—	—
.22	125.5	.0359	0	36.1	36.1	.72	.2°	87.8	88.0	1.56		111.8	112.0	411	.0876	890	.1114
.24	137.0	.0406	0	40.8	40.8	.74	.2	88.8	89.0	1.56		111.8	112.0	422	.0885	890	.1114
.26	148.3	.0442	$.2^{E}$	44.0	44.4	.76		89.5	89.7	1.60		112.0	112.2	434	.0892	912	.1118
.28	159.9	.0485	0	48.7	48.7	.78		90.9	91.1	1.64	$.5^{F}$	112.8	113.3	445	.0907	936	.1129
.30	171.2	.0515	$.1^{E}$	51.7	51.8	.80		91.3	91.5	1.68	$.3^{R}$	113.2	113.5	456	.091	959	.113
.32	182.8	.0545	$.1^{E}$	54.8	54.7	.82				1.72	$.2^{F}$	114.0	114.2	468		981	.1138
.34	194.0	.0576	$.1^{E}$	58.0	57.9	.84		93.0	93.2	1.76		114.8	115.0	480	.0926	1004	.1142
.36	205.8	.0610	$.1^{E}$	60.4	60.3	.88		94.8	95.0	1.80		115.2	115.4	503	.0945	1027	.1149
.38	217	.062	$.1^{R}$	62.2	62.3	.92		96.3	96.4	[illegible]		115.3	113.5	525	.096	1050	.115
.40	228	.0647	$.1^{F}$	64.9	65.0	.96		97.8	98.0	1.88		116.2	116.4	549	.0975	1072	.1159
.42	240	.0670	$.1^{R}$	67.3	67.4	1.00		98.8	99.0	1.92		116.9	117.1	572	.0985	1096	.1165
.44	251	.0683	$.1^{R}$	68.5	68.6	1.04		100.0	100.2	1.96		117.4	117.6	594	.10	1119	.117
.46	262	.0706	$.2^{R}$	70.8	71.0	1.08		110.2	110.4	~~2.00~~		118.0	118.2	616		1140	.1176
.48	274	.072	$.2^{R}$	72.2	72.4	1.08		101.2	101.1					616	.101		
.50	286	.0738	$.2^{R}$	74.0	74.2	1.12		102.2	102.4					640	.102		

Ammeter read low by .01 a
Add .01 a to each reading

am. 21667

Mag curve for ple #D 10 aug 1954

I	H_{dc}	θ_1	θ_2	2θ	ΔL	I	θ_1	θ_2	Δθ	H	Δθ
.040		0	1.8	1.8		1.15	[illegible]	[illegible]	2032	67	[illegible]
.058	2.2	.1	2.0	3.1	[illegible]	1.175	0		2142	7.3	2.35
.063	[illegible]	.1	6.	[illegible]		[illegible]			217.	7.5	2.16
.110	[illegible]	1.0	15.8	16.8		1.2	.25		[illegible]		2.3
.140	8	.5	[illegible]	21.7		1.1			221.8	8	2.20
.163	3.1	.5	32.3	33.5		[illegible]			262	8	2.26
.189	[illegible]	.7	48	48.5	[illegible]	[illegible]			228		[illegible]
.218	[illegible]	0	[illegible]	61.7		[illegible]			[illegible]	[illegible]	
.260	[illegible]	[illegible]	[illegible]	[illegible]					21.	1.62	[illegible]
[illegible]	[illegible]	0	[illegible]	106.1		[illegible]			[illegible]	[illegible]	[illegible]
[illegible]	[illegible]	0	[illegible]	[illegible]		[illegible]			[illegible]	[illegible]	[illegible]
.312	[illegible]	[illegible]	[illegible]	[illegible]		[illegible]			[illegible]	[illegible]	
.117	[illegible]	[illegible]	[illegible]	[illegible]		[illegible]			[illegible]	[illegible]	
.490	[illegible]	[illegible]	[illegible]	[illegible]							
[illegible]	[illegible]			[illegible]							
[illegible]	[illegible]			[illegible]							
[illegible]	[illegible]										
.172	[illegible]			[illegible]							
.673	3.2										

I Δ Z₂

I_1	I_2	H	Δθ	ΔL/L
+ 2.009			0	
2.004	1.894		0	
	1.797	[illegible]	.3	
	1.735	[illegible]	.5	
	1.620	[illegible]	.7	
	1.550	[illegible]	1.0	
	1.470	[illegible]	1.1	
	1.395	[illegible]	1.3	
	1.312		1.5	
	1.208		1.9	
	1.100		2.1	
	1.002		2.4	
	.895		3.0	
	.817	[illegible]	3.2	
	.750	[illegible]	3.7	
	.698		4.0	
	.644	[illegible]	4.2	
	.600	344	4.5	
	.550	[illegible]	5.0	
	.499	[illegible]	5.4	
	.447	226	5.8	.177
	.402	200	6.3	[illegible]
	.337	183	7.2	.0716
	.302	[illegible]	7.9	.0786
	.248	[illegible]	8.9	[illegible]
	.200	[illegible]	10.1	[illegible]
	.156	[illegible]	11.3	[illegible]

I_2	Δθ	H	Δθ
.122	12.4		
.100	13.3		.132
.060	15.0	24	.110
.032	16.3		
0	16.3		
0	16.4		

I_1	I_2	H	Δθ	ΔL/L	
−2.00	0		18.5	.184	.368
	+.033		29.8	.207	.414
	+.052	20.8	27.6	[illegible]	[illegible]
	+.080	45.3	25.1	[illegible]	[illegible]
	.106	60.8	28.5	.283	.565
	.150	[illegible]	36.3	.31	[illegible]
	.178	[illegible]	43.3	.430	[illegible]
	.202	115.8	51.0	.508	1.016
	.252	141.4	59.3	.63	[illegible]
	.295	[illegible]	70.5	[illegible]	[illegible]
	.348	[illegible]	78.3	[illegible]	
	.402	[illegible]	83.3	[illegible]	
	.452	[illegible]	87.2	[illegible]	
	.505	[illegible]	90.5	[illegible]	
	.558	[illegible]	93.2		
	.602	[illegible]	95.3	.948	
	.702	403	99.0	[illegible]	
	.802	460	103.4	[illegible]	[illegible]
	.898	515	104.9	1.042	
	1.006	[illegible]	107.3	[illegible]	
	1.140	654	[illegible]	[illegible]	
	1.228	[illegible]	111.	[illegible]	
	1.398	[illegible]	113.0	[illegible]	
	1.518	926	[illegible]	[illegible]	
	1.605	[illegible]	116.3	[illegible]	
	1.764	[illegible]	117.3	[illegible]	
	[illegible]	[illegible]	117.5		
	[illegible]		117.5		
+	[illegible]		117.6		

Sample AC

I_1	I_2	θ_0	θ_F	$\Delta\theta$	I_1	I_2	θ_0	θ_F	$\Delta\theta$	I_1	I_2	θ_0	θ_F	$\Delta\theta$	H	H	H	ΔB	ΔB	$\Delta B/2$
+2.00				mm	+2.00	.36	0	6.9	6.9	-2.00	0.032	0	2.00	2.9	230	123		0	.0667	.139
	1.961	0	0	0		.328	0	7.3	7.3		.083	0	2.49	2.19	1121	181	475	0	.0726	.248
	1.893	0.3	0.4	.1		.287	0	8.1	8.1		.143	0	3.39	3.39	1072	164		.01	.0806	.336
	1.883	0.0	0.2	.2		.250	0	8.8	8.8		.209	0	5.12	51.2	1024	148	495	.02	.0875	.513
	1.700	0	.4	.4		.215	0	9.8	9.8		.265	0	6.65	66.5	972	132	[illegible]	.009	.0975	.661
	1.658	0	.6	.6		.182	0	10.1	10.1		.323	0	7.58	7.58	947	104	[illegible]	.006	.1005	.734
	1.602	0	.8	.8		.150	0	11.2	11.2		.383	0	8.26	8.26	916	858	219	.008	.1114	.823
	1.560	0	.9	.9		.109	0	12.8	12.8		.429	0	8.59	8.59	892	623	245	.003	.1272	.850
	1.522	0	1.0	1.0		.088	0	13.6	13.6		.490	0	9.07	9.07	871	583	270	.010	.1352	.933
	1.490	0	1.0	1.0		.060	0	14.8	14.8		.569	0	9.48	9.48	852	343	325	.010	.1471	.943
	1.441	0	1.1	1.1		.041	0	15.5	15.5		.657	0	9.81	9.81	825	234	[illegible]	.011	.1541	.977
	1.390	0	1.2	1.2		.035	0	16.0	16.0		.740	0	10.12	10.12	795	[illegible]	[illegible]	.012	.1592	1.008
	1.304	0	1.4	1.4		0	0.1	18.4	18.3		.795	0	103.0	103.0	756		455	.014	.1820	1.023
	1.255	0	1.8	1.8							.890	0	105.9	105.9	717		501	.018		1.052
	1.190	0	2.0	2.0							.943	0	107.0	107.0	680		539	.020		1.065
	1.129	0	2.1	2.1							1.010	0	108.5	108.5	645		576	.021		1.07
	1.060	0	2.2	2.2							1.099	0	109.9	109.9	606		627	.0219		1.09
	.983	0	2.6	2.6							1.190	0	111.0	111.0	[illegible]		680	.0259		1.105
	.920	0	3.0	3.0							1.250	0	112.1	112.1	52[illegible]		715	.0256		1.118
	.872	0	3.1	3.1							1.331	0	113.1	113.1	[illegible]		756	.0271		[illegible]
	.810	0	3.3	3.3							1.432	0	114.0	114.0	413		818	.0256		[illegible]
	.750	0	3.8	3.7							1.530	0	115.0	115.0	429		875	.0278		1.145
	.690	0	4.0	4.0							1.648	0	116.1	116.1	395		940	.1278		[illegible]
	.632	1	4.5	4.4							1.755	0	117.0	117.0	361		1022	.0438		1.164
	.592	0	4.7	4.7							1.836	0	117.5	117.5	331		1050	.0457		1.173
	.520	1	5.0	5.1							1.924	0	118.0	118.0	291		1100	.0503		1.175
	.459	1	5.3	5.4							+2.000	0	118.3	118.3	262 232		1142	.0537 .0667		1.179
	.405	0	6.3	6.3																

4/9 54

I_1	I_2	θ_0	θ_F	$\Delta\theta$	ΔB	H_{dc}	I_1	I_2	θ_0	θ_F	$\Delta\theta$	ΔB	H_{dc}
+2.000	1.842	0	.66		.006	1052	2.00	0	0	36.0	36.0	.358	0
	1.738	0	1.0		.00995	992		[illegible]	0	41.[illegible]		.412	20.0
	1.628	0	1.4		.01305	930		.082	0	50.0		.497	46.8
	1.540	0	1.9		.0189	880		.142	0	68.0		.676	81.1
	1.445	0	2.1		.0209	825		.190	0	92.3		.917	108.4
	1.335	0	2.6		.0258	774		.250	0	[illegible]		1.245	142.9
	1.245	0	3.1		.0308	711		.320	0	148.9		1.480	182.8
	1.163	0	3.8		.0378	665		.372	0	[illegible]		1.619	212.1
	1.066	0	4.2		.0418	620		.445	0	173.2		[illegible]	254
	1.004	0	4.8		.0478	563		.515	0	184.3		[illegible]	294
	0.949	0	5.1		.0507	542		[illegible]	0	[illegible]		1.901	340
	.875	0	5.9		.0587	500		.618	0	199.2		[illegible]	387
	.809	0	6.5		.0646	462		.750	0	[illegible]		2.042	428
	.720	1	[illegible]	[illegible]	.0716	417		[illegible]	0	[illegible]		2.07	475
	.658	0	[illegible]		.0806	376		.910	0	[illegible]		2.13	520
	.582	0	[illegible]		.0925	332.5		[illegible]	0	[illegible]		2.18	570
	.508	0	10.8		.1072	290		1.105	0	[illegible]		2.215	622
	[illegible]	0	[illegible]		.1162	262		[illegible]	0	[illegible]		2.25	[illegible]
	.401	0	12.8		.1272	229		[illegible]	0	[illegible]		2.28	[illegible]
	.345	0	14.3		.1421	197		1.370	0	[illegible]		2.29	[illegible]
	[illegible]	0	[illegible]		.157	165.[illegible]		1.450	0	[illegible]		2.318	829
	.235		[illegible]		.189	124.1		1.520	0	[illegible]		2.33	[illegible]
	.190	0	[illegible]		.203	108.3		[illegible]	[illegible]	[illegible]	[illegible]	2.36	[illegible]
	[illegible]	[illegible]	[illegible]	23.3	.232	81.1		1.685	0	[illegible]		2.38	1020
	[illegible]	[illegible]	[illegible]	[illegible]	.258	56.0		[illegible]	0	[illegible]		[illegible]	1062
	[illegible]	[illegible]	[illegible]	[illegible]	.288	36.0		[illegible]	0	[illegible]		2.40	[illegible]
	[illegible]	[illegible]	[illegible]	[illegible]	.32	20.0		+2.00	0	[illegible]		2.415	1144
	0	[illegible]	[illegible]	[illegible]	.36	0							

I B 2

4

1/9 54

[illegible]

Hac - 805 [illegible]

[illegible] of hysteresis with 1000 [illegible] 3rd [illegible] 26 Jan 1954 ③

IB3

f	I_A	ΔE	H_dc	I_1	I_2	Θ_o	Θ_f	ΔΘ	f	I_3A	H_dc	ΔB	I_1	I_2	Θ_o	Θ_f	ΔΘ
60	1.0	.0756	1000	+.000	1.825	0		.8	60	1.0	615	2.322	-2.000	1.075	2.322		253.9
		.0159	9[illegible]		1.725	0		1.6			712	2.28		1.241	2.28		239.1
		.0272	8[illegible]		1.5			2.8			825	2.395		1.442	2.395		230.5
		.0218	[illegible]		1.440			2.2			970	2.4[illegible]		1.695	2.47		248.0
		.0468	70[illegible]		1.341			4.1			1120	2.495		1.960	2.46		250.2
		.0487	7[illegible]		1.231			5.0			1144			2.000			off scale
		.0593	62[illegible]		1.095			6.0									
		.0717	5[illegible]		.962	.5*	7.0⁸	7.5									
		.0856	49[illegible]		.861	0		8.6	60	1.0			-2.000	.858			225.2
		.10[illegible]	420		.745			10.6						1.010			233.2
		.12[illegible]	300		.630			12.7						1.218			239.2
		[illegible]	310		.542			14.8						1.362			242.1
		.1612	272		.475			16.2						1.535			245.3
		.1950	2055		.359			19.6						1.705			248.5
		.210	143		.250			24.1						1.820			249.7
		.370	50.9		.089			37.2						1.950			250.+
		.419	20		.035			42.1						2.000			off scale
		.470	0		0			47.2									
		.470		-2.000	0	0	47.2	47.2									
		.550	2[illegible]3		.029			55.2		1.02				1.400			242.0
		1.022	90.8		.159			102.9									242.2
		1.450	142		.248			145.5									242.0
		1.728	197		.345			173.8									242.0
		1.990	303		.530			199.9									
		2.121	389		.680			213.5									
		2.24	505		.882			225.0									

4

Combined Hysteresis with 180N to [illegible] impedance 28 Jan. 54 ⑥

I B 2

f	I3	I1	I2	Gc	Gr	ΔG	ΔE	Hdc
180	1.0	+2.000	1.860	0		[illegible]	.009	1022
			[illegible]	[illegible]	[illegible]	1.6	.0159	973
			1.5[illegible]		[illegible]	[illegible]	.0258	872
			[illegible]	1.0	[illegible]	[illegible]	.0372	[illegible]
			1.225	1.[illegible]		.5	.0448	[illegible]
			[illegible]	[illegible]		[illegible]	.0527	613
			[illegible]		5.0	4.[illegible]		
			[illegible]		[illegible]	[illegible]	.0724	[illegible]
			[illegible]		[illegible]	[illegible]	.0856	4[illegible]
			.648		[illegible]	10.[illegible]	.1075	3[illegible]
			.460		[illegible]	12.9	.1382	[illegible]
			[illegible]2		[illegible]	17	.169	207
			.2[illegible]		[illegible]	22.1	.23	136
			[illegible]		[illegible]	[illegible]	.336	27.3
			[illegible]9	0	[illegible]	38.[illegible]	.378	[illegible]
			[illegible]			41.2	.430	0
		−2.000	[illegible]	0		50.0	.477	[illegible]
			[illegible]			81.1	.207	19.5
			[illegible]			142.0	1.45	1523
			.410			1[illegible].6	1.785	[illegible]4
			[illegible]			[illegible]	2.042	[illegible]
			[illegible]			[illegible]5	2.121	453
			[illegible]			[illegible]	2.26	54[illegible]
			1.112			[illegible]	2.312	63[illegible]
			[illegible]			[illegible]	2.38	749
			1.445			[illegible]	2.40	826
			[illegible]	[illegible]	[illegible]	248.9	2.435	909
			[illegible]	0		[illegible]	2.459	989

f	I2	I1	I2	Gc	Gr	ΔG	ΔE	Hdc
[illegible]	[illegible]	+2.000	1.8[illegible]	0		[illegible]	2.42	1671
			1.925	50.[illegible]	[illegible]	24[illegible]	[illegible]	1125
			1.9[illegible]	5[illegible]	155.9	238.9	[illegible]	817
			1.902	[illegible]	[illegible]	24[illegible]	[illegible]	[illegible]4
			1.700		[illegible].5	24[illegible].5	2.412	[illegible]
			[illegible]		195.0	245.0	[illegible]	1010
			1.970		196.2	246.2	2.43	[illegible]
			2.000		19[illegible]	[illegible].2	[illegible]	1142
			0	[illegible]	[illegible]	42.[illegible]		
			.039	[illegible]	[illegible]	50.0		
			.190	[illegible]	59.2	108.2		
			[illegible]		[illegible]	[illegible]		
			[illegible]		[illegible]	183.2		
			.57[illegible]		148.1	199.1		
			.090		157.5	208.5		
			.350		16[illegible].2	210.2		
			.272		174.0	224.0		
			1.0[illegible]		179.8	22[illegible]		
			1.235		183.0	232.9		
			1.295		18[illegible]	237.1		
			1.5[illegible]		[illegible].0	241.0		
			1.725		[illegible]	243.0		
			[illegible]		[illegible]	24[illegible]		
			[illegible]	29.2	190.2	246.1		
			+2.000	0		[illegible].2		

4

Combined Hysteresis with Iron to pure impedance 1 February 1954 ⑦

I B 6

I	I1	I2	[illegible]	G	ΔG	ΔE	Hdc	Hdc meter
[illegible]	+	1.860			[illegible]	.009	1022	[illegible]
		1.625			1.8	.0179	946	
		1.504			2.[illegible]	.0259	850	
		1.3[illegible]			3.5	.0348	77[illegible]	
		1.205			4.4	.0438	6[illegible]	
		1.04[illegible]			5.[illegible]	.0527	595	
		.925			7.1	.0727	522	
		.780			7.[illegible]	.0855	446	
		.618			[illegible].0	.1095	352	
		.4[illegible]			[illegible].2	.1394	260	
		[illegible]			[illegible].1	.180	[illegible]	
		[illegible]			[illegible]4	.223	14[illegible]	
		.04[illegible]			[illegible].4	.362	28.[illegible]	
		0			[illegible]	.427	0	
		0			[illegible].4	.412	0	
		.04[illegible]	[illegible]	[illegible]	5[illegible].0	.508	[illegible]	
		[illegible]	[illegible]	121.[illegible]	[illegible]1.2	1.238	126.4	
		[illegible]	[illegible]	16[illegible]	[illegible]	1.278	2[illegible].4	

Combined Hysteresis with 420 [illegible] 28 Jan 54 ⑦

No.	f	I_a	I_1	I_2	G_i	G_f	$\Delta\Theta$	Δt	f	I_3	I_n	I_2	G_0	G_f	$\Delta\Theta$	Δt	I	E7		
[illegible]	420	1.0	+2.000	.035	0		.2		420	1.0	-2.000	+2.000	0		[illegible]	420	2.0	-2.000	+2.000	247.2
				.140			26.8								[illegible]					247.6
				[illegible]			[illegible]					[illegible]	0		[illegible]					247.0
															[illegible]					246.8
	420	1.0	+2.000	.039			34.0					1.150			232.8					247.8
1129				1.975	0		.1	.001				1.242			236.5					248.0
1024				1.786			1.0	.0002				1.442	0		240.8		.5			247.8
948				1.660			1.8	.018				1.670			241.2		.6			248.0
869				1.571			2.2					1.820	0		247.8		.735			248.5
767				1.342			2.2	.032				1.950	0		249.0		.869			[illegible]
[illegible]				1.170			[illegible]					+2.000			249.5		.967			249.0
[illegible]				1.045			6.0										1.24			249.1
[illegible]				.275			[illegible]		420	.50	-2.000	+2.000			248.0		1.59			249.2
[illegible]				.742			[illegible]					+2.000	0		[illegible]		2.03			250.0
[illegible]				.590						1.50	-2.000	+2.000	0		250.0		2.42			247.3
[illegible]				.450			[illegible]						0		249.8		2.92			[illegible]
[illegible]				.350						2.00	-2.000	+2.000	0		[illegible]		2.25			[illegible]
[illegible]				.125			[illegible]								249.8		2.35			250.0
[illegible]				[illegible]			[illegible].6								246.1		2.35			[illegible]
				0	.9	42.0	11.1								246.1		4.11		138.2	238.2
				0	0		12.1			.25	-2.000		0		247.8		2.00	116	132.2	243.2
0				0			[illegible]			.25			0		247.1					
[illegible]				[illegible]			.5			0					[illegible]					
[illegible]				[illegible]			[illegible]								246.1					
[illegible]				[illegible]			[illegible]						0		246.0					
[illegible]				[illegible]			17.0			.1					246.8					
[illegible]							.8								247.0					

Combined [illegible]

f	I_{3A}	I_{3B}	I_1	I_2		$\Delta\Theta$	I_{3C}				I_1	I_2	G_0	G_f	$\Delta\Theta$
420		[illegible]	.00	[illegible]	.4	.4	1.86	[illegible]	2.0	1.36	-2.00	[illegible]			224.0
		.810								1.44		1.014			[illegible]
		.850					.85			1.55		1.201			224.0
		.870		1.[illegible]		[illegible]	1.77			1.65		1.324			[illegible]
		.63		[illegible]		[illegible]	1.665			1.72		1.430			[illegible]
420	2.0	.50		[illegible]		[illegible]	~~1.42~~			1.78		1.610			[illegible]
		.23		[illegible]		[illegible]	1.57			1.90		1.820			[illegible]
		.85		[illegible]		[illegible]	[illegible]			.97		1.971			245.2
		.15		.87		[illegible]	[illegible]			2.00		2.00			[illegible]
		[illegible]		.73		9.6	1.23								
				[illegible]		12.4	1.11								
				.4		15.1	1.02								
				[illegible]		[illegible]	[illegible]								
				[illegible]		[illegible]		420	.5	.25	-2.00	[illegible]			[illegible]
				[illegible]		[illegible]	.960	420	[illegible]	.25	2.00	.218			152.2
				0		42.0	[illegible]	0	0	0	-2.00	.218			143.2
				0		42.1	.870	150	.51		[illegible]	[illegible]			153.0
				[illegible]		41.0	.760	300	.50		[illegible]	[illegible]			[illegible]
				[illegible]		[illegible]	.310	[illegible]		0	[illegible]	[illegible]			[illegible]
				.245		[illegible]	[illegible]	[illegible]	.5		[illegible]	.248			150.1
				[illegible]				420	1.0						
				[illegible]			1.76	[illegible]	1.76		[illegible]	[illegible]			152.0
				[illegible]			1.10	420	2.00		[illegible]	[illegible]			
				[illegible]		[illegible]	1.[illegible]	420	2.28		[illegible]	[illegible]			150.2
				[illegible]		[illegible]	[illegible]								

Combined Static Magnetization Curve 175 turn
Core
23 March 56 II A-1

D Sampled demagnetized from 5/7 ps Hickok ammeter 0-5 amp
Weston ammeter Serial 30016 Weston 0-[illegible]
(2)

½I	θ_0	θ_F	$\Delta\theta$	Space	H 703 I	ΔB $9.765\times10^{-3}\Delta\theta$	½ΔB	Space	H corrected 8.82 I	ΔB .02765 Δθ	½ΔB
.040	.1R	14.0B	14.1	3.72	28.19		.0688	.918			
.081	.5R	50.4	50.9	7.58	56.9		.2483	3.44			
.119	0	81.9	81.9	11.13	83.6		.400	5.33			
.191	0	116.6	116.6	17.85	134.1		.57	7.60			
.281	.2B	146.0	145.8	26.3	192.5		.712	9.48			
.342	0	160.1	160.1	32.0	240.1		.783	10.44			
.417	.2R	175.8	176.0	39.0	293		.860	11.48			
.526	0	195.2	195.2	49.9	369.8		.953	12.70			
.635	0	211.2	211.2	59.5	446		1.030	13.20			
.741	0	223.4	223.4	69.5	521		1.090	14.51			
.840	0	229.1	229.1	78.8	591		1.118	14.88			
.931	0	237.0	237.0	87.4	655		1.157	15.39			
.988				92.5	694						
.990	0	242.2	242.2	92.8	697	2.362	1.181	15.72	8.74	23.62	11.81
1.079	0	242.2	242.2	101.0	758		↓				
1.079	200.0R	39.2B	239.2		↓		1.166				
1.079	199.8R	39.8	239.8				1.170				
1.079	100.0R	138.8	238.8				↓				
1.079	0	216.2	216.2		↓		1.200				
1.300					914		[illegible]				

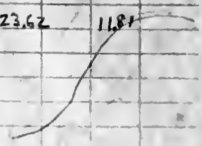

Combined Static Magnetization Curve
II 6 1 2
I A 2 6

Vdc	I_1	θ_0	θ_F	$\Delta\theta$	H_{dc} 572 I rms	H_{ac} 513 I	ΔB $9.95\times10^{-3}\Delta\theta$	H_{dc} 900 I	H_{ac} 807 I
28.9	0			0		0			
	.039	0	2.2B	2.2	22.3		.022	351	
	.080	.8R	8.9	9.7	45.8		.0965	72.0	
	.260	.5R	29.9	30.4	148.6		.302	234	
	.340	.8R	37.0	37.8	194.2		.376	306	
	.460	.8R	46.2	47.0	263.0		.468	414	
	.651	0	58.0	58.0	372.0		.577	586	
	.805	0	65.2	65.2	460		.649	725	
	.940	0	70.0	70.0	538		.697	845	
	1.10	0	74.8	74.8			.745	990	
	1.358	0	80.9	80.9			.805	1220	
	1.598	.2	85.0	85.2			.848	1438	
	1.802	.5	88.1	87.6	1030		.872	1620	
	2.000	.5	91.0	90.5	114		.900	1800	
	[illegible]	.5	91.7	91.2			.938	2022	
	2.70	.8	92.6	97.8			.973	2430	
	3.52	1.0	[illegible]	[illegible]			1.025	3162	
	4.13	1.0	107.9	106.9			1.062	3718	
	4.76	1.0	110.0	109.0			1.082	4250	
	5.02	1.0	111.4	110.4			1.100	4510	

change ammeter to Hickok Uniform Scale 0-5 amp meter serial no. 1827

[illegible]

I₁	θ	ΔΘ	I₁	f	H	ΔB
0			0.1	780		
.016		[illegible]	0.1		28.15	[illegible]
.15[illegible]	0	1[illegible]			[illegible]	.528
.[illegible]17	0	158.3			222.9	.772
.440		[illegible]			3[illegible]2.8	.887
[illegible]		19[illegible]	.1		29[illegible]	.973
.741		221.0			[illegible]	[illegible]
.835	0	2[illegible]3.5	0.1		58[illegible]	1.119
.94[illegible]	0	[illegible]28.0	0.1		[illegible]	1.161
1.07[illegible]		24[illegible] 2[illegible]9.5			[illegible]	1.2[illegible]8
1.160	off scale					
.998		241.5	0.1			1.178

I₁	I₃	f	V	V	θ₀	θ_f	Δθ	H	ΔB
0		.25			0				
.040		.25			0		4[illegible].3	28.15	.238
.1[illegible]0		.25					113.4	277	.553
.320		.25					164.8	225.0	.803
.435		.25					181.0	306	.898
.580		.25					202.[illegible]	408	1.000
.715		.25					220.2	503	1.072
.855		.25					233.[illegible]	601	1.135
0.962		[illegible]					241.4	676	1.175
1.104		.25	off scale					777	
1.030		.25			1.0⁸	247.5	246.5	725	1.200

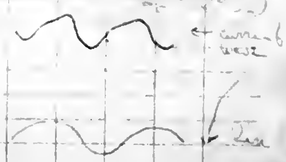

23 Mar 54 II A 4

I1	I3	I4	I5	f	Vdc	Vac	θ0	θ1	Δθ	H	ΔE	tan
.040	1?1		.50				1.?	[illegible]	25.5	28.?		.1244
.16?			.50				4.1	11.?	115.9	112.?		.565
[illegible]			.50				0		175.5	296.9		.905
.?20			.50				.8	214.0	213.2	443		1.03?
.72?			.50				0	229.0	229.0	555		1.117
[illegible]			.50				1.0	235.?	236.5	618		1.154
.9?0			.50				1.0	241.8	241.8	675		1.125
1.035			.50				1.0	246.8	247.3	727		1.208
1.065			.50				1.0	249.6	250.8	763		1.223

23 Mar 54 II A 5

I1	I3	I4	I5	f	Vdc	Vac	θ0	θ1	Δθ	H	ΔE	tan
	141	146	1.0	~~302~~ 190	23.8	18						
.040			1.0				$.5^{R}$	10.8^{B}	16.3	28.15		.0795
.165	62	166	1.0				5.0^{B}	~~47.0~~ 45.?	50.0	116.0		.244
.400	168	171	1.0				5.0^{R}	159.7	164.7	281.5		.803
.579	172	175	1.0				2.0^{B}	200.0	198.0	407.0		.966
.728	173	176	1.0				1.0^{B}	220.5	219.5	519		1.020
.855	176	180	1.0				1.0^{R}	230.0	231.0	601		1.128
.940	175	176	1.0				2.0^{B}	241.5	239.5	661		1.168
1.045	171	175	1.0				1.0^{B}	247.5	246.5	735		1.202
1.095	162	173	1.0	✓	✓	✓	off scale			770		

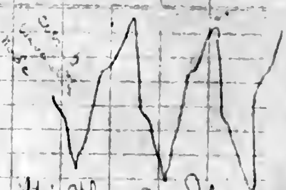

Note: [illegible] the [illegible] voltage [illegible] the [illegible] [illegible] [illegible] no [illegible].

Note: [illegible]

6 May D.C. Hysteresis Loop no ac 1 amp ... S- 6 E+F

							9.66×10						6.5×10⁻³	7.03	7.95×10⁻³ ΔΘ
I₁	I₂	H	Θ₀	Θ_F	ΔΘ	ΔB	span	ΔE	I₂	Θ	Θ_F	ΔΘ	ΔB	H_ac	ΔB
+1.00	.90		1.0	1.0	3.0		2.1	.0314	.81	1.5	7.0	3.5	.0287	.570	.0278
	.755		0	5.0	5.0		6.1	.0918	.60	1.0	11.2	10.2	.0836	.422	.0811
	.612			10.0	10.0		12.9	.1939	.40	0	21.5	21.5	.176	281	.171
	.500			15.1	15.1		20.1	.301	.25	1.5	32.0	33.5	.274	176	.266
	.408			20.0	[illegible]		[illegible]	.343	.20	0	37.1	37.1	.312	142.0	.303
	.341		1.2	24.0	25.2		26.5	.397	.14	0	41.3	44.2	.362	99.4	.351
	.273			30.5	30.5		31.2	.467	.10	2.0	50.0	52.0	.426	70.3	.413
	.160			42.0	42.0		36.2	.599	.05	0	61.0	61.0	.500	35.2	.481
	.080			58.6	58.6		49.0	.666	0	0	74.0	74.0	.687	0	.589
	.039		2.0	67.0	69.0										
	0		2.0	76.8	74.8										
	0		2.0	77.2	74.8										
	.035		2.0	94.0	92.0		55.1	.827				~~755~~	.755	22.	.731
	.052		2.0	115.2	113.2								.33	36.5	
	.071		0	133.0	133.0		79.7	1.06				1	1.09	43.9	1.058
	.09		1.0	148.0	147.0		88.3	1.322					1.205	63.9	1.17
	.12		1.0	164.2	163.2		96.5	1.449					1.339	84.3	1.298
	.165		3.0	179.0	176.0		105.3	1.512					1.44	116.0	1.40
	.200		.5	186.5	186.0		111.5	1.672					1.525	140.5	1.48
	.226		2.0	193.0	191.0		114.	1.72					1.575	158.9	1.52
	.260		0	199.0	199.0		115.5	1.70					1.63	182.0	1.58
	.330		0	207.0	207.0		124.0	1.861					1.695	224.8	1.645
	.381		3.0	218.0	215.0		[illegible]	1.932					1.76	268	1.710
	.500		2.0	227	225.0		135.	2.022					1.845	351.5	1.79
	.71		2.0	243	241.0		144.0	2.165					1.972	429	1.915
	.831		~~20.0~~ 23.0	226.0	249.0		149.	2.24					2.04	584	1.98
	.850		20.0	233	253.0		15.	2.27					2.07	625	2.01
	.960		23.0	233	256.0		153.3	2.35					2.10	675	2.04
	1.00		21.5	235	256.5		[illegible]	2.305					2.10	703	2.04

combined Hysteresis 90~ 0.1 peak — 29 March 54

II B = [illegible]

											H 703 I₂	ΔB 9.765×10⁻³ Δθ	H_ac 703 I₅	span
I₁	I₂	I₃	I₄	I₅	f	V_ac	V_dc	Θ₀	Θ_F	ΔΘ	H	Δ		
+1.000				.1	22.8									
	.899				27.5	32.0	44.0	0	[illegible]	18	632	.176	70.3	1.17
	.814									3.7	572	.0362		2.415
	[illegible]									6.5	496	.0635		4.23
	.615									10.4	433	.1015		6.77
	.530									13.9	372	.1359		9.05
	.412									21.0	290	.2055		13.69
	.309									28.2	217.5	.2753		18.32
	.228									38.4	160.2	.375		25.0
	.070									58.8	4[illegible]	.575		38.3
	.035									67.0	24.6	.655		44.3
	0									77.0	0	.760		50.6
	0									78.0	0	.762		50.8
	.027									102.2	20.0	1.009		66.7
	.118									159.0	[illegible]	1.550		103.6
	.230									186.5	161.8	1.82		121.2
	.315									202.2	213	1.978		131.8
	.447									212.[illegible]	314	2.075		138.0
	.537								[illegible]	220.[illegible]	378	2.14		142.5
	.652								[illegible]	221.5	459	2.215		147.5
	.774									233.[illegible]	545	2.28		152.0
	.859									237.1	604	2.33		154.0
	[illegible]									24[illegible].8	670	2.355		156.0
					27.5					24[illegible]	703	2.37		158.0

0.25

II B2c

I_1	I_2	I_3	I_4	I_5	∠	V_{dc}	V_{ac}	θ_o	θ_f	$\Delta\theta$	203 I_2 H	9.76(10)^3 $\Delta\theta$ ΔB		Squares
+1.000	.955	40	40	.25	27.5	30	40			1.0	672	.0098	1758	.655
	.822									4.2	578	.041		2.73
	.700									8.9	492	.0868		5.78
	.600									13.0	421	.127		8.46
	.458									20.7	322	.202		13.5
	.341									29.2	240	.285		19.0
	.230									40.1	161.5	.392		26.2
	.085									62.0	59.8	.605		40.4
	.035									73.0	24.6	.712		47.5
	0									85.9	0	.836		55.8
	.036									121.2	25.3	1.181		78.9
	.172									180.8	121.0	1.761		117.4
	.296									201.0	208	1.96		130.8
	.397									210.9	279	2.06		137.2
	.500									220.9	352	2.155		143.2
	.640									229.0	450	2.23		149.0
	.774									235.1	544	2.29		152.8
	.870									238.2	612	2.32		154.9
	.942									242.5	662	2.36		157.2
	1.000									299.0	703	2.38		158.9

II B2 Squares

I_1	I_2	1	I_4	I_5	f	V_{dc}	V_{ac}	θ_o	θ_f	$\Delta\theta$	H	ΔB	H_{max}	
1.0	.938	82	86	.5	28.0	[illegible]	[illegible]			1.9	659	.0185	352	1.23
	.825									5.1	580	.0498		3.32
	.695									10.0	489	.0976		6.51
	.600									14.2	422	.1383		9.22
	.465									21.3	341	.208		13.87
	.369									29.5	259	.288		19.2
	.225									43.8	158	.427		28.42
	.120									59.0	84.4	.575		38.35
	.035									78.5	24.6	.766		51.1
	0									93.9	0	.915		61.0
1.	.035									132.0	24.6	1.29		86.1
	.138									173.5	97.0	1.692		112.9
	.219									192.0	154	1.872		124.5
	.315									204.5	221	1.995		133.0
	.425									215.0	298	2.10		140
	.551									224.8	338	2.195		146.1
	.685									233.0	482	2.275		151.5
	.812									238.8	570	2.33		155.5
	.942									243.5	667	2.37		158.0
	1.000									245.2	703	2.39		159.1

I1	I2	I3	I4	I5	Vac	Vdc	—	G0	G1	ΔG	H	ΔB	II C[illegible]
+1.000	.954	1.[illegible]		1.	20	[illegible]	28.0	0		1.8	62	.0128	1.7
	.852									5.0	[illegible]	.0349	3.26
	.709									8.0	[illegible]	[illegible]	5.2
	.[illegible]									15.3	4[illegible]	[illegible]	9.7
	.438									24.1	[illegible]	.255	15.7
	.29									33.7	[illegible]	.331	[illegible]
	.1[illegible]									47.8	[illegible]	.48[illegible]	32.4
	.070									73.1	[illegible]	.712	47.5
	.025									85.0	24.0	.980	55.4
	0									109.0	0	1.015	6[illegible]
−1.000	.025							13.5^{B}	131.2	135.7	81.0	1.322	8[illegible].1
	.129							0		173.0	9[illegible].7	1.630	113.0
	.282									199.0	[illegible]	1.942	129.3
	.431									213.1	[illegible]	2.08	13[illegible].0
	.566									224.9	2[illegible]5	2.2[illegible]	146.9
	.738									233.0	51[illegible]	2.27	151.2
	.862									238.0	[illegible]	2.32	155.0
	.970									242.2	63[illegible]	2.36	157.5
										243.2	7[illegible]	2.37	158.1
	+1.000									243.2	[illegible]	2.37	158.1

[illegible]

I1	J2	J3	I4	I5	ζ	Vac	Vdc	Gc	GT	ΔG		H	ΔB	Hc	II B[illegible]
1.000	.926	14C	15C	1.5	28	45	30			2.3		652	.0224	1053	1.49
	.792									8.5		556	.05[illegible]		5.53
	.630									14.0		443	.137		9.33
	.516									19.5		363	.199		12.8
	.370									30.0		260	.292		19.49
	.230									44.2		1615	A32		28.7
	.065							2.0^{+}	61.6		[illegible]	457			
								3.0	78.5						
	.065							2.0	76.6	74.6			.729		48.6
	.036							3.0	82.5	79.5		25.3	.776		51.8
	0							3.0	107.5	104.5		0	1.02		~~[illegible]~~ [illegible]
−1	.036							3.0	132.5	135.5		25.3	1.322		88.1
	.125							2.0	163.0	165.0		87.6	1.61		107.2
	.279							5.0^{R}	191.0	191.0		192	1.862		124.2
	.416							4.0^{B}	200.2	204.2		292	1.995		132.0
	.552							4.0^{R}	218.6	219.6		388	2.10		140
	.724							6.0^{R}	229.2	223.2		509	2.18		145.1
	.882							$6.[illegible]^{R}$	231.5	230.0		620	2.30		153.1
	.961							7.0	240.0	243.0	G×B	676	2.37		158.0
									~~231~~			880			
	+1.000							2.0^{B}	231.5	233.5		703	2.28		152.0

22 March 54 II 032

I₁	I₂	I₃	I₄	I₅	f	V_AC	V_DC	Θ₀	Θ_F	ΔΘ	H	ΔB	[illegible]	H
+1	.90			[illegible]	60	L	29.1	0	1.9	1.3	[illegible]		[illegible]	.3
	[illegible]							0	[illegible]	[illegible]	5/2		3.[illegible]	
	.630							0	9.2	9.2	[illegible]		[illegible]	
	.5[illegible]0							0	[illegible].1	[illegible].1	[illegible]		[illegible]	
	.442							0	19.9	19.9			[illegible]	
	.301							0	30.5	30.5	[illegible]		[illegible]	
	.210							0	40.2	40.2	[illegible]		26.[illegible]	
	.110							0	51.8	51.8	[illegible]		35.6	
	.040							0	70.8	70.8	[illegible]		46.1	
	0							0	82.6	82.6			53.8	
−1	.029							0	104.1	104.1	[illegible]		67.6	
	.172							0	172.1	172.1	[illegible]		115.2	
	.292							0	198.2	198.2	[illegible]		129	
	.480							1.0E	212.4	211.4	[illegible]		139.8	
	.590							1.0E	222.0	222.0	[illegible]		145	
	.692							.5E	228.0	228.5	[illegible]		148.6	
	.815							.5E	234.[illegible]	235.[illegible]	[illegible]		153	
	.930							0	240.0	240.0	[illegible]		156	
	1.000							0	24[illegible]	[illegible]	7[illegible]		157.2	

Test 1. 11 March 54 II 032

1a p dc 1a p ac peak to peak 60 cycles 75 turn detection coil

[illegible] .4953 0703 I₂ 8850 I₂ .0012 [illegible]

→ DC → AC → f peak to peak

I₁	I₂	I₃	I₄	f	I₅	V_AC	V_DC	Θ₀	Θ_C	ΔΘ	A	ΔB Spec	H₇₀₃	H_AC	H₈₈₅₀	ΔB	μ
+1		[illegible]	[illegible]	60	1	73.1	25.4	put in 2. coil			~~A~~	common voltage		0.16	volts	0	
	.905							.9R	2.1B	3.0		[illegible] 1.27	636	703	1000	.0936	
	.833							1.0L	6.0B	5.0		3.23	583		7420	.1360	
	.762							.1E	8.0E	7.9		5.14	536		6740	.2462	
	.659							.2R	12.0	12.2		7.24	464		5820	.3840	
	.561							2.0E	18.1	16.1		15.47	394.2		4960	.503	
	.479							.2E	22.2	22.0		14.35	336.2		4240	.718	
	.358							0	21.8	21.8		20.65	251.8		3163	.993	
	.242							1.0	44.0	43.0		28.0	170.0		2140	1.341	
	.160							.5E	54.8	54.3		38.	112.1		1415	1.691	
	.080							.5E	86.8	86.3		56.1	21.08		2655	2.62	
	0							.5E	110.5	110.0	[illegible] 0	7[illegible]	0		0	3.438	
	0							.2E	107.8	107.6	put in 3 coil A	7[illegible]				3.36	
		[illegible]	2.5	60	1	71.0	25.3		[illegible]								
−1	.030							.2E	132.0	132.8		86.4	21.08		265.5	4.14	
	.157							.5E	172.0	172.5	[illegible]	114	110.2		1383	5.38	
	.316							1.0E	181.0	180.0		127.5	223.8		2816	5.93	
	.440							1.0E	222.4	223.4	[illegible] 4	[illegible]	303.8		3895	6.96	
	.570							.2R	202.0	199.4			400.5		5049	6.21	
	.320							3.0B	198.5	200.5		131	225.0		2830	6.28	
	.4[illegible]0							2.5B	209.7	212.0		138	295.5		3719	6.62	
	.523							3.0E	217.0	220.0		143	367.8		4630	6.87	
	.682							3.0	[illegible]	232.0		151	479		6040	7.25	
	.818							1.0E	239.1	236.1		155	575		7240	7.38	
	.930							3.0E	237.0	240.0		[illegible]	654		8230	7.30	
	−1.0							1.0E	243	248.0		[illegible] 474	703		8850	7.52	
	+1.0							2.0E	24	240.8						7.58	

~ 45   120 cycles   1a-p-c peak to peak   IIB-C

I_1	I_2	I_3	I_4	I_5	f	V_{dc}	V_{ac}	θ_0	θ_f	$\Delta\theta$	H	ΔE	H_{ac}	[illegible]
	~~[illegible]~~ .149	.15		1	120	228	[illegible]						.733	
	.230	.171	.172		120	288	[illegible]	0	2.1	2.1	.5		.0245	[illegible]67
	.920							1.5	4.0	3.5	[illegible]		.0537	[illegible]
	.683							.5	0.0	0.5	481		.1025	34
	.560							.2	17.0	16.8	[illegible]		.1340	[illegible]
	.461							.2	22.5	22.3	324		.2172	14.
	.303							.5	36.0	35.5	2[illegible]		.344	2[illegible].01
	.175							.8	52.4	51.6	1[illegible].5		.502	[illegible].5
	.050							1.1	71.1	75.5	[illegible]		.736	4[illegible]
	0							.2	102.0	102.2	[illegible]		.927	65.3
-1	[illegible]							[illegible]	[illegible]	111.6	7[illegible]		1.111	21.[illegible]
	.12[illegible]							2.[illegible]	[illegible]	18[illegible]	[illegible]		1.381	112.7
	~~[illegible]~~ .305							2.01	~~[illegible]~~ [illegible]	24[illegible].9	236		[illegible]	142.[illegible]
	.462							.2	220.0	210.8	3[illegible]		[illegible]	[illegible]
	.621							0	228.0	228.0	4[illegible]		2.222	143.2
	.782							[illegible]	229.0	23[illegible]	[illegible]		[illegible]	15[illegible].1
	.940							.3	242.2	24[illegible].9	661		[illegible]	157.1
	1.0							2.5	245.8	243.3	70[illegible]		[illegible]	158.[illegible]

22 Mach 54 IIC1

I_1	I_2	I_3	I_4	I_5	f	V_{ac}	V_{dc}	θ_0	θ_f	$\Delta\theta$	H	ΔE
+1			.1	.16	[illegible]	2		0	1.7	1.7	6[illegible]	
	.781							0	5.0	5.0	[illegible]	[illegible]
	.572							0	8.6	8.6	1[illegible]	[illegible]
	.346							.2	11.[illegible]	11.7	[illegible]	8.[illegible]
	.4[illegible]							0	20.0	20.0		
	.515							0	[illegible]	[illegible].5		[illegible]
	.172								43.5	43.9		[illegible]
	.032							0	68.0	68.0	[illegible]	[illegible]
0	0							.2	[illegible]	[illegible].5	0	
-1	.025							0	10[illegible]	107.1	[illegible]	[illegible]
	.170							.35	174.4	174.9	[illegible]	
	.333							0	[illegible]	12[illegible].8		
	.444							0	212.2	212.2	[illegible]	
	.561							1.6	222.2	221.6	4	
	.678							0	226.[illegible]	[illegible]	4[illegible]	
	.8[illegible]							0	233.8	[illegible].9	[illegible]	
	[illegible]							0	23[illegible]	23[illegible]		
	1.0							1.0	21[illegible]	[illegible]		
								0	[illegible]5.8	7[illegible].9		

17 March

I_1	I_2	I_3	I_4	I_5 peak to peak	f	V_{dc}	V_{ac}	θ_0	θ_F	$\Delta\theta$	H	AB	$\Delta S_?$	Hac
1.0	.950	38	38	.25	180	22.8	61.8	0	1.0^E	1.0	666		.65	175,5
	.782							0	5.1	5.1	549		3.32	
	.659							0	10.0	10.0	463		6.51	
	.519							0	16.1	16.1	364		10.47	
	.320							0	26.0	26.0	260		16.9	
	.238							0	32.1	37.1	167		24.1	
	.072							0	62.8	62.8	50.5		40.8	
	0							0	82.8	82.8	0		53.8	
-1	.039							0	112.0	112.0	27.4		73.0	
	.220							0	187.0	187.0	154.5		121.5	
	.400							0	210.1	210.1	281		136.8	
	.562							0	222.9	222.9	394		145.9	
	.782							0	235.0	235.0	549		153.0	
	.960							1.0^F	240.0	239.0	675		155.4	
	.979							0	241.2	241.2	687		156.9	
	1.000							0	242.9	242.9	703		157.9	

17 March II R4

I_1 dc	I_2 dc	I_3 ma ac	I_4	f	V_{dc}	V_{ac}	θ_0	θ_F	$\Delta\theta$	I_5 peak to peak ac	H	AB	Δgauss	Hac
1.0		72	78	180						.5				
1.0	.922	73	82		22.8	51	$.5^B$	1.0^{13}	1.5	.5	647			
	.801						$.2^B$	6.0^B	5.8		563		3.77	
	.701						$.2^B$	9.2	9.0		492		5.85	
	.560						0	16.1	16.1		392		10.48	
	.435						$.2^B$	24.0	23.8		305		15.50	
	.253						$.2^B$	39.8	39.6		182		25.78	
	.170						0	50.6	50.6		119		32.9	
	0						1.4^E	115.0	113.6		0		73.9	
-1	.038						$.2^B$	135.1^R	135.3		26.7		90.8	
	.170						0	183.0	183.0		119		119.0	
	.298						$.2^R$	202.0	201.8		209		131.0	
	.412						0	211.0	211.0		289		139.1	
	.520						$.2^F$	223.2	223.0		372		145.9	
	.650						$.2^F$	231.2	231.0		453		150	
	.802						1.0^F	238.5	237.5		564		154.2	
	.902						$.8^F$	243.2	242.4		634		158.0	
	.981						1.2^F	245.2	244.0		689		158.8	
	1.001						1.0	245.8	244.8		703		159.2	

DE4 R/

[illegible]	[illegible]	[illegible]	[illegible]	[illegible]	[illegible]	[illegible]	[illegible]	[illegible]	[illegible]	H	ΔΘ	[illegible]	H
1.0	.[illegible]	[illegible]	[illegible]	.75	[illegible]	[illegible]	[illegible]	[illegible]	1.1	669		.715	527
	.172						[illegible]	[illegible]	6.[illegible]	543		4.5	
	.[illegible]							[illegible]	[illegible]	450		8.0	
	.1[illegible]							21.9	[illegible]	336		14.25	
	.20[illegible]						[illegible]	[illegible]	[illegible].4	212		23.0	
	.16[illegible]						.5	[illegible].0	[illegible].5	114.5		34.2	
	.03[illegible]						[illegible]	80.[illegible]	[illegible].0	21.1		52.7	
							1.0	9[illegible]	97.5	0		63.5	
-1	.0[illegible]						0	13[illegible]	[illegible]	26.7		87.8	
	.162						[illegible]	18[illegible].2	1[illegible].7	114		117.9	
	.32[illegible]						[illegible]	206.5	206.5	232		134.2	
	.1[illegible]						[illegible]	231.0	[illegible]0.5	350		143.5	
	.6[illegible]						[illegible]	[illegible]	[illegible].4	458		15[illegible].0	
	.[illegible]40						[illegible]	[illegible]	[illegible]1.6	0-[illegible]			
	.[illegible]						0	245.[illegible]	24[illegible]				
	.959						0	242.0	242.0	674		157.3	
	1.000						0	244.9	244.9	703		159.2	

I_{ac}

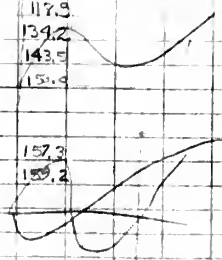

1.00
1.50

Test 2 180 cycle load ac peak to peak lode 11 march 54

I_1	I_2	I_3	I_4	f	I_5	V_{ac}	V_{dc}	Θ	$Θ_f$	ΔΘ	H	ΔΘ	H_{ac}	II B4 Square
+1		164	166	150	1	49.8	25.0				carry the voltage .40			
	.938							0	1.9^E	1.9	658	.275	703	1.23
	.815							$.4^B$	6.0^B	5.6	573	.0596		3.64
	.725							0	8.9	8.9	509	.0863		5.79
	.610							0	14.2	14.2	428	.1388		9.25
	.518							1.5^B	19.8	19.3	364	.1882		12.54
	.406							$.5^R$	25.4	25.9	234	.253		16.85
	.202							1.5^R	34.1	35.6	2.138	.348		23.2
	.180							1.5^R	49.7	50.2	126.4	.430		32.62
	.030							0	81.2	81.2	21.03	.793		52.9
	0							$.5^R$	112.5	112.0	0	1.102		73.5
-1	.034							1.5^B	139.6^R	140.5	23.9	1.37		91.4
	.160							1.5	185.0	186.5	126.4	1.82		121.1
	.320							$.5^R$	210.0	209.5	260	2.041		136.1
	.481							0	220.0	220.0	368	2.142		143.0
	.670							0	232.0	232.0	471	2.26		150.8
	.892							1.0^E	242.0	241.0	613	2.35		156.7
	.960							0	244.5	244.5	675	2.38		159.0
	+1.0							1.0^R	248.0	248.0	703	2.41		160.8

Jackson
Effect on hysteresis loops of superposing alternating magnetizing forces.

DEC 8
MAY 18
AP 16 56
14 APR 72

339
BINDERY
DISPLAY
4107
20662

25260

Thesis
J22

Jackson
Effect on hysteresis loops of superposing alternating magnetizing forces.

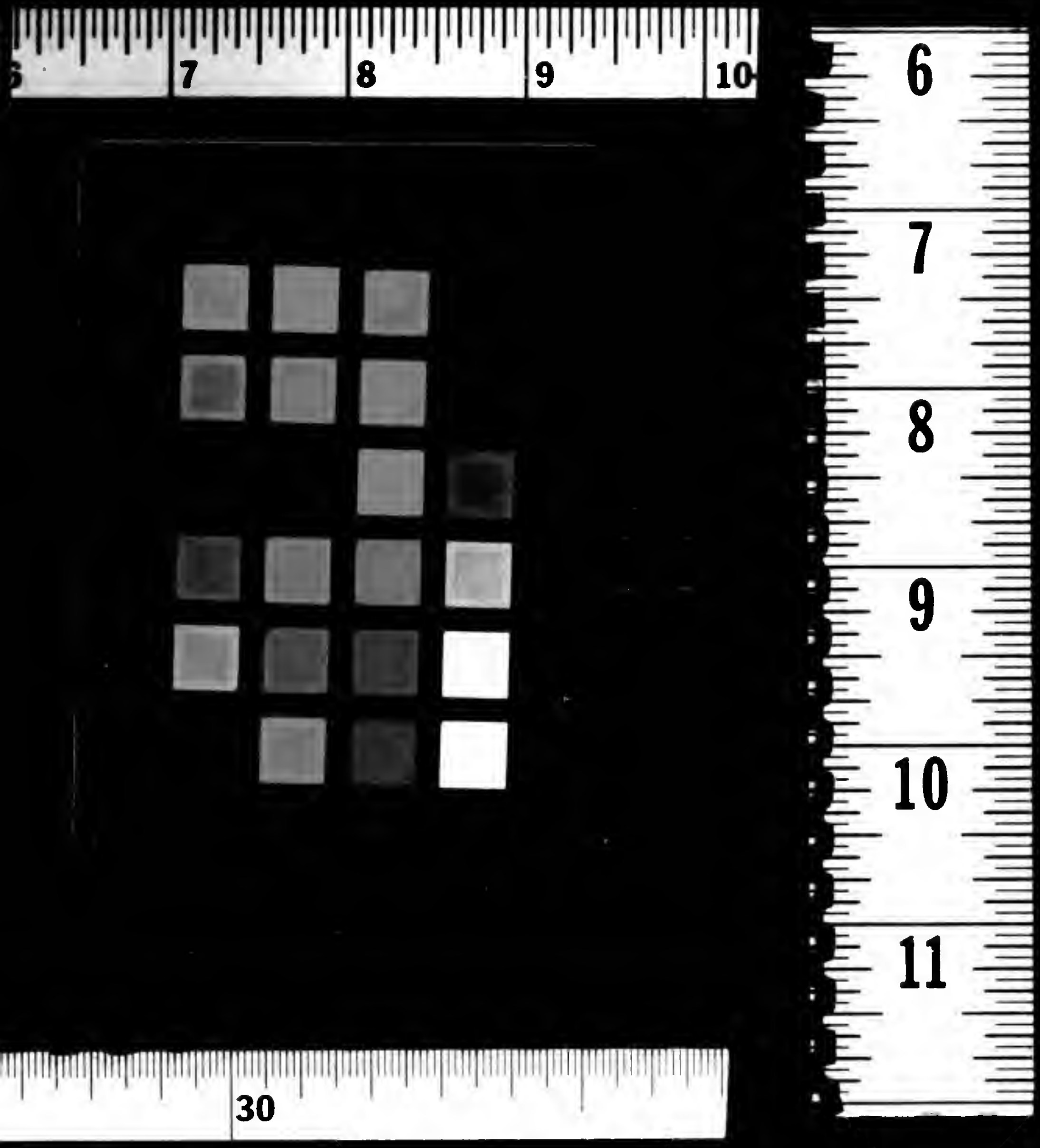
7
8
9
10
30
6
7
8
9
10
11